Inaugural dissertation

for

obtaining the doctoral degree

of the

Combined Faculty of Mathematics, Engineering and Natural Sciences

of the

Ruprecht - Karls - University

Heidelberg

Presented by

Eshita Varma M.Sc.

Born in: Kanpur, India

Oral-Examination: 19.09.2022

mRNA Binding Proteins in the Heart

Referees:

Prof. Dr. Marc Freichel

Dr. Mirko Völkers

Table of Contents

I. List of Figures

II. List of Tables

III. Index of Abbreviations

Abbreviation	Full form
µ	Micro
2C	Complex Capture
2D	2 Days
AAV9	Adeno-associated virus 9
AdCo	Adenovirus without coding insert
AICAR	5-Aminoimidazole-4 carboxamide 1-ß-D-Ribofuranoside
AKT	Protein Kinase B
AREBP	AICAR response element binding protein
AV	Adenovirus
BSA	Bovine serum albumin
BW	Body Weight
cDNA	Complementary DNA
CHX	Cycloheximide
CIRP	Cold-inducible RNA Binding Protein
Cm	Centimeter
Col1a1	Collagen type I alpha 1
CSD	Cold Shock Domain
CTD	C-terminal Domain
CVD	cardiac dysfunction
DAPI	4′,6-Diamidino-2- phenylindole
DCM	Dilated cardiac myopathy
DEPC	Diethyl pyro carbonate
DMEM	Dulbecco’s Modified Eagle Medium
DMSO	Dimethyl sulfoxide
DNA	Deoxyribonucleic acid
dNTP	Nucleoside triphosphates
EC	Endothelial Cells

ECG	Echocardiography
ECL	Enhanced Chemiluminescence
EDTA	Ethylene diamine tetra- acetic acid
eEF	elongation factors
eEF2	elongation factor 2
eEF2K	eukaryotic elongation factor 2 kinase
EF	Ejection fraction
eIF4A	eukaryotic translation initiation factor 4 A
eIF4B	eukaryotic translation initiation factor 4 B
eIF4E	eukaryotic translation initiation factor 4 E
eIF4G	eukaryotic translation initiation factor 4 G
eRF	peptide chain-releasing factors
et al.	Et alii (and others)
FBS	Fetal bovine serum
FC	Fold Change
FDR	False discovery rate
FITC	Fluorescein isothiocyanate
Fluc	Firefly Luciferase
FS	Fractional shortening
FT	Flow-through
Fw	Forward
G	Gram
GAPDH	Glyceraldehyde 3-phosphate dehydrogenase
H	Hours
HEK293	Human embryonic kidney 293 cells
HEPES	4-(2-Hydroethyl)-1-piper-azineethane- sulfonic acid
hnRNPL	Heterogeneous nuclear ribonucleoprotein L
HPRT	Hypoxanthine phospho- ribosyl transferase 1
HuR	Human antigen R
HW	Chain
IgG	Immunoglobulin G
IP	Immunoprecipitation

IRES	Internal ribosomal entry sites
K	Kilo
KD	Knockdown
KEGG	Kyoto Encyclopaedia of Genes and Genomes
L	Litre
LB	Lysogeny broth
log2	Logarithm to the base 2
log2FC	Log2 of fold change
LV	Left Ventricle
M	Meter
M	Molar Concentration
MAPK	Mitogen-Activated Protein Kinase
MBNL-1	Muscle blind-like 1
Min	Minutes
Mio	Million
Mol	Moles
mRNA	messenger RNA
mRNPs	ribonucleoprotein particles
mTOR	mammalian target of rapamycin
N	Sample size
Neg	Negative
NFAT	Nuclear factor of activated T-cells
Nm	Nanometre
Nppa	Natriuretic precursor Peptide a
Nppb	Natriuretic precursor Peptide b
NRCM	Neonatal rat cardiomyocyte
NRVM	Neonatal rat ventricular myocyte
Nt	Nucleotide
NX	Uncrosslinked
OE	Over Expression
ORF	Upstream Open Reading Frame
P	p-value
p70S6K1	Ribosomal protein S6 Kinase beta 1

PBS	Phospho-buffered Saline
PCR	Polymerase Chain reaction
PE	Phenylephrine
PEI	Polyethyleneimine
PI3	Phosphoinositide 3-kinase
PVDF	Polyvinylidene difluoride
QKI	Quaking RNA binding protein
R-	Without RNase
R+	With RNase
RBM20	RNA-Binding motif protein 20
RBP	RNA Binding Protein
rcf	Relative centrifugal force
rev	Reverse
Ribo-Seq	Ribosomal Profiling/Sequencing
RIP	RNA Immunoprecipitation
RIP-qRTPCR	RIP-quantitative PCR
RIP-Seq	RNA Immunoprecipitation Sequencing
Rluc	Renilla Luciferase
RNA Seq	RNA Sequencing
RV	Right ventricle
S6K	S6 Kinase
SDS	Sodium Dodecyl sulphate
Secs	Seconds
siRNA	small interfering RNA
SMC	Smooth Muscle Cells
SRSF1	Serine/Arginine splicing factor 1
TAC	Transverse Aortic Constriction
TBS	Tris-buffered Saline
TBST	TSB-Tweed
TE	Tris-EDTA
tiRNA	tRNA-derived stress induced RNAs
TOP	Terminal Oligo Pyrimidine
tRNA	transfer RNA

UTR	Un-translated Region
UV	UV crosslinked
V	Volt
Ybx-1	Y-box Binding protein 1

IV Abstract

Cardiac diseases result in altered protein and gene expression levels due to altered signal transduction pathways. RNA binding proteins (RBPs) are an emerging group of post-transcriptional regulators that control RNA between protein and RNA levels. Analysing the role of RNA binding proteins in cardiac dysfunction would be vital in understanding the coordination of multiple post-transcriptional events during such diseases. However, the specific role of RBPs in controlling protein expression in the diseased myocardium is still not completely understood. Ribosomal sequencing and RNA sequencing was used to identify mTOR-dependent and translationally regulated transcripts in response to TAC surgery. Ybx-1 showed up to be one RNA binding protein that is upregulated only during pathological hypertrophy in our screen. Experiments in isolated cardiomyocytes *in vitro* showed that Ybx-1 depletion prevents cellular growth by inhibiting protein translation. Furthermore, Ybx-1 expression depends on mTOR signalling and is independent of mRNA transcription. Ybx-1 knockdown *in vivo* preserves heart function during pathological cardiac hypertrophy. eEF2 mRNA was identified as a potential mRNA that binds to Ybx-1 and is upregulated during cardiac hypertrophy. Cardiac hypertrophy involves upregulation of protein synthesis, and elongation factors such as eEF2 regulate it. Identifying the crosstalk between Ybx-1 and eEF2 can help understand how these factors contribute to cardiac dysfunction.

V Abstrakt

Herzerkrankungen führen aufgrund veränderter Signaltransduktionswege zu veränderten Protein- und Genexpressionsniveaus. RNA-bindende Proteine (RBPs) sind zentrale posttranskriptionalle Regulatoren, die den gesamten RNA Metabolismus kontrollieren. Eine verbesserte Analyse der Rolle von RNA-bindenden Proteinen bei Herzfunktionsstörungen wäre daher entscheidend für das Verständnis der Koordination von posttranskriptionellen Ereignissen im Rahmen von Herzmuskelerkrankungen. Die spezifische Rolle einzelner RBPs in der Kontrolle der Proteinexpression im erkrankten Myokard ist jedoch noch nicht vollständig verstanden. Ribosomale Sequenzierungen und RNA-Sequenzierung wurden daher verwendet, um translationsregulierte Transkripte als Reaktion auf chronische Druckbelastung des linken Ventrikels zu identifizieren. Das Protein Ybx-1 erwies sich in diesem Screen als ein RNA-bindendes Protein, das nur während pathologischer Hypertrophie hochreguliert wird. In-vitro-Experimente an isolierten Kardiomyozyten zeigten, dass eine Ybx-1-Depletion das Zellwachstum verhindert, indem eine Verminderung der Ybx-1 Expression generelle Proteintranslation hemmt. Darüber hinaus hängt die Ybx-1-Expression von der mTOR-Signalgebung ab und ist unabhängig von der mRNA-Transkription. Ybx-1-Knockdown in vivo bewahrt die Herzfunktion im Rahmen pathologischer Herzhypertrophie. eEF2-mRNA wurde als potenzielle mRNA identifiziert, die an Ybx-1 bindet und während der Herzhypertrophie hochreguliert wird. Herzhypertrophie beinhaltet eine Hochregulierung der Proteinsynthese, und Elongationsfaktoren wie eEF2 regulieren die mRNA Translation im Rahmen von Zellwachstum. Die Identifizierung der Regulation von RBPs wie Ybx-1 und deren Ziel mRNAs wie z.B eEF2 kann helfen zu verstehen, wie posttranskriptionelle Faktoren zur Herzfunktionsstörung beitragen.

1. Introduction

The heart is a complex organ in the human body, and its vital function is to deliver oxygen and nutrients to various body organs and transport carbon dioxide to the lungs. Any dysfunction in the heart can result in a wide range of disorders, making heart diseases a significant health issue. Altered signal transduction pathways affect gene and protein expression in the heart and, therefore, are associated with cardiac dysfunction and disease progression. Gene and protein expression in the cell is controlled by transcription and translation. Many gene expression studies based on profiling mRNA abundance in human or experimental heart failure models have been performed, providing large datasets describing transcriptional regulation networks after pathological stress. However, the role of post-transcriptional gene control in cardiac biology and pathophysiology needs to be further explored.

1.1 Heart Diseases

Prolonged cardiac dysfunction can lead to heart failure, resulting in reduced longevity. Heart failure affects 1-2% of the adult population, and the risk of developing heart failure is approximately one in five for a person of 40 years of age [1]. The prevalence of cardiovascular diseases in adults over 20 years of age is 49.2% and was shown to increase with age [2,3]. Heart failure is a progressive disease, and the leading cause of mortality due to heart failure is cardiac death or multiple organ failure [4]. An understanding of the pathophysiology and natural history of heart failure underpins the therapeutic approaches used to achieve the goals of treatment, which are to relieve symptoms and prolong life [1]. Despite the impressive number of effective treatments available, heart failure has still a poor outcome, with nearly 25% to 50% mortality rate in 5 years after diagnosis [4]. Cardiac dysfunction currently claims more lives yearly than combined cancer and chronic lung disease. In 2019, ≈18.6 million (95% UI, 17.1–19.7 million) deaths were attributed to CVD globally [3].

1.1.1 Cardiac Hypertrophy

Cardiac hypertrophy is a coping mechanism of the heart to handle stress caused due to increased blood pressure or increased blood volume [5–8]. Cardiac hypertrophy involves increased cardiac muscle mass and can be classified as physiological or pathological cardiac hypertrophy. Cardiac hypertrophy with normal or increased contractile function coupled with standard architecture and organisation of cardiac structure is called physiological cardiac hypertrophic. In contrast, a hypertrophic heart with increased cardiomyocyte death and fibrotic remodelling and reduced systolic and diastolic function is called pathological cardiac hypertrophy [9]. Physiological hypertrophy is generally seen in response to the postnatal growth of the body, pregnancy or exercise, and it is considered adaptive and is not a risk factor for heart failure [10]. When the heart is stressed due to an additional load or a cardiac incidence, it undergoes a compensatory response by increasing cell size and normalising wall stress [11]. During this compensatory response, the heart increases in size and mass, followed by biochemical, molecular, structural and metabolic changes to preserve cardiac function [4]. Pathological cardiac hypertrophy often progresses toward heart failure, making it a vital focus for prevention or treatments. Analysing and unravelling the mechanisms with which the molecular, structural and metabolic changes happen in the heart during cardiac hypertrophy become vital to understanding and controlling pathological hypertrophy.

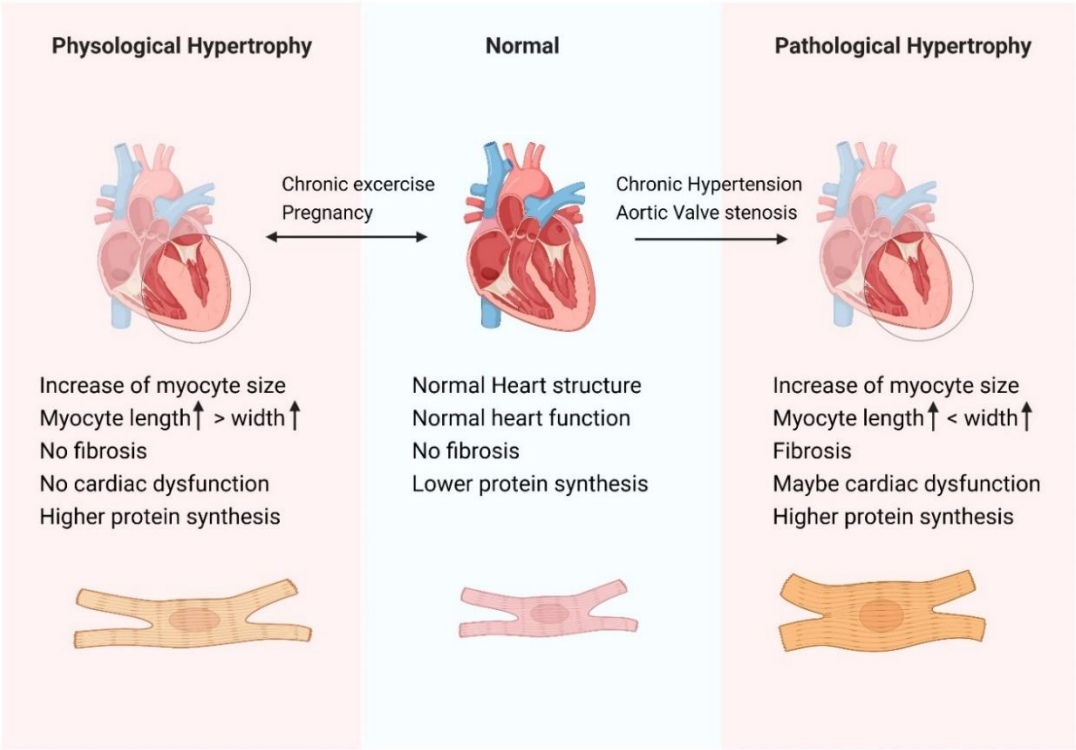

Figure 1.1: Cardiac hypertrophy. The difference between physiological and pathological cardiac hypertrophy with a focus on the cardiac myocyte.

The human heart contains various cells such as cardiomyocytes, vascular smooth muscle cells, fibroblasts, immune cells and endothelial cells. Cardiomyocytes account for 30% of the total cell number but 70-80% of total cell mass [12]. An intrinsic feature of cardiomyocyte cells is that they usually cannot divide; therefore, cardiac hypertrophy is associated with cardiomyocyte enlargement [4,13]. Enlargement of the cell is often associated with increased protein synthesis in the cell and activation of various signalling pathways. The signalling pathways involved in physiological cardiac hypertrophy differ from those in pathological cardiac hypertrophy [14]. There are multiple complex pathways involved in cardiac cell growth and remodelling, and they are often initiated at the cell membrane in response to stress, such Mitogen-Activated Protein Kinase (MAPK) signalling, calcineurin-NFAT (Nuclear Factor of Activated T cells) circuit, PI3(phosphatidylinositol 3-kinase)-AKT (Protein Kinase B) signalling and mTOR (mechanistic target of rapamycin) signalling [15]. The mTOR signalling pathway acts as a master regulator of energy production, biomolecule synthesis, and nutrient uptake that necessitate reprogramming all aspects of cellular metabolism [16].

1.1.2 mTOR Pathway – Regular of Cardiac Hypertrophy

mTOR is an evolutionarily conserved serine/threonine kinase that acts on different downstream targets to regulate cellular proliferation and growth rates [17]. The role of mTOR in various cell types and diseases has been studied in detail because of its unique position in various cell signalling pathways, including those that regulate protein synthesis, nutrition, cell size, cell growth and protein degradation [18]. Activation of mTOR signalling is thought to play a central role in cell proliferation, tumorigenesis and various kinds of cancer. mTOR forms a part of several complexes, such as mTOR complex 1 (mTORC1) and mTOR complex 2 (mTORC2), that have different compositions, downstream targets and sensitivity to mTOR inhibitor rapamycin [19]. The two mTOR complexes are formed based on their interaction with two mutually exclusive binding partners that influence substrate recruitment and subcellular localisation [20]. Raptor (regulatory associated protein of mTOR) forms the mTORC1 complex, contributing to metabolic regulation and cell growth. Rictor (Rapamycin-insensitive companion of mTOR) forms mTORC2. mTORC2 complex is insensitive to the effects of rapamycin and is involved in the regulation of cell survival and cytoskeletal remodelling [18,21]. Studies *in vivo* and *in vitro* have demonstrated that mechanical stimulation such as i*n vivo* pressure-overload of the heart and agonist stimulation of cardiomyocytes *in vitro* can activate the mTOR signalling pathway [18,19]. The involvement of mTORC1 in metabolism and cell growth makes it a protein of interest for hypertrophic growth in cardiomyocytes.

Upstream signals such as growth factors, stress and amino acids activate mTORC1 and result in downstream responses (Figure 1.2). mTORC1 serves as a vital bridge between growth signals and heightened biosynthetic activities. mTORC1 controls protein synthesis by phosphorylating various substrates downstream, and the two best-established effectors of mTORC1 on protein synthesis are the eukaryotic translation initiation factor 4E (eIF4E)-binding proteins and ribosomal protein S6 kinases (S6Ks) [19]. mTORC1

phosphorylates 4E binding protein (4E-BP), and 4E-BPs are considered translational repressors because they prevent cap-dependent translation in their non-phosphorylated state[22]. mTORC1 also phosphorylates 70S6K1, contributing to increased protein and nucleotide synthesis [23]. In addition, activated P70S6K phosphorylates multiple substrates, including the 40S ribosomal S6 protein and eukaryotic translation initiation factor 4B(eIF4B), which are both needed for active protein translation [24,25].

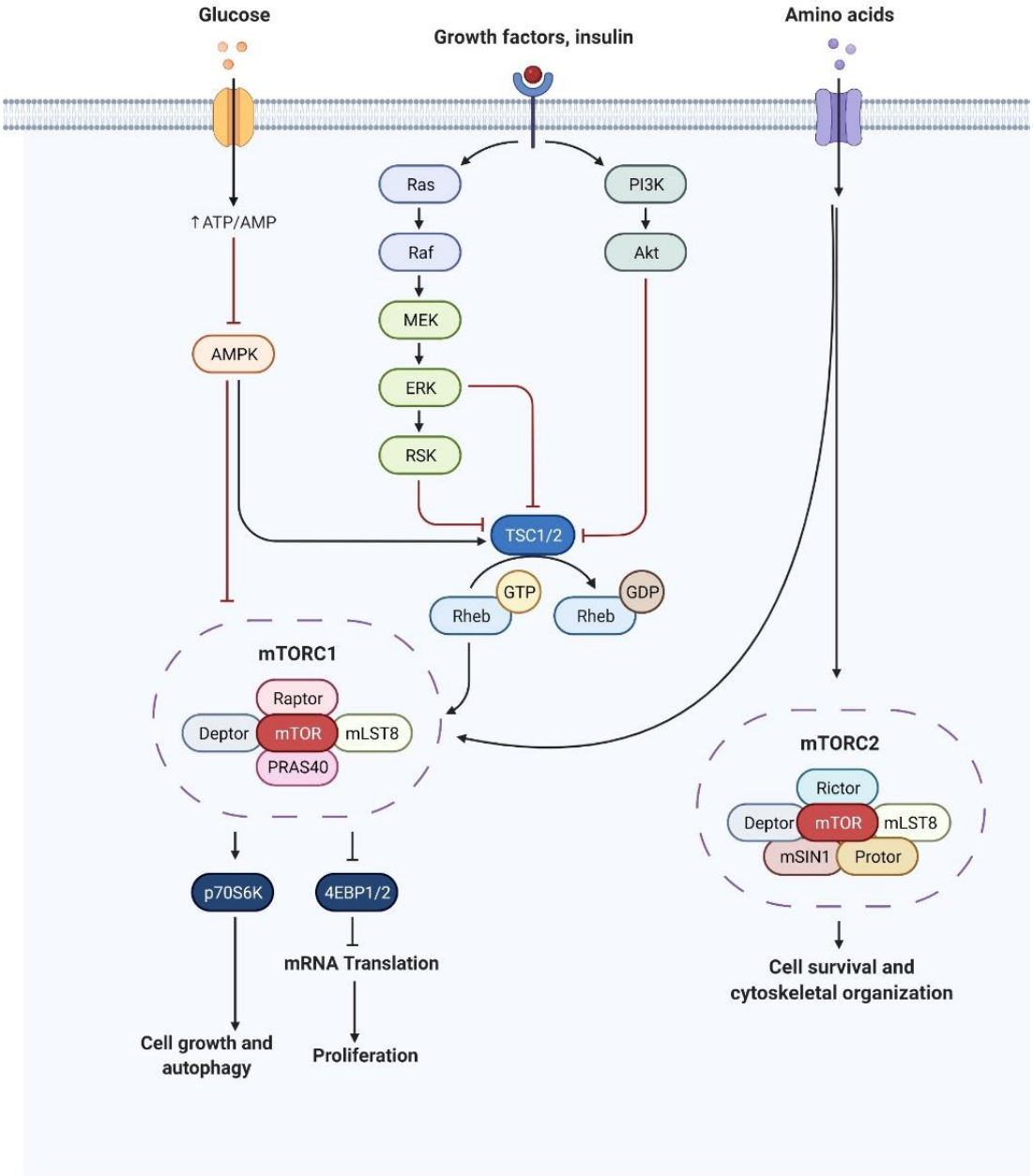

Figure 1.1: mTOR pathway in the cell. The signalling pathway mTOR in an eukaryotic cell and its effect on cell growth, protein translation and cell survival

Phosphorylation of 4E-BPs (1 and 2) by mTORC1 stimulates the release of 4E-BP from its inhibitory binding with eIF4E at the 5'-cap of mRNAs, allowing eIF4E to bind to eukaryotic translation initiation factors 4G (eIF4G) and 4A (eIF4A) [26,27]. Eukaryotic initiation factors play a vital role in protein translation. Protein translation in a cell occurs in three phases, i.e., initiation, elongation and termination. Translation initiation is considered the rate-limiting step of protein synthesis, and mTORC1 affects translation initiation via 4EBPs. The cap-dependent translation consists of various well-defined steps, as described in figure 1.2 and 1.3, and eIF4E-driven translation has been implicated in promoting cell growth and proliferation [28].

1.2 Post Transcriptional and Translational Mechanisms during Cardiac Hypertrophy

Adult cardiomyocytes do not have the ability to differentiate, and heart growth in adult cells is mainly due to increased cardiomyocyte size, also known as hypertrophic growth [29]. Pathological cardiac hypertrophy is characterised by a global increase in protein synthesis, fibrosis and reactivation of foetal genes at a molecular and cellular level. The central dogma of molecular biology involves transferring information from DNA to RNA to protein. While the process may seem simple and lateral, it is quite complex and involves various other processes influencing protein production. Post-transcriptional regulation is vital for determining when and where an mRNA will be translated and what would be its half-life, thus affecting a protein level in the end [30]. Cardiac hypertrophy involves rapid and massive changes in the abundance of different proteins in the cell. It is a stressful event for the cell, and translational regulation is recognised as a means for tissue to rapidly respond to environmental stress [31].

1.2.1 Translation Initiation

Translation of mRNA is the final step in gene expression, and regulation of this process allows the immediate and direct adaptation of protein levels, independent of nuclear pathways [32]. Research has shown that experimental pressure overload enhances protein synthesis through increased translation

rate and capacity [33,34]. There are three main parts of protein translation, i.e., initiation, elongation and termination. Translation initiation is the rate-limiting step of protein synthesis in a cell. Translation initiation factors (eIFs) recruit mRNA to the small ribosomal subunit (40S) during the initiation. The mechanism of this cap-dependent translation is shown in figure 1.3. The 40s subunit binds the eIF2-GTP-Met-tRNAi complex and eukaryotic initiation factors eIF1, eIF1A, and eIF3 to form the 43S preinitiation complex(PIC) [31]. PIC is recruited to the 7-methylguanosine cap of the RNA transcript by the eukaryotic initiation factor 4F complex (eIF4F). The eIF4F complex is made up of eIF4E (m7G cap-binding protein), eIF4A (RNA helicase) and eIF4G (a large scaffold protein that facilitates interactions between proteins and the small ribosomal subunit). eIF4E interacts with the cap structure at the 5'-end of the mRNA and binds with eIF4G and eIF4A, which then binds to the poly(A)-binding protein (PABP) to stabilise the complex. mRNA is scanned from 5' to 3' direction by the initiation complex until the initiation codon is reached where the large ribosomal subunit (60S) meets the complex resulting in the creation of active ribosomes [35]. The complexity of the translation initiation offers multiple points of regulation. Elongation factors (eEFs) help the ribosomes move along the coding region and synthesise the encoded polypeptide with multiple ribosomes covering them with RNA to form polysomes. At the termination codon, peptide chain-releasing factors (eRFs) are required to release the polypeptide from the ribosome [36].

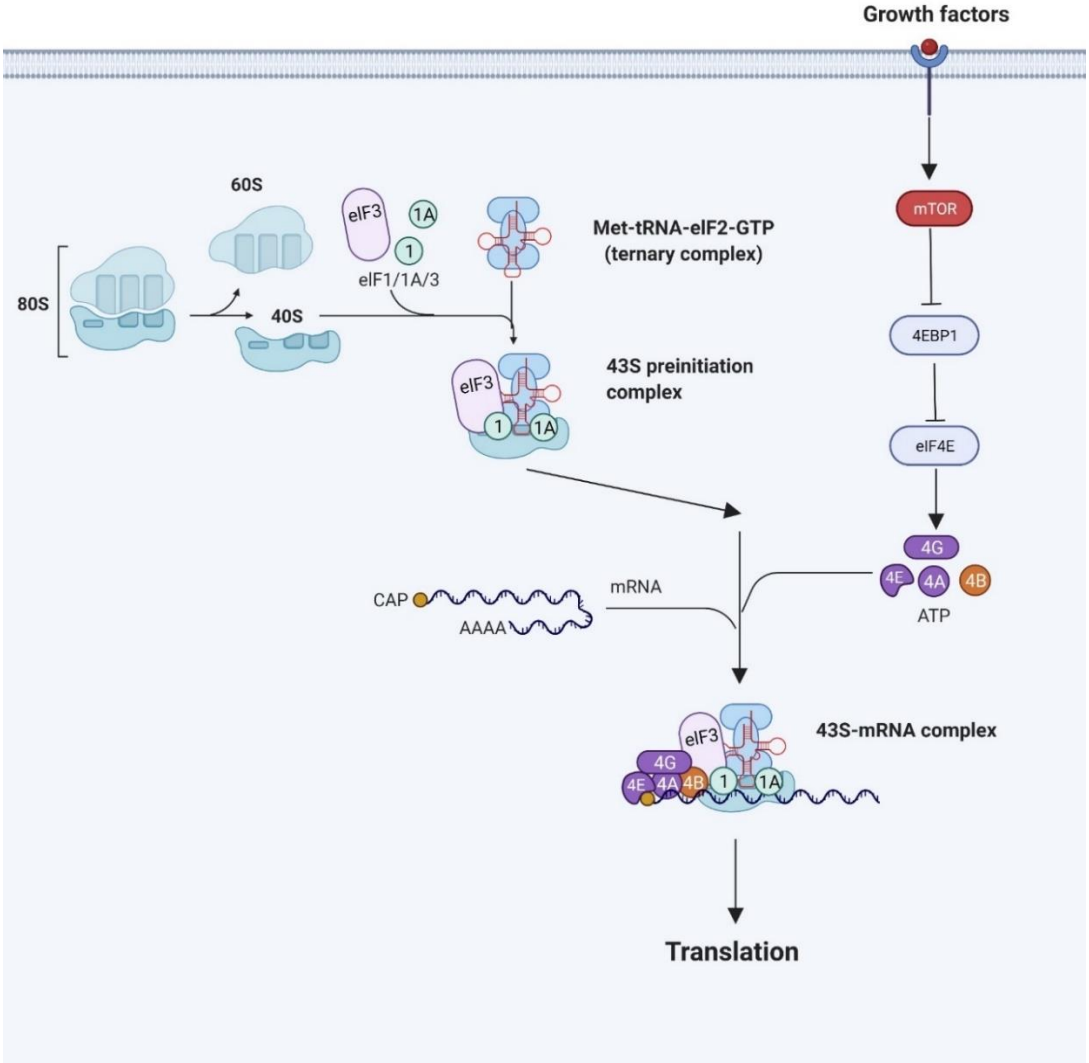

Figure 1.3: Cap Dependent Translation in Eukaryotes

1.2.2 Translation – Elongation

The initiation phase of protein synthesis is considered a key regulator in the process; however, the elongation phase consumes the most energy out of the three phases. Studies have shown that elongation is a tightly regulated process, and compared to the initiation, it has been relatively less explored [37]. Additional peptides are added to a growing peptide change during the elongation phase, and eukaryotic elongation factors 1A and 1B are involved in recruiting new aminoacyl-tRNA to the ribosome [38]. Elongation factor 2 (eEF2) is a GTPase that stimulates the peptidyl-tRNA's ribosomal translocation and helps start the new elongation cycle [37,39]. eEF2 can be inhibited by phosphorylation of eEF2 on the Thr-56 site by eEF2K (eukaryotic

elongation factor 2 kinase), also known as Ca^{2+} and calmodulin-dependent protein kinase [40]. eEF2 inhibition results in elongation inhibition and, thus, a decrease in global translation. eEF2K is involved in regulating eukaryotic translation elongation and is a crucial link between mTORC1 and translation [41]. When mTORC1 becomes activated, it blocks eEF2K by phosphorylating it with the help of S6 Kinase (S6K), resulting in enhanced elongation during growth. This suggests a strong interplay between initiation and elongation in eukaryotic cells [42]. Therefore, these processes directly affect protein synthesis in the cell, making the eEF2 pathway a significant regular of protein translation.

1.2.3 Control of translational mechanisms

There are two primary translational control mechanisms, i.e., global and selective. Global translational control acts on all mRNAs in a non-specific manner; for example, the accessibility of eIF4E is regulated by 4E-BP, which displaces eIF4G from eIF4E and thus inhibits translation initiation [32]. On the other hand, selective translation regulation targets a subset of mRNAs, for example, the regulation that can be carried out by RNA binding proteins that bind to specific sequences or structural elements in untranslated regions of protein-coding transcripts [36,43]. Following transcription in the nucleus, messenger RNA binding proteins bind to nascent mRNA precursors and mediate various RNA processing reactions, including 5′end-capping, splicing, editing, 3′-end cleavage, and polyadenylation.

After transcription in the nucleus, the mRNA (pre-mRNA) undergoes several steps before it becomes mature mRNA for translation. These nuclear processing steps include 5′end-capping to generate a 7-methylguanosine cap, splicing out of introns, and 3′-end cleavage/polyadenylation to create a mature, polyadenylated mRNA [43]. Many of these steps in the nucleus happen with the help of RNA binding proteins.

1.3 RNA Binding Proteins

Post-transcriptional gene regulation is regulated majorly with the help of RNA binding proteins (RBP). With the advancement of the latest technologies and next-generation sequencing methods, researchers have identified a wide range of RBPs, their protein cofactors and their RNA targets. Studies have identified a census of human RNA binding proteins, and the role of RBPs in various RNA processing has been uncovered [44]. RBPs recognise and bind with binding motifs to form ribonucleoprotein (RNP) complexes to regulate multiple RNA processes like RNA export, RNA stability, pre-mRNA splicing, mRNA decay, translocation and localization. RBPs are also involved in RNA degradation and decay through deadenylating and decapping enzymes [45]. Over 1500 RBPs have been identified in the human genome, and their roles in human diseases are still being uncovered [44,46,47]. The potential of RBPs being implicated in heart diseases is emphasized by the discovery that over 390 RBPs are explicitly expressed in the cardiomyocytes [48].

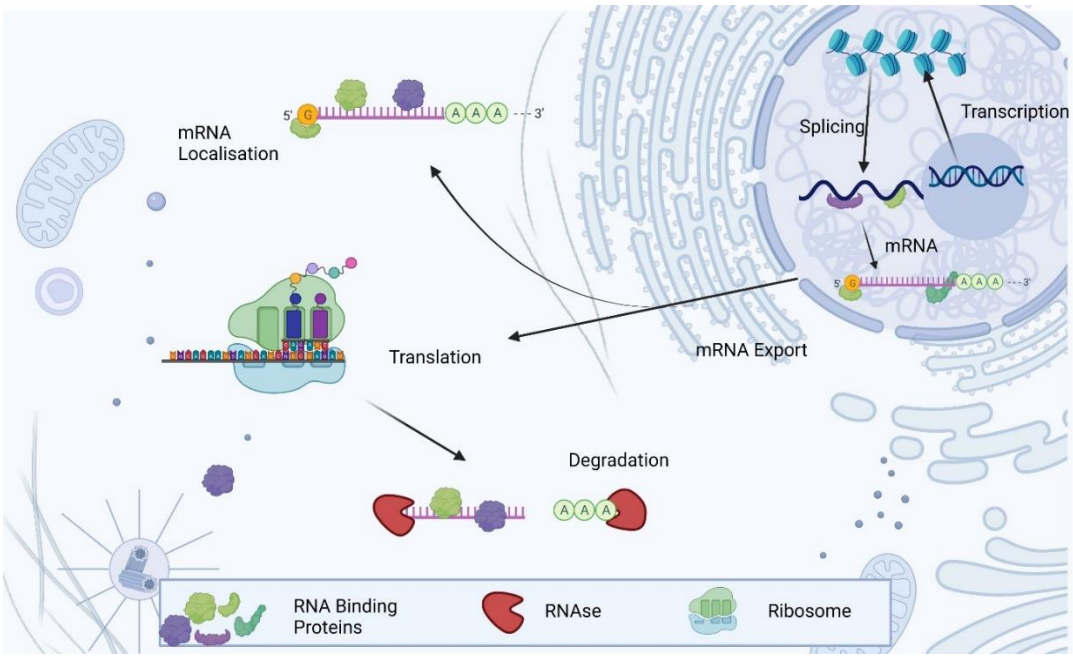

Figure1.4: RNA binding proteins. The various functional roles of RNA binding proteins in the cell

The heart is a complex tissue containing various kinds of cells. RBPs are involved in different stages of heart development, and mutation in RBPs has resulted in numerous cardiac diseases [49]. Studies have also shown that enrichment of translationally regulated genes by RBP targets contributes to

fibrotic remodelling of heart diseases [50,51]. An example of this can be seen when reduction in RNA-binding motif protein 20 (RBM20) leads to DCM in the heart [52]. Moreover, genome-wide studies into RBM20 targets have discovered that RBM20 inhibits splicing by binding introns proximal to alternatively spliced exons [53]. Moreover, changes in splicing patterns in cardiomyocytes have been shown to disturb the cardiomyocyte function and illustrate the role of RBPs as molecular switches in gene networks with robust cardiac networks. However, the exact mechanism and role of RBPs in cardiomyocytes have not been fully understood due to their complex interaction with other networks and pathways in the cell.

Table 1.1: RNA Binding proteins in cardiac diseases

Disease	**Cellular Phenotype**		**RBPs(pre-) mRNAs regulated**
	Normal	**Disease**	
Atherosclerotic plaque	Monocytes	Macrophage foam cell	• AREBPs • ROQUIN
	Resting EC	Inflammatory EC	• hnRNPL • SRSF1
In-stent(re)stenosis	Contractile SMC	Synthetic SMC	• QKI • HuR
Capillary Rarefaction	Perivascular stromal cell	Myofibroblast	• HuR • MBNL-1
Cardiac Hypertrophy	Cardiomyocyte	Hypertrophic cardiomyocyte	• RBM20 • CIRP • SRSF1

1.4 Ybx-1

RBPs are involved in multiple processes in the cell and control protein levels post-transcriptionally; however, Y-box binding protein 1 (Ybx-1) is one RBP that was initially discovered as a DNA binding protein and was only later that the role of Ybx-1 as RBP was found.Ybx-1 was named after its ability to bind to DNA containing the Y-box motif (5'-CTGATTGGCCAA-3'), and therefore Ybx-1 was thought to be a transcription factor [54–56]. Ybx-1 is a part of a large family of proteins containing an evolutionary conserved cold shock domain. In humans and mice, there are three Y-box proteins (Ybx-1, Ybx-2 and Ybx-3) [57]. The Y box proteins have 3 domains, i.e., the N-terminal, the cold shock domain and the C-terminal domain. The RNA, CSD single and double-stranded DNA binding properties of Y-box proteins are due to the cold shock domain [58]. The role of Ybx-1 in cancer has been widely studied due to its role in proliferation, inflammation and malignant cell transformation [54,59–61]. Ybx-1 is a vital protein associated with various translationally inactive mRNAs in different cells, and its functions in translational regulation in highly conserved [62].

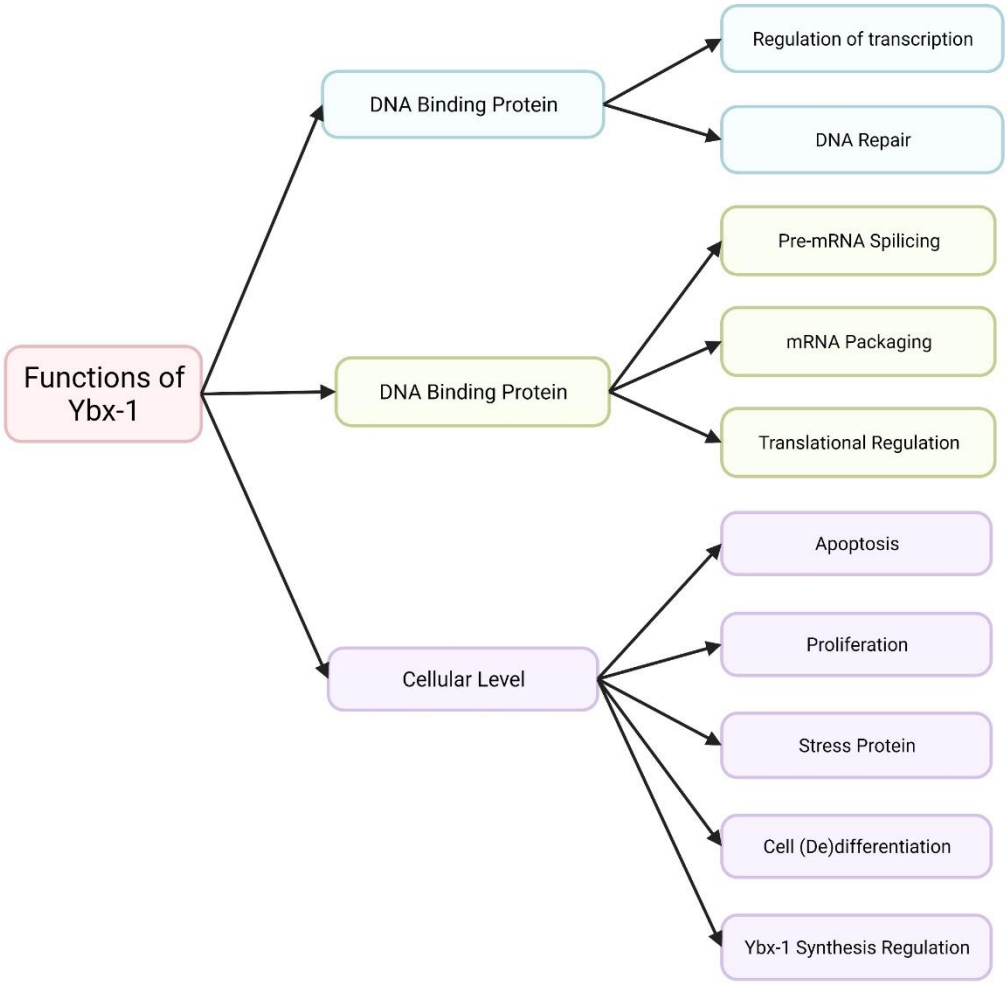

Figure 1.5: Ybx-1 and its various functions

1.4.1 Structure of Ybx-1

The Ybx-1 protein has three main parts, i.e., the alanine and proline-rich N terminal (the A/P domain), the cold shock domain (CSD) and the C- terminal domain (CTD) [63]. The c-terminal domain contains alternating clusters of positively and negatively charged amino acids. Analysing the RNA-binding specificity of Ybx-1 is vital to understanding its cellular and molecular functions [64]. The A/P and CTD domains have no regular secondary structures and are intrinsically disordered, and the disorder is common in many free RNA-binding proteins. RBPs such as Ybx-1 may acquire different fixed structures, depending on their binding to mRNAs or their various protein partners [54]. Ybx-1 is known to bind to both DNA and RNA in specific and no specific ways. *In vitro* studies with Ybx-1 have shown that it binds specifically

to a CA(U/C) C consensus sequence, and the *in vivo* Ybx-1 binding sites contain a UYAUC motif [64]. The CSD plays a central role in the sequence-specific binding of Ybx-1, where the essential regions of the CTD are involved in the nonspecific binding of Ybx-1 [65]. The CSD is the most evolutionary conserved nucleic acid-binding protein domain identified in bacteria and eukaryotes and is known to bind to single-stranded RNA oligomers [66]. The CSD is a simplified version of the oligosaccharide-binding fold lacking the alpha-helix, and the NMR structure of Ybx-1 CSD was the first eukaryotic CSD to prove the conservation of crucial structural features of CSD from bacteria to man [67]. Thus, YB-1 functions as a nucleic acid chaperone and, via its interaction with numerous proteins, exerts pleiotropic functions in cellular processes such as proliferation, differentiation, DNA damage repair, RNA splicing, and cellular stress responses [56].

1.4.2 Role of Ybx-1 in Transcription

Initially, Ybx-1 was regarded as a Y-box transcription factor; however, it is involved in changes in levels of genes with and without the Y-box sequence in their promoter. Experiments with Ybx-1 showed that an increase in Ybx-1 in the cell or its translocation from the cytoplasm was accompanied by decreasing or increasing amounts of mRNAs/proteins encoded by many genes responsible for cell division, differentiation, proliferation, and multiple drug resistance [54]. Furthermore, studies have shown the presence of single-stranded DNA in areas of transcriptionally active promoters, and Ybx-1 has shown a high-affinity binding to single-stranded DNA, thereby highlighting its role as a DNA binding protein [66]. In the nucleus, Ybx-1 can also act as a nucleic acid chaperone, i.e., it melts double helices, including those in the promoter region and case of G-rich motifs, Ybx-1 stabilizes double helices, thus promoting DNA binding to transcription factors with an affinity for DNA duplexes [68,69]. Ybx-1 is vital to cells, and knockout of Ybx-1 in mice results in embryonic lethality due to malformations, neural tube defects and haemorrhages [70].

Ybx-1 has been shown to translocate to the nucleus and is involved in the activation of genes involved in cell survival during stress [55,71]. Ybx-1 is also involved in splicing as it recognises specific sequences within pre-mRNAs and brings splicing factors to these sequences, thereby acting as a splicing regulator for some mRNAs [54,72].

1.4.3 RNA Binding Functions of Ybx-1/Translation

A protein named p50 was identified in the 1970s during the analysis of the protein composition of cytoplasmic mRNPs from different eukaryotic cells, and it was only twenty years later that it was identified as Ybx-1 [73]. So initially, in the cytoplasm, Ybx-1 was identified as a significant packaging protein of mRNPs, regulates mRNA translation, provides for its stability and is involved in localization [63]. The relationship between Ybx-1, mRNA, and the translational dependence of Ybx-1 is bell-shaped, as shown in figure 1.6 [54]. There is inhibition of translation initiation when Ybx-1 is knocked out [74]. In the absence of Ybx-1 in the cell, the RNA-binding initiation factors are not accumulated at the 5' UTR; instead, they are scattered over the entire mRNA, which reduces the translation initiation efficiency [75,76]. At a low Ybx-1/mRNA ratio, Ybx-1 is bound to mRNA as a monomer by two RNA binding domains which result in the unfolding of mRNPs, resulting in inaccessibility of mRNA for interaction with translation initiation factors [63]. Ybx-1 is also known to have RNA-chaperone activity, which could increase protein translation in the cell [68]. Studies have shown that when there are higher levels of Ybx-1 as compared to mRNA in the cell, Ybx-1 displaces eIF4F and PABP, resulting in inhibition of translation [77,78]

Another possible effect of high amounts of Ybx-1 in the system is the interaction of Ybx-1 with mRNA, mainly through the cold shock domain resulting in the formation of large multimeric Ybx-1 complexes. Such large complexes pack mRNA fragments and make them inaccessible for translation [63].

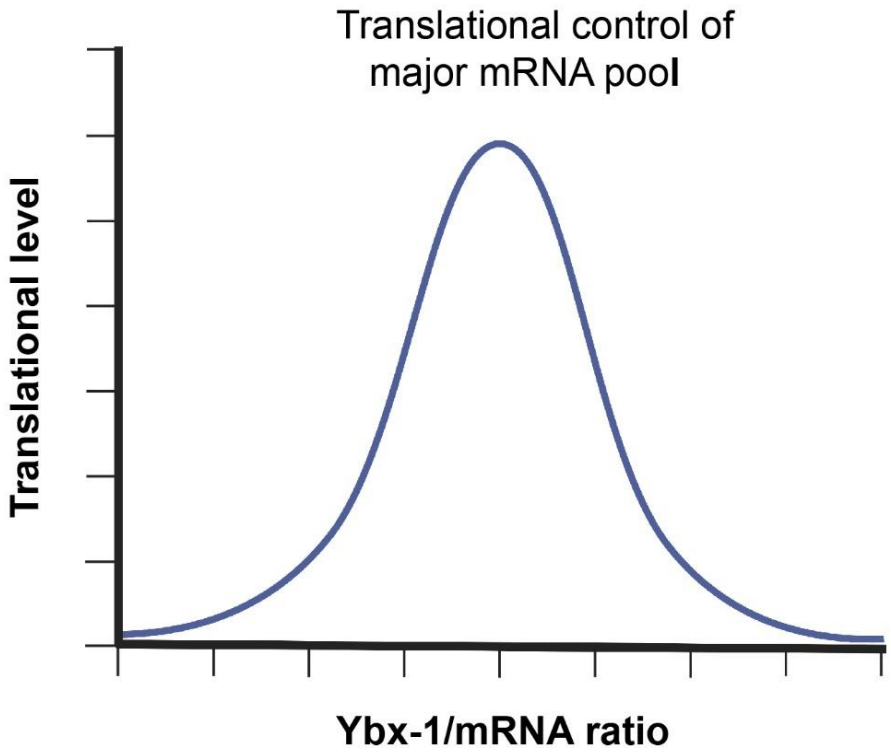

Figure 1.6: Translational control of Ybx-1 in a cell

Figure 1.6 shows a potential model for the effect of Ybx-1 on translation. In eukaryotes, the ordinary concentrations of Ybx-1 are optimal for the translation of many mRNAs by the cap-dependent mechanism. Some mRNAs that bind specifically with Ybx-1 work well at low Ybx-1 concentration, while some other mRNAs that are cap-dependent suppress translation at higher Ybx-1 levels. This leads to the possible conclusion that mRNAs that bind to Ybx-1 differ depending on the kind of cell, the extracellular stimuli and the concentration of Ybx-1 in the cell [54].

The role of Ybx-1 in translation repression has been discussed above, but there are also reports of Ybx-1 mediating mRNA stabilization in a cap-dependent manner [79]. It has been mentioned above that Ybx-1 binds to some mRNAs preferentially over others, and the majority have a well-structured 5' UTR and are GC rich. These mRNAs are translated in the presence of high concentrations of initiation factors, and in the absence of cell growth stimulation, Ybx-1 inhibits translation by displacing eIf4E from the cap-dependent region [54]. Multiple experiments with Ybx-1 have identified Ybx-1

bound transcripts as growth- and stress-related proteins, transcription factors and metabolic enzymes [79]. This data suggests that Ybx-1 mediated translation inhibition affects mRNAs that are cap-dependent. The proximity of Ybx-1 to the cap region on the mRNA also sheds light on its potential role as an RNA chaperone.

1.4.4 Ybx-1 as a Stress Protein

Ybx-1 is found both in the cytoplasm and the nucleus; therefore, the stress response of Ybx-1 depends on its location in the cell. When cells are irradiated with UV rays, Ybx-1 protein translocates to the nucleus and reduces the cell sensitivity to the stress by acting as a transcription factor or modulating transcription factors [54]. However, the method for translocation of Ybx-1 is still not precise and needs further exploration.

Ybx-1 is also known to be associated with stress granules and processing bodies. Stress granules are involved in the sorting or processing of untranslated messenger RNAs for degradation, reinitiating or packaging into ribonucleoprotein particles (mRNPs). Studies have shown that Ybx-1 is involved in forming stress granules along with a simultaneous increase in Ybx-1 secretion by the cells [80]. Stress granules formation via tRNA-derived stress-induced RNAs (tiRNAs) happens by the association of Ybx-1 CSD and tiRNA, where the CSD binds to the angiogenic-produced tiRNA, displacing eIF4F from capped mRNA, inhibiting translation and inducing stress granules formation [67]. In addition, the Ybx-1 CSD helps Ybx-1 bind to coding and non-coding transcripts, including tRNA [81].

1.5 Hypothesis and Aims

The PhD project can be divided into three main aims:

1. Identify post-transcriptional regulators that are involved in cardiac hypertrophy.

2. Analysis of the effect of manipulating Ybx-1 levels on cardiomyocyte growth, survival and contractility *in vitro* and on cardiac function *in vivo*

3. Identify the mRNAs bound to RNA-bound proteins to understand their molecular function in cardiomyocytes

Aim 1: To identify potential post-transcriptional regulators, we performed Ribosome Profiling (Ribo-Seq) on *in vivo* hypertrophy mouse models. We used phenylephrine (PE) *in vitro* to induce hypertrophy, and the mTORC1 inhibitor Torin1 was used to inhibit hypertrophy. Transverse aortic constriction (TAC) surgery was used on our mice models to mimic pathological hypertrophy. Our results showed Ybx-1 to be one such RNA binding protein that is up-regulated only in pathological hypertrophy.

Aim 2: *In vitro* manipulation of the Ybx-1 levels in neonatal rat ventricular myocytes (NRVMs) can easily be performed by knocking down or overexpressing Ybx-1. *In vivo*, Ybx-1 levels are increased by cardiomyocyte-specific Ybx-1 overexpression by AAV9 infection. After subjecting the mice to transaortic constriction surgeries (TAC), heart function is assessed by echocardiography, and heart growth is assessed by measurement of the heart weight. Ybx-1 knockdown in mice is planned to be done using the shRNA virus.

Aim 3: To identify mRNAs bound to Ybx-1, we plan to use immunoprecipitation and RIP-Seq analysis. We plan to use neonatal rat cardiomyocytes stimulated with phenylephrine for the IP. Bioinformatical assessment of RNA bound to the Ybx-1 samples will help identify the mRNAs. We also plan to use the complex capture 2C procedure to study the interacting partners of Ybx-1

2. Materials

2.1 Reagents

Table 2.1: List of reagents

Reagent	Supplier	Catalog-No.
(+-)-Norepinephrine (+)-bitartrate salt	Sigma-Aldrich/Merck	A0937
(R)- (-)-Phenylephrine hydrochloride	Sigma-Aldrich/Merck	P6126
4-(2-Hydroethyl)-1-piper-azineethanesulfonic acid (HEPES)	Thermo Fisher Scientific	15630056
Acetic acid	Honeywell	64-19-7
Agarose	Jena Bioscience	AC-001S
Ambion™ Nuclease Free Water	Thermo Fisher Scientific	AM9937
Ammonium hydroxide solution	Honeywell	5002
Bouin's solution	Sigma-Aldrich/Merck	HT10132
Bovine serum albumin (BSA)	Sigma-Aldrich/Merck	A6003
Cadmium chloride (CdCl2)	Honeywell	20899
Chloroform	Merck	32211
Claycomb media	Sigma-Aldrich/Merck	51800C
Cycloheximide (CHX)	Sigma-Aldrich/Merck	C1988
DC™ Protein Assay	Bio-Rad	5000111
D-Glucose	Sigma-Aldrich	50-99-7
Dialized serum	Gibco™ /Thermo Fisher Scientific	A3382001
Diethyl pyrocarbonate (DEPC)	BioChemica	A0881,0100
Dimethyl Sulfoxide (DMSO)	Sigma Aldrich	D8418-50ML
Dithiothreitol (DTT)	Sigma-Aldrich/Merck	43819
DMEM, glucose-free	Thermo Fisher Scientific	A1443001
DMEM/F-12, HEPES	Thermo Fisher Scientific	11330057
DNA loading dye	Thermo Fisher Scientific	R0611
dNTP mix	Promega	U1511
Dulbecco’s Modified Eagle Medium (DMEM)	Sigma-Aldrich/Merck	D5796-24X

Dynabeads ™ M-280 Sheep anti-Mouse IgG	Invitrogen (by Thermo Fisher Scientific)	11201D
Dynabeads ™ M-280 Sheep anti-Rabbit IgG	Invitrogen (by Thermo Fisher Scientific)	11203D
Dynabeads ™ Protein G	Invitrogen (by Thermo Fisher Scientific)	10003D
ECL: Western Lightning Plus	PerkinElmer	NEL104001EA
eEF2K Inhibitor: A-484954	Merck	324516-10MG
Ethanol	Sigma-Aldrich/Merck	51976
Ethidium bromide	Sigma-Aldrich/Merck	E1510
Ethylenediaminetetraacetic acid-(EDTA)-disodium salt	Honeywell	6381-92-6
FBS	Gibco™/Thermo Fisher Scientific	10270
Fetal bovine serum (FBS), superior	Biochrom/Merck	S 0615
Fibronectin from bovine plasma	Sigma-Aldrich/Merck	F1141
Formaldehyde (35 %, v/v)	Carl-Roth	50-00-0
Gelatine	Sigma-Aldrich/Merck	G9391-100G
Gene Ruler 1 kb DNA ladder	Thermo Fisher	SM0313
Gene Ruler 50 bp DNA ladder	Thermo Fisher	SM0373
Hank's buffer salt solution, Ca^{2+} and Mg^{2+} free (HBSS)	Thermo Fisher	14170088
Heparin-Natrium-25000- ratiopharm®	Ratiopharm	N68542.04
HiPerFect Transfection Reagent	Qiagen	301704
Hydrochloric acid (HCl, [37%])	Honeywell	30721
Immobilized γ-Aminophenyl-m7GTP (C10-spacer)	Jena Bioscience	AC-155S
Isoflurane Baxter	Baxter	HDG9623
Isopropanol	Sigma-Aldrich/Merck	I9516
iTaq™ Universal SYBR® Green Supermix	Bio-Rad	1725124
Kanamycin sulfate	Thermo Fisher Scientific	11815024
Laemmli buffer	Bio-Rad	161-0747

LB-Agar	Carl Roth	6671
LB-Medium	Carl Roth	X964.3
Magnesium chloride ($MgCl_2$)	Sigma-Aldrich	P9333-1KG
Magnesium sulfate ($MgSO_4$)	Sigma-Aldrich	M2643-500G
Mammalian Polysome Buffer	Epicentre/Illumina	5X ASBHMR1212
Methanol	VWR Chemicals	20847.307
MOPS	Bio-Rad	161-0788
Nonidet® P-40 Substitute (NP-40)	Sigma-Aldrich/Merck	74385-1L
Oligo(dt) beads	New England BioLabs	S1419S
Penicillin-Streptomycin	Gibco™ /Thermo Fisher Scientific	15140122
Penicillin-Streptomycin-Glutamine	Gibco™/Thermo Fisher Scientific	10378016
Percoll	GE Healthcare	17-0891-02
Phenol: Chloroform:IAA 25:24:1	Thermo Fisher Scientific	AM9730
Phospho-buffered Saline (PBS)	Sigma-Aldrich/Merck	D8537
PhosStop	Sigma-Aldrich/Merck	4906837001
Ponceau BS	Sigma-Aldrich/Merck	B6008.25G
Ponceau S	Sigma-Aldrich/Merck	P3504
Precision Plus Protein™ Dual Color	Bio-Rad	1610374
Protease Inhibitor Cocktail tablets	Sigma-Aldrich/Merck	11873580001
Qiazol	Qiagen	79306
RNaseZap™ RNase Decontamination Solution	Thermo Fisher Scientific	AM9780
Skim milk powder	Carl Roth	T145.2
Sodium Chloride (NaCl)	Carl Roth	9265.2
Sodium deoxycholate	AppliChem GmbH	A1531.0025
Sodium dodecyl sulfate (SDS)	Serva	20765.03
Sodium Hydroxide (NaOH)	Sigma-Aldrich/Merck	30620
Sucrose	Sigma-Aldrich/Merck	84100
SUPERase•In RNase Inhibitor	Thermo Fisher Scientific	AM2696

Transfer Buffer: Invitrogen Novex NuPAGE (20X)	Thermo Fisher Scientific	NP00061
Tris	Carl Roth	4855.1
Tris hydrochloride (Tris-HCl)	Carl Roth	9090.2
Triton X-100	Sigma-Aldrich/Merck	X100
Trypsin	Thermo Fisher Scientific	15090046
Trypsin-EDTA	Thermo Fisher Scientific	25200056
Tween® 20	Carl Roth	25300-120
VectashieldÒ antifade mounting media	Vector Laboratories	H-1000
Water, nuclease-free	Thermo Fisher Scientific	AM9937
Western Lightning Plus-Enhanced Chemiluminescence Substrate	PerkinElmer	NEL104001EA
Westernbright Chemiluminesznez substrat fur film und CCD kamera	Biozym	541005
Xylol	Carl Roth	9713.5
B-Mercaptopethanol	Sigma-Aldrich/Merck	M6250

2.2 Antibodies

Table 2.2 List of antibodies

Target	**Species**	**Dilution**	**Supplier**	**Catalog No.**
Western Blot				
GAPDH	Mouse	1:5000	Santa Cruz Biotechnology	sc-365062
4E-BP1	Rabbit	1:2000	Cell Signalling Technology	9452
Actin	Mouse	1:1000	Santa Cruz Biotechnology	sc-8432
Troponin T	Rabbit	1:2000	Abcam	ab209813
eEF2	Rabbit	1:5000	Cell Signalling Technology	2332S
eIF4A	Rabbit	1:1000	Cell Signalling Technology	2013
eIF4E	Rabbit	1:5000	Cell Signalling Technology	9742s

eIF4G	Rabbit	1:5000	Cell Signalling Technology	2498
phospho-eEF2	Rabbit	1:1000	Cell Signalling Technology	2331
Phospho-p70 S6 Kinase	Rabbit	1:500	Cell Signalling Technology	9205L
Phospho-S6 Ribosomal Protein	Rabbit	1:5000	Cell Signalling Technology	4858S
Puromycin	Mouse	1:1000	Merck-Millipore	MABE343
S6 Ribosomal Protein	Music	1:1000	Cell Signalling Technology	54D2
Ybx-1	Rabbit	1:2000	Cell Signalling Technology	D2A11
B-Tubulin	Rabbit	1:1000	Abcam	Ab6046
Peroxidase-AffiniPure Anti-Mouse	Donkey		Jackson Immuno Research	715035151
Peroxidase-AffiniPure Anti-Rabbit	Goat		Jackson Immuno Research	111035144

Immunohistochemistry

eEF2	Rabbit	1:200	Cell Signalling Technology	2332S
Sarcomeric Actin	Mouse	1:100	Santa Cruz Biotechnology	sc-8432
Ybx-1	Rabbit	1:200	Cell Signalling Technology	D2A11
Anti-rabbit IgG-FITC	Donkey	1:100	Jackson Immuno Research	711-095-152
Anti-rabbit IgG-Cy3	Donkey	1:100	Jackson Immuno Research	711-165-152
Anti-Mouse IgG-FITC	Donkey	1:100	Jackson Immuno Research	715-095-151
Anti-Mouse IgG-Cy3	Donkey	1:100	Jackson Immuno Research	715-165-151

Immunoprecipitation

eIF4G	Rabbit	Cell Signalling Technology	2498
Ybx-1	Rabbit	Cell Signalling Technology	D2A11

2.3 Enzymes

Table 2.3: List of enzymes

Enzyme	Supplier	Catalog No.
DNAse I	Sigma-Aldrich/Merck	10104159001
DNAse I	Thermo Fisher Scientific	EN0525
Gateway™ LR Clonase™ II Enzyme Mix	Thermo Fisher Scientific	11791100
Rnase Inhibitor, Murine	New England BioLabs	M0314L
Rnase A	Thermo Fisher Scientific	EN0531

2.4 Kits

Table 2.4: List of kits

Kit	Supplier	Catalog-No.
Agilent RNA 6000 Nano kit	Agilent	5067-1511
DC™ protein assay	Bio-Rad	5000112
Dual-Luciferase® Reporter Assay System	Promega	E1960
iScript™ cDNA Synthesis Kit	Bio-Rad	1708891
Pierce Silver Stain Kit	Thermo Fisher Scientific	24612
Plasmid Miniprep Kit: Gen Elute™	SigmaAldrich/Merck	PLN70
Plasmid Plus Maxi Kit	Qiagen	12965
Qubit™ RNA BR assay kit	Thermo Fisher Scientific	Q10210
Qubit™ RNA HS assay kit	Thermo Fisher Scientific	Q32855
Quick RNA™ Miniprep	Zymo Research	R1055
RNA Clean & Concentrator	Zymo Research,	R1013
SuperScript™ III First-Strand Synthesis Super Mix	Thermo Fisher Scientific	18080400

TruSeq Ribo Profile (Mammalian) Library Prep Kit	Illumina	ASLPA1212

2.5 Plasmids

Table 2.5: List of plasmids

Target	Name	Cloning Method	Supplier	Backbone	Species
Ybx-1	pAd_huYBX1	Gateway		pAd_CMV_nV5_Dest	Human
eEF2	pAD_EEF2	Gateway		pAd_CMV_nV5_Dest	Human
Ybx-1	shRNA_sh1_YB1		Amsbio	pAVCMV-CreOn-shRNA	Mouse
Ybx-1	shRNA_sh2_YB1		Amsbio	pAVCMV-CreOn-shRNA	Mouse
Ybx-1	shRNA_sh3_YB1		Amsbio	pAVCMV-CreOn-shRNA	Mouse
Ybx-1	scAAV-CMV-YB-1-shRNA-tandem		Biocat		
Scrambled	shRNA_Control		Amsbio	pAVCMV-CreOn-shRNA	Scrambled
Ybx-1	psiCheck2_HuYB	Restrictions-enzyme (NheI)		psiCHECK2	Human
	psiCheck2		Biocat	psiCHECK2	Human
Sec61B	pCDNA3_Sec61B-V5-Apex	Restrictions-enzyme (NotI & XhoI)		pCDNA3.1	Human
cMyc	psiCheck2_cMyc		Biocat	psiCHECK2	Human
eEF2	psiCheck2_MuEe	Restrictions-enzyme (NheI)		psiCHECK2	Mouse

2.6 Primers

Table 2.6:List of primers

Gene	Strand Direction	Primer
Mouse		
18S	Forward	CGAGCCGCCTGGATACC
	Reverse	CATGGCCTCAGTTCCGAAAA
Col1a1	Forward	GCTCCTCTTAGGGGCCACT
	Reverse	CCACGTCTCACCATGGGGG
HPRT	Forward	GGGGCTGTACTGCTTAACCAG
	Reverse	TCAGTCAACGGGGGACATAAA
Nppa	Forward	TTGTGGTGTGTCACGCAGCT
	Reverse	TGTTCACCACGCCACAGTG
Nppb	Forward	TTTGGGCTGTAACGCACTG
	Reverse	CACTTCAAAGGTGGTCCCAGA
Ybx-1	Forward	CAGGAGAGCAAGGTAGACCAGT
	Reverse	TGCTGACCTTGGGTCTCATCTC
α-Mhc	Forward	GCAAAGGAGGCAAGAAGAAAGG
	Reverse	TGAGGGTGGGTGGTCTTCAG
β-Mhc	Forward	AGGGCGACCTCAACGAGAT
	Reverse	CAGCAGACTCTGGAGGCTCTT
Rat		
18S	Forward	CGAGCCGCCTGGATACC
	Reverse	CATGGCCTCAGTTCCGAAAA
Acat	Forward	CATGGGCATCACAGCTGAAAAC
	Reverse	GCCCTTGATGACTGACTGGAT
Aldoa	Forward	CCCTCCTTACTCCTTTCGCC
	Reverse	CACAACACCACCCTTGGACT
Carns	Forward	TCGTCTTCTGATTGGTGAGGG
	Reverse	TCCAATGACACCTGCACACA
eEF2	Forward	AAGTCCACGTTGACCGACTC

	Reverse	TGTCAGTGAAGCGTGTCTCC
Foxp1	Forward	ACGTGCCCATTTCTTCAGCAG
	Reverse	TGACGCACTGCATTCTTCCA
HPRT	Forward	GGGGCTGTACTGCTTAACCAG
	Reverse	TCAGTCAACGGGGGACATAAA
Ide	Forward	CGGTTCATCTCACTGGGTCC
	Reverse	ATACAACACGGGAGTGCAGA
Nppa	Forward	TACAGTGCGGTGTCCAACACAGAT
	Reverse	TGGGCTCAATCCTGTCAATCCTA
Nppb	Forward	GAACAATCCATGATGCAGAAGC
	Reverse	GCTGTCTCTGAGCCATTTCCT
Ybx-1	Forward	AAGTGATGGAGGGTGCTGAC
	Reverse	TGCCATCCTCTCTAGGCTGT
Human		
eEF2	Forward	GACAGCGAGGACAAGGACAA
	Reverse	AGGCGTAGAACCGACCTTTG
HRPT	Forward	CCTGGCGTCGTGATTAGTGA
	Reverse	CGAGCAAGACGTCCAGTCCT
β-ACTIN	Forward	GTCACCAACTGGGACGACAT
	Reverse	ACATGATCTGGGTCATCTTCTCG

2.7 siRNA

Table 2.7:List of siRNAs

Name	Catalog No.	Manufacturer
Ybx1	4390771	Ambion
Scrambled	AM4637	Ambion

2.8 Consumables

Table 2.8:List of consumables

Item	Supplier	Catalog-No.

96 well lates, 0.2ml	Greiner	655180
Amersham Hybond-N+ membrane	GE Healthcare	RPN203B
Aspiration Pipettes, sterile 2 ml	Greiner bio-one	710183
Bis-Tris Protein Gel: 4-12% Criterion™ XT, 18 well	Bio-Rad	3450124
Bis-Tris Protein Gel: 4-12% Criterion™ XT, 26 well	Bio-Rad	3450113
Cell Scraper	Greiner bio-one	341070
CL-XPosure™ Film, 20 x 25 cm	Thermo Fisher	34091
Conical Centrifuge Tubes 15 ml	Greiner bio-one	188271
Conical Centrifuge Tubes 50 ml	Greiner bio-one	352070
Cover slips (24 x 60 mm)	Marienfeld GmbH	101242
E-Plate Cardio 48	ACEA Biosciences	300600940
Filter Tip1 10 µl	Neptune Scientific	976-010
Filter Tip1 1000 µl	Neptune Scientific	976-1250
Filter Tip1 20 µl	Neptune Scientific	976-020
Filter Tip1 200 µl	Neptune Scientific	976-200
Gel loading Tips: Gel-Saver	Kisker, Steinfurt	GSII054R
MicroAmp™ Fast Optical 96 well, 0.1 ml	Applied Biosystems™	4346907
Nunclon R Cell Culture, 15 cm	Merck	Z755923-150EA
Nunc™ Cell Culture/Petri Dishes	Thermo Scientific	168381
Nunc™ Lab-Tek™ Chamber Slide	Thermo Fisher	177429PK
Parafilm	Sigma-Aldrich/Merck	P7793
PCR plate, 96-well	Steinbrenner	SL-PP96-3L
Pipette Tips 10 µl	StarLab	S1111-3700
Pipette Tips 1000 µl	StarLab	S1111-6810-C
Pipette Tips 20 µl	StarLab	S1111-070
Pipette Tips 200 µl	StarLab	S1111-0706
Primer bundle for qPCR	Steinbrenner Laborsystemes	SL-PP-PB3LB

PVDF-Membrane Immobilion-P	Millipore/Merck	IPVH00010
Scalpel	Feather	02.001.30.010
Serological Pipette, 10 ml	Sarstedt	356551
Serological Pipette, 25 ml	Sarstedt	861.685.001
Serological Pipette, 5 ml	Sarstedt	356543
Tissue culture flasks T25	Sarstedt	833.910.002
Tissue culture flasks T75	Sarstedt	833.911
Well Plates 12-wells	Greiner bio-one	665180
Well Plates 6-wells	Greiner bio-one	657160
White opaque 96 well Microplate, Optiplate	PerkinElmer	6005290
Zymo-Spin IC Columns	Zymo research	C1004-250
Zymo-Spin IIICG columns	Zymo research	C1006-250-G

2.9 Lab Equipment

Table 2.9:List of lab equipment

Devices	**Supplier**
Agilent 2100 Bioanalyzer	Agilent
Axio Observer Z1 fluorescence microscope	Zeiss
Cell Incubator: Hera Cell® 240i	Thermo Fisher Scientific
Criterion Cell System	Bio-Rad
Enspire Multimode Plate Reader	Perkin Elmer
Gel Imaging System, UV Transilluminator	Biostep
Gradient Station	BioComp
Harvard volume-cycled rodent ventilator	Harvard Apparatus
Horizontal electrophoresis system	Bio-Rad
Hypoxia cell incubator	Binder
Laminar Flow Hood: Herasafe 2030i	Thermo Fisher Scientific
Laser Scanning Microscope: Cell Observer SD	Zeiss
Multi Shaker, Plattform 409 x 297 mm	NeoLab
Magnetic stirrer: neo-Mag® 1500 UpM	NeoLab

Mini Trans-Blot Cell	Bio-Rad
Nanodrop™ spectrometer	Thermo Fisher Scientific
Optima XPN-80 Ultracentrifuge	Beckman Coulter
Power Pac™ HC	Bio-Rad
Real-time PCR system: Viia 7	Thermo Fisher Scientific
Stratalinker 2400 UV Crosslinker	Stratagene/Agilent
Thermal Cycler: C1000 Touch™	Bio-Rad
Tissue homogenizer, Bullet Blender	Next Advance
Vevo 2100 Imaging System VisualSonics	VisualSonics
xCelligence® RTCA Cardio ECR	ACEA Biosciences

2.10 Softwares

Table 2.10:List of software used

Software	Publisher
Biorender	Biorender
Blast	NCBI
Galaxy	Galaxy Project Freiburg
Image J (Fiji)	SciJava
Microsoft Office	Microsoft
Primer-Blast	NCBI
Prism	GraphPad
R Studio	RStudio, Inc
RTCA Cardio Software	ACEA Biosciences

2.11 Buffers and Solutions

2.11.1 Buffers for general use

10x PBS pH 7.4
1,37 M NaCl
26,8 mM KCl
14,7 mM KH_2PO_4
63,3 mM Na_2HPO_4 x 2 H_2O

TE-Buffer
100 mM TrisHCl pH 8
1 mM EDTA pH 8

10x TBS
0.2 M Tris
1.5 M NaCl Adjusted to pH 7.6

1x TBST
1x TBS
0.05 % (v/v) Tween

2.11.2 Buffers and solutions for biological methods

Agarose Gel electrophoresis

50x TAE buffer
50 mM EDTA disodium salt
2 M Tris
1 M Acetic Acid

Agarose gel 1.5 %
in 1x TAE buffer
1.5 % (m/v) Agarose
0.2 µg/ml ethidium bromide

Cloning
LB-Agar plates In distilled water
0.35 % (m/v) LB-Agar

LB-Media
In distilled water
0.2 5 (m/v) LB

Sucrose gradient (Polysome Profiling)

2x Sucrose buffer
In DEPC water
20 mM Tris-HCl pH 8.0
200 mM KCl
10 mM $MgCl_2$
0.2 mg/ml CHX
1x Protease inhibitor cocktail

10 % Sucrose solution
In DEPC water
10 % (m/g) sucrose
50 % (v/v) 2x Sucrose buffer

50 % Sucrose solution
In DEPC water
50 % (m/g) sucrose

50 % (v/v) 2x Sucrose buffer

2.11.3 Buffers and solutions for biochemical methods

RIPA Buffer

150 mM NaCl

1 % (v/v) NP-40

0.5 % (v/v) Na-Deoxycholate

0.1 % (v/v) SDS

50 mM Tris-HCl pH 8

Ponceau S staining solution

0.1% (w/v) Ponceau S

5%(v/v) acetic acid

Mammalian lysis buffer

In Mammalian Polysome Buffer

20 mM Tris pH 7.4

10 mM MgCl

200 mM KCl

2 mM DTT

100 µg/ml CHX

1% Triton X-100

1U DNAse/µl

2.11.3.1 Immunoprecipitation

RIP Immunoprecipitation

Polysomal Lysis Buffer (1 ml)

5X Mammalian Polysomal Buffer (200ul)

DEPC Water 1X (669 ul)

10% Triton (100 ul)

100 mM DTT (10 ul)

DNase 1 (10 ul)

Murine RNAse Inhibitor (11ul)

High Salt Wash Buffer(1 ml)

5X Mammalian Polysomal Buffer (200ul)

IM KCL in DEPC Water to make the buffer 1X (680 ul)

10% Triton (100 ul)

100 mM DTT (10 ul)

DNase 1 (10 ul)

Wash Buffer

5X Mammalian Polysomal Buffer (200ul)

DEPC Water 1X (680 ul)

10% Triton (100 ul)

100 mM DTT (10 ul)

DNase 1 (10 ul)

CAP Immunoprecipitation

NP 40 Buffer

50 mM Tris-HCL ph=7.4

100 mM NaCl

1mM EDTA pH = 8.0

0.5% NP-40

1x Phosphoinhibitor

1x Protease Inhibitor

2.11.4 Cell culture and media solutions

NRVM preparation and culture

Digestion solution

In HBSS

0.25 % (v/v) Trypsin

300 U/ ml DNase II

0.4 M HEPES

0.0016 M NaOH

2% (v/v) Penicillin-Streptomycin

Stop solution 4 % (v/v) FBS

300 U/ ml DNase II

2% (v/v) Penicillin-Streptomycin

ADS, 10 x

1.16 M NaCl 180 mM HEPES

8.45 mM $NaHPO_4$

55.5 mM Glucose

53.7 mM KCl

8.31 mM MgSO4 Adjusted to pH 7.35±0.5

red ADS buffer 116 mM NaCl

18 mM HEPES

845 µM $NaHPO_4$

5.55 mM Glucose

5.37 mM KCl 831 µM MgSO4

0.002 % Phenol Red Adjusted to pH 7.35±0.5

Stock Percoll

Top Percoll (density= 1.059 g/ml)

90 % (v/v) Percoll
10 % ADS, 10x

83 % (v/v) Stock Percoll
17 % ADS, 1x

Bottom Percoll (density 1.082 g/ml)
65 % (v/v) Stock Percoll
35 % (v/v) red ADS

Percoll gradient
4ml Top Percoll (pipetted first)
3 ml Bottom Percoll (pipetted underneath)

NRVM Culture media
In DMEM/F-12 medium
10 % (v/v) FBS
1 % Penicillin-Streptomycin-Glutamine

NRVM Treatment media
In DMEM/F-12 medium
0.5 % (v/v) FBS
1 % Penicillin-Streptomycin-Glutamine

Media for cell lines

Supplemented Claycomb media
In Claycomb media
10 % FBS
1 % Penicillin-Streptomycin-Glutamine
100 µM Norepinephrine

HEK Culture media
DMEM with 4500 mg/L glucose
10 % (v/v) FBS, SUPERIOR
1 % Penicillin-Streptomycin-Glutamine

3. Methods

3.1 Isolation and Cultivation of primary cardiomyocytes

3.1.1 Isolation and cultivation of neonatal rat ventricular myocytes

One-to-three-day-old neonatal rat ventricles were used to isolate neonatal rat ventricular myocytes (NRVMs). Rats were sacrificed to excise the hearts. The

hearts were then flushed with HBSS to eliminate any remaining blood. The atria and residual vessels were separated, and the ventricles were cut into 1-3 mm sections. The tissue fragments were then transferred to a 10 ml digestion solution and incubated for 10 min at 37 °C. The stop solution was used to stop the digestion, and then the tissue dispersion was pipetted up and down several (± 20) times to detach cells from the tissue pieces. The supernatant was accumulated and kept on ice after the undigested tissue parts settled, while the digestion step was repeated (in total 6-10 times) on the left-over tissue pieces. The supernatants were pooled and pelleted by centrifugation for 15 min at 500 rcf at 4 °C and resuspended in NRVM culture media. Cells were counted and then pelleted again by centrifugation at 250 rcf for 5 min. ADS buffer was then used to resuspend the cells in the appropriate volume to obtain 20-30 Mio cells/ml. Two ml of the suspension per gradient were carefully transferred to the top of the Percoll gradient. The Percoll gradient was centrifuged at room temperature for 30 minutes at 1500 rcf with no deceleration brake. Cardiomyocytes from the layer between the bottom red ADS layer and the middle transparent ADS layer were harvested, washed twice with 50 ml of ADS, resuspended in NRVM Culture medium, and then counted.

Then, about 80.000 cardiomyocytes/cm2 were seeded in NRVM Culture medium into 6-well plates for protein extractions, 12-well plates for RNA isolations or apoptosis experiments, and chamber slides for cell size measurements and other microscopical examination. Before plating, culture plates were coated with 5 g/ml fibronectin, and chamber slides were coated with 10 g/ml in serum-free DMEM/F-12 medium for 1 hour. After 20 hours of culture, NRVM Treatment media were added. Unless otherwise specified, cells were grown at 37 °C and 5% CO2. NRVMs were treated according to the following descriptions for investigation of hypertrophy for further analysis (Figure 3.1).

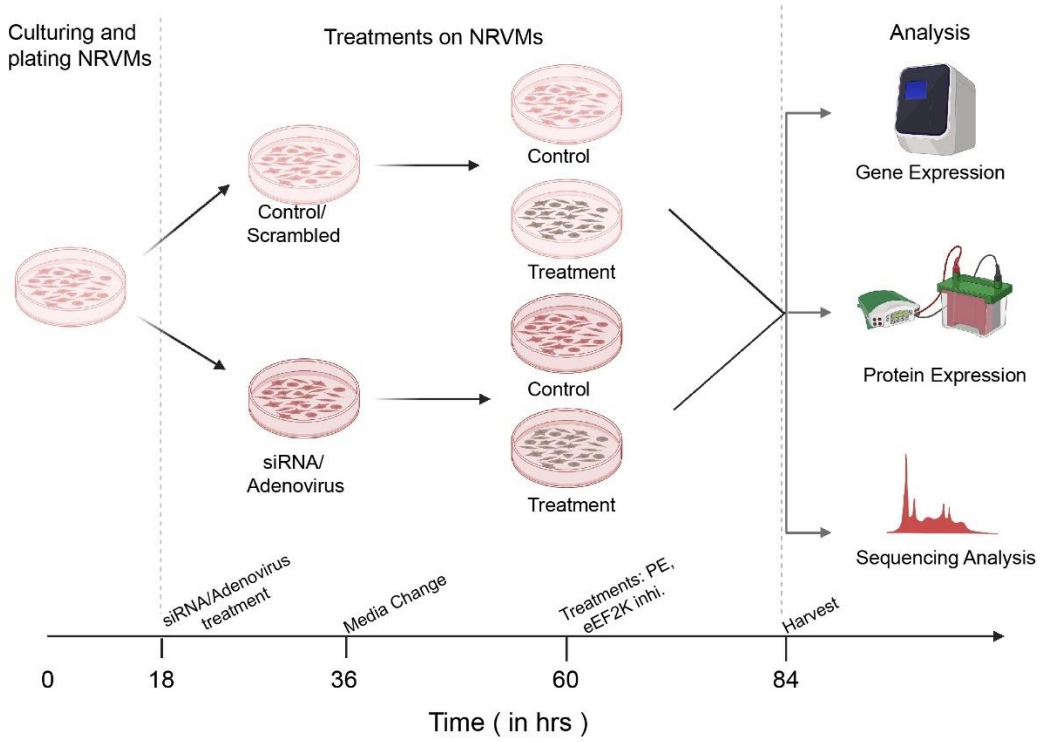

Figure 3. 1 Culturing and treating NRVMs

3.1.1.1 Knocking down Ybx-1 with siRNA

Eighteen to twenty hours after plating, the NRVMs were transfected with either 25 nM scrambled small interfering (si) RNA or siRNA targeting rat Ybx-1. The transfection was done in 0.5% FCS (starving) media using HiPerfect reagent according to the manufacturer's protocol. The media was changed on the cells after overnight incubation of approximately 18 hours.

3.1.1.2 Transduction of NRVMs with adenovirus for Ybx-1 overexpression or eEF2 overexpression

Eighteen to twenty hours after plating, NRVMs were transduced with the recombinant adenovirus encoding for Ybx-1 (Ybx-1 OE) or adenovirus encoding for eEF2 (eEF2 OE) or with an equivalent amount of empty control-virus (AdCo) in NRVM culture media. Media was replaced by fresh media 24 hrs later

3.1.1.3 Treatment with phenylephrine

24 hours after adenoviral transduction or siRNA transfection, NRVMs were treated with 100 uM phenylephrine in an NRVM treatment medium for 24 hours to evaluate the induction of hypertrophy. Hypertrophy was evaluated by either cell size measurement using NRVMs planted on chamber slides (3.4) or semi-quantitative examination of hypertrophy marker gene expression by RT-qPCR of extracted RNA (3.3.2 and 3.3.4).

3.1.1.4 Treatment with Torin 1

The NRVMs were treated with 200 nM Torin 1 for 3 or 24 hours before harvesting the cells. The media was not changed while treating the cells with Torin 1. First, Torin1 was dissolved in DMSO to get a stock concentration of 200 uM. Then, cells were harvested for RNA pr protein for further analysis.

3.1.1.5 Treatment with eEF2k inhibitor – A-484954

24 hours after adenoviral transduction or siRNA transfection, NRVMs were treated with 100 uM A-484954 (eEF2K inhibitor) in an NRVM treatment medium for 24 hours. Cells were harvested for protein or RNA analysis. Cell size was measured by immunofluorescence.

3.1.2 Cultivation of HEK 293T cells

The human embryonic kidney (HEK) 293 T cell line was cultured in DMEM media supplemented with 10% FCS and 1% PSG. Cells were passaged 1:10 when reaching 100 % confluence. Incubation conditions of HEK293T cells were identical to those of NRVMs with 37°C and 5 % CO_2. HEK 293T cells were frozen in 95% FBS containing 5% DMSO using a Nalgene slow freezer Mr. Frosty container at -80 ° C and then the vials were transferred to the liquid nitrogen tank. To plate frozen HEK 293T cells, a vial was removed from liquid nitrogen and thawed in a 37°C water bath. Then the cell dispersion was transferred to a sterile 15 mL conical tube, where 9 ml supplemented DMEM

media was added dropwise. Next, cells were pelleted by centrifuging at 300 rcf for 5 min, resuspended in 12 ml supplemented DMEM media and transferred to a T25 tissue culture flask.

3.2 Animal procedures

3.2.1 Neonatal rats

1 to 3-day-old Sprague-Dawley rats were used to cultivate the ventricular myocytes of newborn rats. All animal research was approved by the institution's animal care and use committee.

3.2.2 Experimental animals

Male C57BL/6N mice raised at the university hospital's Heidelberg animal facility were used in experiments. Ribo-seq investigations were conducted on homozygous Ribo-tag animals with cardiac myocytes. These were crossed with Jackson Laboratory-purchased Ribo-tag mice to produce the MHC-Cre mouse strain. Random assignment of animals to experimental groups. Under a 12-hour light/dark cycle, the animals had unrestricted access to water and normal food. All animal research was approved by the institution's animal care and use committee. Eight-week-old mice were injected with the AAV9 vector encoding the recombinant Ybx-1 gene. Two weeks later, other operations were conducted.

3.2.3 Transverse aortic constriction surgery on mice

Mice aged 10 weeks were anaesthetized in an induction chamber with 2% isoflurane and 0.5 - 1.0 l/min of 100% O2. Endotracheal intubation is conducted after placing the mouse in a supine posture on a heating pad to maintain its body temperature. The intubation was then linked to a Harvard volume-cycled rodent ventilator cycling at 125-150 breaths per minute and sustaining anaesthesia with 1.5-2 percent isoflurane and 0.5-1.0 l/min of 100 percent O2. The thorax was partly opened to the second rib using a microscope. With forceps, the thymus and fatty tissue detached from the aortic arch with care.

After identifying the transverse aorta, a silk suture was put between the innominate and left carotid arteries and wrapped around the aorta with a little blunt needle positioned in parallel. After the second knot, the needle was discarded. A similar surgery was conducted on Sham-mice; only the aorta was not ligated. A 6.0 suture was used to seal the rib cage and the skin. The mouse was injected intra-peritoneally with buprenorphine (0.1 mg/kg) for postoperative analgesia and subcutaneously with sterile saline to prevent dehydration. Following the operations, mice were killed 2 weeks later. The heart was removed together with the atria and the right ventricle. The weights of intact hearts and left ventricles were normalized to the total body weight or tibial length. The hearts were shock-frozen in liquid nitrogen and kept at -80 degrees Celsius until processing.

3.2.3.1 Cardiac function assessed by echocardiography

Echocardiography (ECG) was utilized to evaluate heart function following AAV9-Ybx-1 injections and TAC surgery. Mice were administered 1-2 percent isoflurane, and supine images were captured using a Vevo 2100 Imaging System. A heating pad maintained a core temperature of 37 °C, and heart rates were kept constant between experimental groups (400–500 bpm). Utilizing the conventional 2D quantification software, LV volumes, fractional shortening (FS), and ejection fraction (EF) were measured.

3.2.3.2 Preparation of murine heart lysates

Using a tissue homogenizer, murine left ventricular tissue was lysed in 700 ul Mammalian lysis buffer. The tissue was further homogenized by passing the lysate 10 times through a 23-gauge syringe cannula. The supernatant from homogenates centrifuged at 4°C and 18,000 rcf for 10 minutes was utilized immediately in subsequent procedures. The samples were held on ice for 10 minutes to ensure complete lysis and then centrifuged at 20,000 rcf to precipitate cell debris.

3.3 Molecular biological methods

3.3.1 Isolation of total RNA from cell culture for sequencing

For RIP-Seq, Ribosome Profiling or Ribo-Seq RNA was isolated using Qiazol. For gene expression analysis by RT-qPCR, RNA from NRVMs was isolated by the Quick RNA MinipPrep. After washing with PBS, cells were harvested by adding the appropriate amount of RNA Lysis Buffer supplied by the kit to the cell monolayer and subsequent scraping. RNA was isolated according to the manufacturer's manual and eluted in nuclease-free water. RNA concentrations were determined using a NanoDrop™ spectrometer.

3.3.2 Isolation of total RNA from cell culture for sequencing

For RIP-seq, Ribosome Profiling or Ribo-seq RNA was isolated using Qiazol. The cardiomyocytes were extracted with 100 ul of Mammalian lysis buffer per 10 cm2 of cell culture dish surface. In Mammalian lysis buffer, 1 ml of Qiazol was added per 1000 ul of cells, and cell lysis was ensured by vortexing. The homogenized samples were incubated at room temperature for 5 minutes. The homogenate was then blended for 15 seconds with 0.2 ml chloroform per 1 ml of Qiazol. The mixture was incubated at room temperature for 5 minutes before being centrifuged at 12000 rcf at 4 degrees Celsius for 5 minutes. Transferring the top aqueous phase to a second tube, the same volume of 95 per cent ethanol was added and carefully mixed. Following the DNase I treatment, the mixture was transported to the Zymo-SpinTM IC Column of the RNA clean & concentrator™ -5 according to the manufacturer's instructions. RNA concentrations were quantified using the Qubit™ RNA BR test kit following the manufacturer's instructions and the estimated quantity of extracted RNA.

3.3.3 Isolation of total RNA from *in vivo* samples

For RNA isolation from 100 µl of the left ventricular extracts, obtained by the procedure explained in 3.3.3.2, 1 ml Qiazol was added. Then, RNA isolation with Qiazol followed by clean-up using the RNA clean & concentrator ™ -5 was performed as explained in 3.4.2. Finally, the concentration of RNA was

measured using the Qubit™ RNA BR assay kit according to the manufacturer's instructions.

3.3.4 Reverse Transcription of RNA and Real-Time quantitative PCR

Following the manufacturer's instructions, cDNA was generated from 200 ng of extracted RNA using the iScript reverse transcription supermix for RT-qPCR. 1:10 dilution of cDNA using nuclease-free water. As a template, 3 µl of 1:10 dilutions of cDNA were used with 5 µl of iTaq universal SYBR-Green supermix and 3 mM of forward and reverse primer. Ct values of the target genes were adjusted to the geometric mean of two or three reference genes (see 2.6). The fold change was determined using the ΔΔCt technique.

3.3.5 RNA Isolation after RNA Immunoprecipitation (RIP-Seq)

RNA was isolated from the elutes after immunoprecipitation using 1 ml Qiazol per sample. RNA was isolated in a similar way to 3.3.3. RNA was eluted in 20ul of DNase-free water. Quality control was performed on the RNA using the Bioanalyzer.

3.3.6 Electrophoretic assay for RNA by Bioanalyzer

According to the manufacturer's manual, the Agilent RNA 6000 Nano kit was used to assess the quality of isolated RNA for sequencing procedures. In brief, 9 µl, freshly prepared gel-dye mix was loaded on the chip, followed by 5 µl RNA 6000 marker into all wells. The RNA samples and the ladder were denatured at 70 °C for 2 min before loading them. Next, 1 µl RNA or ladder was added to the wells of the chip. After vortexing, the chip was placed into Agilent 2100 Bioanalyzer, and the chip run was started.

3.3.7 Polysome Profiling

RNA extracted from NRVM cells was separated using a 10-50 percent sucrose gradient (220,000 rcf, 2.5 h, 4°C) in an ultracentrifuge (220,000 rcf).

Using the BioComp Gradient Station with 2 mm steps at 0.3 nm/sec, absorbance at 256 nm was measured in parallel while continuous fractionation was done.

Based on the polysome profile signal pattern, cytosolic, 40S subunit, 60S subunit, monosome, and polysome I-IV fractions were combined. RNA was isolated from the pooled fractions using the Quick RNATM Miniprep Kit from Zymo Research. As an internal control, samples were spiked with Renilla Luciferase (Rluc) mRNA that had been *in vitro* transcribed, followed by cDNA synthesis and qPCR (3.4.4). Ct values were standardized to Rluc, and the sample input fold change was computed.

3.3.8 Ribosomal sequencing (Ribo-seq)

NRVMs cultured on 15 cm dishes were harvested and lysed in 600 µl Mammalian lysis buffer containing 0.1 mg/ml cycloheximide on ice. Lysates were incubated on ice for 10 min, pipetted repeatedly using a 25-gauge needle and then centrifuged at 20000 rcf for 10 min at 4 °C. Cleared supernatants were transferred to new tubes. Absorbance at 260 nm per ml of a 1: 10 dilution of the samples was recorded on a Nanodrop spectrometer to calculate the required amount of RNase for the generation of ribosome footprints (RFPs). 7.5 units of TruSeq Ribo Profile Nuclease for each A260 were added to the lysates and incubated for 45 min with gentle mixing at room temperature. The RNA digestion is stopped by adding 15 µl SUPERase•In RNase Inhibitor. RFPs were then purified by ultracentrifugation with 220,000 rcf for 2.5 h at 4°C, subsequent fractionation using the BioComp Gradient Station and RNA isolation with Qiazol as explained in 3.4.1.

3.3.9 Production of the eEF2 adenovirus

3.3.9.1 Cloning of the eEF2 into pAd vector by gateway cloning

eEF2 was amplified from HEK cells using primers designed against human eEF2. 600 ng RNA of MCF7-cells was used with eEF2 primers with the touch-down PCR setting with 18 cycles. The samples were stored o/n at 4 °C. 20 µl 6x Loading Dye was added to both samples. Next, they were loaded onto a

1 % Agarose gel for insert purification. According to Thermo Fisher Scientific, the mutant construct was cloned into a pAD vector using the LR Recombination Reaction. The LR reaction mix was transformed into NEB alpha-5 *E. Coli* following the High- Efficiency Transformation Protocol from New England Biolabs. Again, an agarose gel was run for band separation, and the bands at a size of 3 kb were excised. After gel extraction, BP-reaction was performed. The samples were kept on ice for 30 s, heated up to 42 °C for 45 s and then cooled down on the ice for 2 min. Next, 100 µl SOC medium was added, and the samples were incubated at 37 °C for 1 h at 300 rpm. Finally, cells were plated on an LB-kanamycin (LB-Kan) agar plate and incubated o/n at 37 °C. Positive colonies were picked and transferred into 5 ml LB-Kan and incubated for 23 h with 100 rpm. A 200 µl aliquot of each miniprep was taken, 200 µl 50 % glycerol was added, and the aliquots were then stored at - 80 °C. Miniprep samples were centrifuged at 3900 rpm for 15 min, the supernatant was removed, and the pellet was stored at -20 °C. The plasmid DNA was purified using the peqGOLD Plasmid Miniprep Kit I (VWR Peqlab, Catalog 13-6943-xx) according to the manufacturer's instructions. The samples were sent in for sequencing to Eurofins afterwards.

3.3.9.2 eEF2 adenovirus production

HEK293A cells were grown up to 70-80 % confluency. Transfection was performed by mixing the eEF2 plasmid with 450 µL HEK Culture media and 140 µL 1x PEI with 340 µL media. Both solutions were incubated separately for 10 minutes at room temperature, then mixed and incubated for another 15 minutes. The media of the HEK293A cells was exchanged, and the PEI mixture was added to the cells drop-wise. Cells were split the next day. After 5 days, cells and media were collected in a Falcon tube and spun down at 3000 rcf for 10 minutes. The collected supernatant was used for the transfection of new HEK293A cells. After 3 days of incubation, the viral supernatant was collected and stored. This supernatant was used as a viral transduction agent for the following experiments.

3.4 Biochemical Methods

3.4.1 Western Blot

3.4.1.1 Measurement of protein concentrations

After washing with PBS, cardiomyocytes were harvested in 80 µl Ripa buffer with 1x Protease Inhibitor, 1x PhosSTOP per 6-well and lysates were immediately placed on ice. To extract DNA from samples, they were centrifuged for 15 minutes at 15,000 rcf at 4 °C, and the supernatant was transferred to a fresh tube. Lysates produced from the homogenization of murine and human left ventricular tissues (3.2.3.2) required no additional treatment for protein determination and Western Blot examination. Protein concentrations were measured using the DCTM protein assay according to the manufacturer-recommended methodology.

3.4.1.2 Western Blot analysis

Lysate containing 20 µg of total protein was loaded on a 4-12% Bis-Tris gel in 1x Laemmli buffer. Electrophoresis was performed using the Criterion Cell system in 1x MOPS buffer at 100 V for 10 min and then increased to 200 V. The gel was blotted on a methanol-activated 0.45 µm PVDF membrane using the Mini Trans-Blot Cell system for 35 min at 100 V. The membranes were stained with Ponceau S staining solution to control an equal amount of loaded protein and successful blotting. Proteins of interest were detected by incubating the membrane in a primary antibody solution overnight at 4 °C and a horseradish peroxidase-conjugated secondary antibody incubating for 1 hour at room temperature. All antibodies were diluted according to Table 3.2 in 5 % skimmed milked in TBST. Detection was performed using Western Lightning Plus-Enhanced Chemiluminescence (ECL) Substrate. The developed films were scanned in greyscale, and scans were used for semi-quantitative densitometry using ImageJ. In brief, densitometry values for one protein of interest were normalized to densitometry values of the reference proteins Actin, GAPDH or β- Tubulin. Additionally, fold changes were calculated by normalizing each value to the controls.

Table 3.1: List of antibodies used for western blot

Target Protein	Species	Dilution	kDa
Ybx-1	Rabbit	1:2000	49-50
eEF2	Rabbit	1:5000	90
eIF4G	Rabbit	1:5000	220
eIF4E	Rabbit	1:5000	25
eIF4A	Rabbit	1:2000	48
GAPDH	Mouse	1:5000	37
B-Tubulin	Rabbit	1:10000	50
Actin	Mouse	1:5000	42
Donkey-anti-mouse HRP	Donkey	1:5000	-
Goat-anti-rabbit HRP	Goat	1:5000	-

3.4.2 Silver Staining

Protein lysates were loaded onto a Nu-PAGE Bis-Tris Gel and run at 100 V until the ladder reached the bottom of the well. Then the gel was treated with reagents from the Pierce staining kit according to the protocol in the kit. The gel is washed twice with ultrapure ddH_2O for 5 minutes each. It is then fixed for 15 minutes in 30% ethanol:10% acetic acid solution twice. The gel is then washed for 5 minutes twice in 10% ethanol and twice again for 5 minutes each in ultrapure water. Sensitizer working solution is prepared according to the instructions in the kit, and the gel is sensitized for 1 minute in the solution. Following, it is quickly washed with water for 1 minute twice. Meanwhile, the stain working solution is prepared, and the gel is stained with the stain working solution for 30 minutes after the washing. The developer working solution is prepared using the 0.5 mL enhancer with 25 mL developer. The gel is washed with ultrapure water for 20 seconds twice and developed for 2 or 3 minutes until bands appear. The reaction is stopped with 5% acetic acid for 10 minutes, and the gel is scanned.

3.4.3 Immunocytochemistry and quantitative analysis of cell surface area

Following treatment procedures described above, NRVMs plated on chamber slides with 100000 cells/well density were fixed with 4% PFA for 15 minutes at room temperature. After washing three times with PBS, samples were permeabilized with 500 µl 0.3 % Triton in PBS for 10 min and blocked with 10 % horse serum in PBS for 1 h, following antibody incubation diluted in 10 % horse serum overnight at 4°C. The following day samples were washed five times with PBS and then incubated with secondary antibody diluted in 10 % horse serum for 1 hour at room temperature. After washing five times with PBS, cells were incubated with DAPI diluted in PBS for 5 minutes, washed again and then mounted using Vectashield→ antifade mounting media and coverslips. Immunofluorescent microscope pictures were taken to assess protein localization, overexpression, and cell size analysis. Cell size measurements were conducted by analysis of 20 x magnification images of the respective sample by ImageJ. A minimum of 50 cells per picture was used to evaluate cell size.

Table 3. 2: : List of antibodies used for immunofluorescence

Target Protein	Species	Dilution
Ybx-1	Rabbit	1:200
Actin	Mouse	1:100
Flag	Rabbit	1:100
Anti-rabbit FITC	donkey	1:200
Anti-mouse Cy3	Goat	1:200

3.5 RNA Methods

3.5.1 RNA Immunoprecipitation-sequencing

3.5.1.1 Harvesting cells and protein determination

4 x 10^6 NRVMs were plated in 10-cm dishes and cultivated in DMEM-F12 media containing 10% FCS. 2 dishes were harvested and pooled for one sample. The dishes were washed with ice-cold PBS twice. 400 ul of Mammalian Polysomal buffer was used to lyse the cells in one dish, and then

the cell was scraped, and two plates were pooled together. The samples were needled with a 25G size needle approximately 10 times. The samples were centrifuged at a maximum speed of 4ºC for 15 mins. The supernatant was transferred to fresh Eppendorf, and protein determination was done according to 3.3.1.1.

3.5.1.2 RNA-immunoprecipitation and -sequencing

NRVM lysates were incubated with Ybx-1 antibody overnight at 4˚C, then for 1 hr at RT with prewashed sheep anti-rabbit IgG Dynabeads (ThermoFisher), .10 ug of antibody was used per sample. Coprecipitate was washed once with ice-cold wash buffer, three times with ice-cold high salt buffer, and finally with wash buffer. Samples were divided for use for protein or RNA. Protein elution was performed by heating the samples with lamelli buffer at 95ºC for 5 mins. RNA was eluted by using Trizol and the following extraction using chloroform. According to the manufacturer's instruction, library generation was done using the Lexogen Quant-Seq kit. Libraries were then multiplexed and sequenced on a NextSeq550.

3.5.2 Capture Complex

NRVMs were plated in 15 cm dishes with 10% FCS 1% PSG DMEM-F12, then UV cross-linked with 2000 mA of energy with a crosslinker. Cells were harvested in 1 ml of Mammalian Polysomal buffer, and protein determination was performed using Bio-Rad Assay. The Zymo RNA isolation kit was used to perform RNA isolation. 2 mg of protein sample(X) was mixed with 4X lysis buffer and 5X 100% ethanol. RNA isolation was performed according to the Bio-Rad kit and was eluted in 50 ul nuclease-free water. The samples were run on a speed vacuum until the RNA concentration in the samples was approximately 1ug/ul. RNA concentration was measured on Nanodrop, and then samples were treated with or without RNase (1 U/100 ug) for 30 mins at 50ºC. Samples were then used for silver staining or western blot.

3.5.3 Isolation of tRNAs

To purify small (17-200 nt) and large (>200 nt) RNA into separate fractions, the RNA Clean and Concentrator kit – 5 was used. First, cells were harvested in 1 ml Qiazol lysis reagent. If not processed immediately, samples were stored at -80°C. After mixing, samples were incubated for 5 min at room temperature. Then, 200 µl of chloroform was added to each millilitre of Qiazol, mixed vigorously and incubated for an additional 3 min at room temperature. To separate the different phases, samples were centrifuged at 12,000 x g for 15 min at 4°C, and the upper aqueous phase was transferred into a new tube. The aqueous phase containing the RNA was mixed with an equal volume of ethanol (600 µl/700 µl), transferred to a Zymo-Spin Column and centrifuged at 13,000 x g for 30 sec at room temperature. RNAs larger than 200 nt bind to the column, while RNAs of a size of 17-200 nt are primarily in the flow-through. Therefore, to also capture the small RNAs, the flow-through was mixed with an equal volume of ethanol and transferred to a new Zymo-Spin Column. Once RNAs were bound to the columns, purification followed the manufacturer's protocol. Finally, RNA was eluted in 15-30 µl for small RNAs and 35-50 µl for large RNAs, respectively, and the concentration was measured using a UV/Vis microvolume spectrophotometer.

3.6 Dual Luciferase Assay

3.6.1 Transfection

By cloning Ybx-1, eEF2, and cMyc 5'UTRs into piCheck2 plasmid upstream of Renilla luciferase, 5'TOP-reporter constructs were generated. First, HEK 293 cells were transfected for 24 hours with 5'UTR-reporters using ViaFect reagent per the manufacturer's instructions (Promega). HEK cells were then treated with 250 nM Torin1 for six hours.

3.6.2 Dual Luciferase Assay

HEK 293T cells were lysed 24–48 h after transfection/infection in passive lysis buffer (Promega) from the Dual luciferase kit. The samples were produced following the methodology provided by the manufacturer (Promega) and

quantified using a LUMIstar OPTIMA plate reader. The signals of Luciferase were adjusted to the total protein quantity obtained using the RC-DC kit (BioRad)

3.7 Statistical analysis

Cell culture experiments were done at least two to four times with n = at least two biological replicates (cultures) for each treatment. *In vivo* experiments were performed on at least three biological replicates (mice) for each treatment. The investigators were blinded to the sample group allocation and examination of the experimental outcome during the experiment. Unless otherwise noted, values displayed are mean ± SEM, and statistical treatments are one-way ANOVA followed by Bonferroni's post hoc comparisons. The data was presented and analyzed using the GraphPad Prism (R studio for analysis of the sequencing datasets).

4 Results

With the advancements in modern technology, studies have discovered RNA binding proteins as crucial players in post-transcriptional regulation. Multiple diseases in the human body have dysregulation of proteins and unravelling the functions of RNA binding proteins will help control them. This study aimed to identify the RNA binding proteins involved in cardiac hypertrophy and analyse their function and binding partners to understand the disease. The objectives can be divided into the following parts:

Aim 1: was to Identify post-transcriptional regulators involved in cardiac hypertrophy.

Aim 2: was to analyse the effect of manipulating Ybx-1 levels on cardiomyocyte growth, survival and contractility *in vitro* and *in vivo*

Aim 3: was to Identify the mRNAs bound to RNA-bound proteins to understand their molecular function in cardiomyocytes

4.1 Identifying RBPs involved in Cardiac Hypertrophy

Cardiac hypertrophy involves dysregulation of protein levels and identifying the RNA binding proteins (RBPs) involved in this process was the first step of the study. A list of mRNA targets regulated after transverse aortic constriction (TAC) surgery on Ribo-tagged mice [81] as generated using *in vivo* Ribosomal sequencing data [82]. Figure 4.1 (A) shows a diagrammatic flow of ribosomal sequencing and RNA sequencing. Previously published *in vivo* Ribo-Seq and RIP-Seq data set was used to identify mRNA targets of the mTOR pathway translationally upregulated after transverse aortic constriction (TAC) surgery. 680 RNA binding proteins in NRVM were identified using RNA interactome capture, and this data was overlapped with mTOR responsive mRNA *in vitro* to create a list of 86 targets that are common between the two [82,83]. These 86 targets were then overlapped with mRNAs upregulated after 2 Days of TAC surgery to finally get 9 translationally upregulated RNA binding proteins during cardiac hypertrophy (Figure 4.1 B). Ybx-1 was one of the hits; interestingly, it was upregulated only on a protein level (Figure 4.1 C). Ybx-1 is significantly upregulated 2 days after TAC, whereas no changes are

observed in the RNA seq data at different time points (Figure 4.1 D). Ybx-1 decreased on a protein level in NRVM treated with mTOR inhibitor Torin 1 for 3 hours, showing the effect of the mTOR pathway on the Ybx-1 expression level. No change was observed in mRNA levels of Ybx-1 in NRVM (Figure 4.1 E). Immunoblots were done with left ventricle lysates 2 days after TAC surgery on mice showed that Ybx-1 is upregulated on a protein level and remains unchanged on an mRNA level, therefore highlighting the translational control of the mTOR pathway on Ybx-1(Figure 4.1 F).

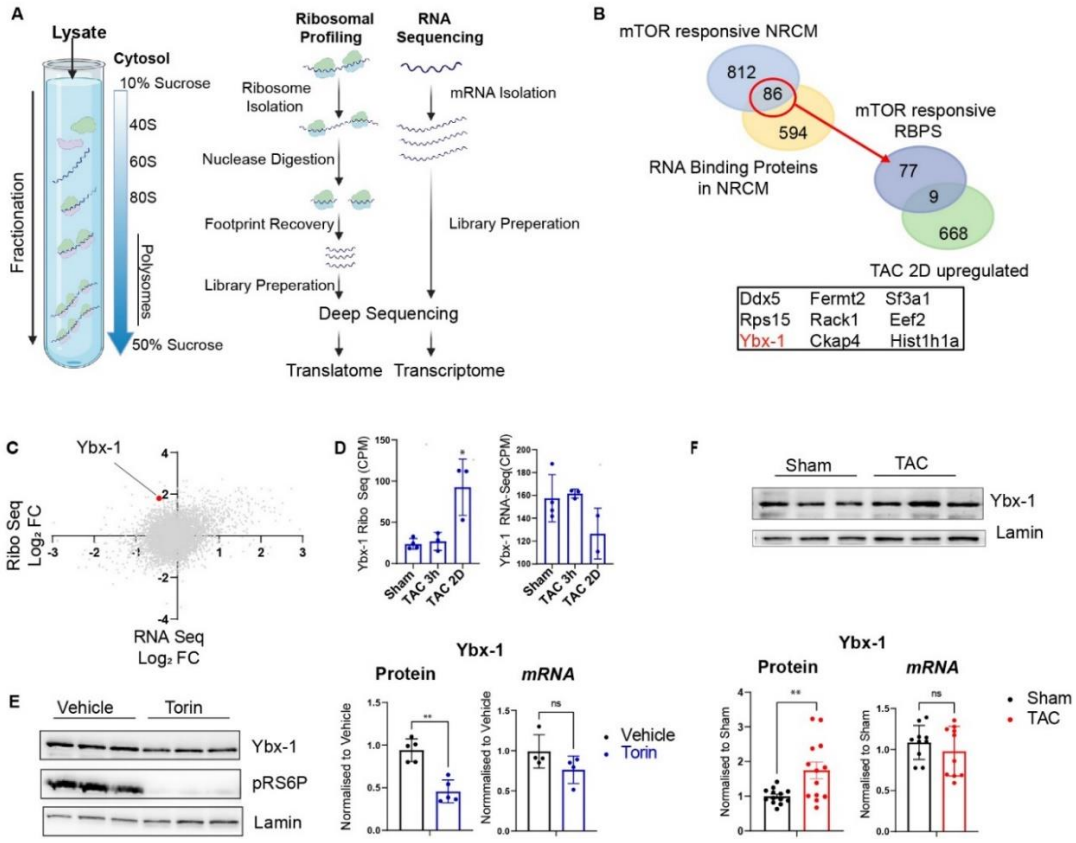

Figure 4.1: Identifying RNA Binding proteins involved in cardiac hypertrophy. (A) Schematic representation of translational profiling of mTOR-dependent mRNAs *in vitro* and *in vivo*. (B)Venn Diagram showing the overlap of PE and Torin responsive mRNAs from NRVM and RNA binding proteins in NRVM Data from **Doroudgar et al.** and **Riechert et al**. was used to identify the 9 RNA binding proteins [82,83](C) Scatter plot of Ribo Seq and RNA seq data 2 days after TAC. Ybx-1 is highlighted in red. (D)Graphs depicting quantitative values of Ybx-1 in Ribo-Seq and RNA-Seq Data from sham, TAC 3 hours and TAC 2 days mice. (E)Representative immunoblot and quantification of Ybx-1 expression levels in NRVM after inhibition by Torin for 3 hours. Lamin is used as a housekeeper. n= 5 independent experiments (F) Representative immunoblot and quantification of Ybx-1 protein levels after 2 Days TAC and Sham *in vivo*. Error bars indicate means± SEM n =13 * p≤ 0.05, ** p≤ 0.01, t-test

4.2 Ybx-1 is an RNA Binding Protein

Ybx-1 was initially identified as a DNA binding protein; however, its role as an RBP has been explored in-depth [54,65,66]. Complex capture was performed on NRVM to confirm that Ybx-1 binds to RNA in cardiomyocytes 15. NRVM were harvested after UV cross-linking them, followed by RNA isolation using a Zymo RNA kit, and the isolated RNA was then treated with and without RNase (Figure 4.2 A). Silver staining showed almost no protein in the uncrosslinked samples (Figure 4.2 B). However, a more significant protein is observed in the cross-linked sample treated with RNase than in the untreated UV cross-linked sample. Immunoblotting with the RNA isolated after complex capture and treated with RNAse for Ybx-1 confirmed Ybx-1 as an RNA binding protein in cardiomyocytes (Figure 4.2 C). Ribosomal S6 protein was used as a positive control, and Actin was used as a negative control.

4.2.1 Ybx-1 binds to tRNAs

Ybx-1 plays multiple roles in the cell and acting as an mRNA stabiliser is one of them. Research work by Goodarzi et al. was able to immunoprecipitate Ybx-1 along with tRNAs and highlight the role of Ybx-1 in stabilising tRNA fragments and enhancing protein regulation downstream in oncogenic cells[85]. To ascertain if Ybx-1 binds to tRNAs in cardiomyocytes, I used complex capture along with a few additional steps. tRNAs are smaller RNA fragments than mRNA, so small RNA fragments were purified from cardiomyocytes after crosslinking them (Figure 4.2 D). After the RNA isolation, elutes were treated with RNAse for digestion, followed by western blot with the samples. 3 10-cm dishes of cardiomyocytes were used per sample, and around 5 ugs of small RNAs were isolated. Ybx-1 was visible on the blot from the crosslinked samples showing that Ybx-1 binds to tRNAs in cardiomyocytes (Figure 4.2 E).

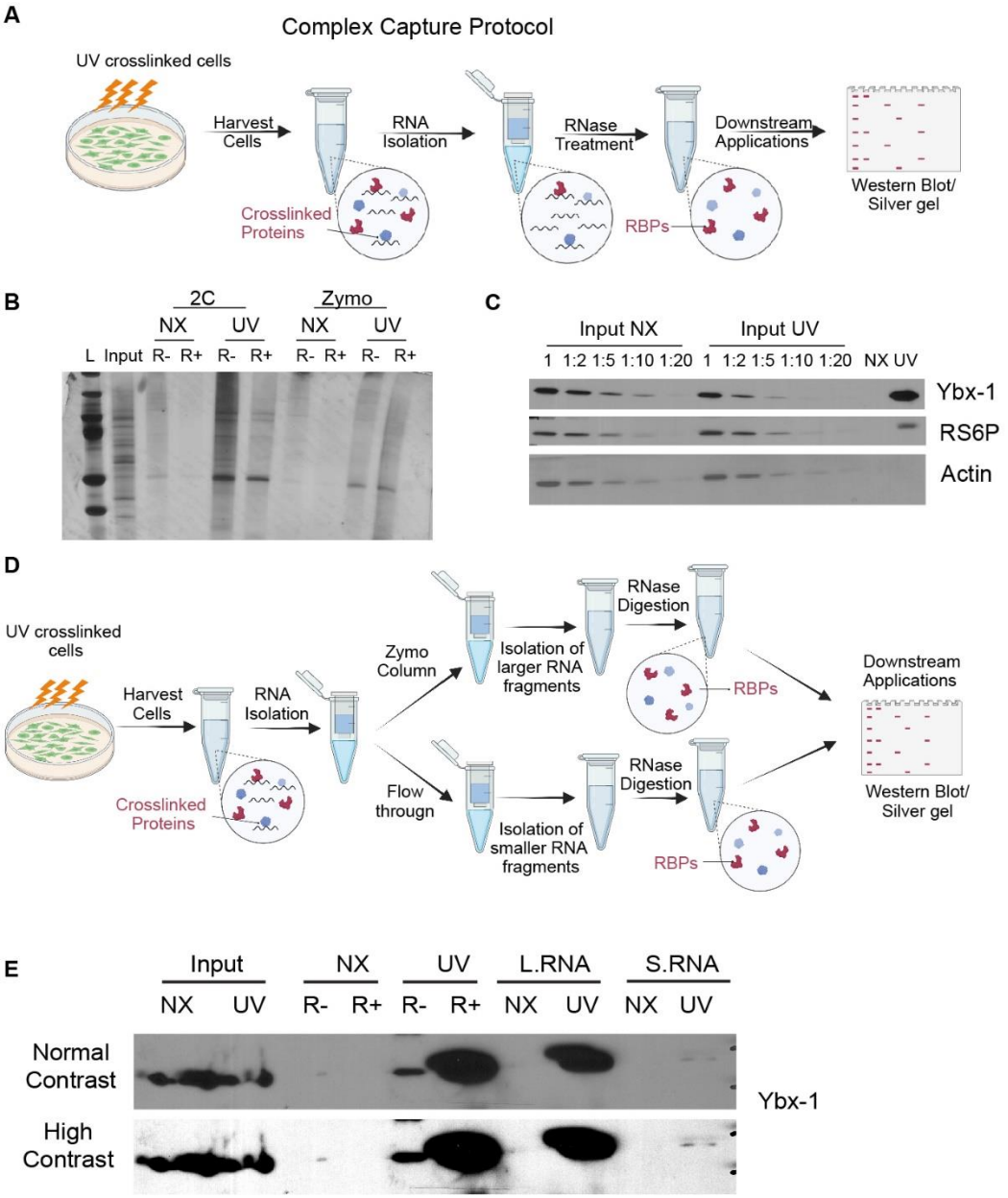

Figure 4.2: Ybx-1 is an RNA binding protein. (A)Experimental design of complex capture protocol. Cells were irradiated with 150 mJ/cm^2 at 254 nm UV crosslinker, and then RNA was purified from the samples. Samples were digested with RNases and then used for silver staining or Western Blot. (B) Silver Gel of NRVM samples that were uncrosslinked (NX) or cross-linked (UV) and then treated with(+) or without(-) RNase. (C) Western blot of NRVM lysates after complex capture. Inputs were diluted in various concentrations, and the samples were treated with RNAse before loading them on the gel (D) Schematic design of isolation of protein linked with tRNAs.samples were treated in a similar way to (A) Immunoblot for Ybx-1 in NRVM lysates after isolation of different RNA fragments with (+) or without (-) RNAse digestion.

4.3 Ybx-1 has a TOP-like MOTIF

Protein synthesis demands a lot of cell energy and resources. Protein translation supports cell growth and proliferation via ribosomal proteins, initiation, and elongation factors. A 5' Terminal Oligopyrimidine (5’ TOP)

pattern distinguishes mRNAs encoding proteins required for translation. Several structural characteristics distinguish members of the TOP mRNA family: a) an invariable C residue at the cap site, followed by a length of 4 to 15 pyrimidines that is unbroken. B) a comparable number of C and U residues in most members' pyrimidine stretch; c) a CG-rich region immediately downstream of the 5′TOP motif; and d) substantial conservation of the 5′TOP motif and its surrounding transcribed sequence across mammals [86]. The mTORC1 and PI3K pathways, which are tightly linked, may be used to induce the translation of TOP mRNAs by replenishing growth hormones and nutrition. The relevance of the mTORC1 signalling pathway in the regulation of TOP mRNAs has been established in many studies [87]. When inhibitors like rapamycin and Torin1 disrupt mTORC1 signalling, the translation of transcripts with the 5' TOP motif is significantly reduced [88]. TOP-like motifs are highly conserved between species, and Ybx-1 has a conserved TOP-like motif. To check if the 5'UTR region of Ybx-1 is a TOP-like motif, we designed a plasmid with two luciferase reporter constructs, i.e., Renilla and Firefly. Renilla luciferase was used as control luciferase. 5'UTR region of Ybx-1, eEF2 (positive control) and c-Myc (negative control) was inserted into the dual luciferase plasmid, and then HEK cells were transfected with the plasmids. The cells were treated with Torin1 for 3 hours to block mTORC1 signalling, and the luciferase activity was measured using the dual luciferase assay. The Ybx-1 and eEF2 showed a significant reduction in firefly expression level compared to the Renilla, thus cementing the presence of the TOP-like motif in the 5'UTR region of Ybx-1.

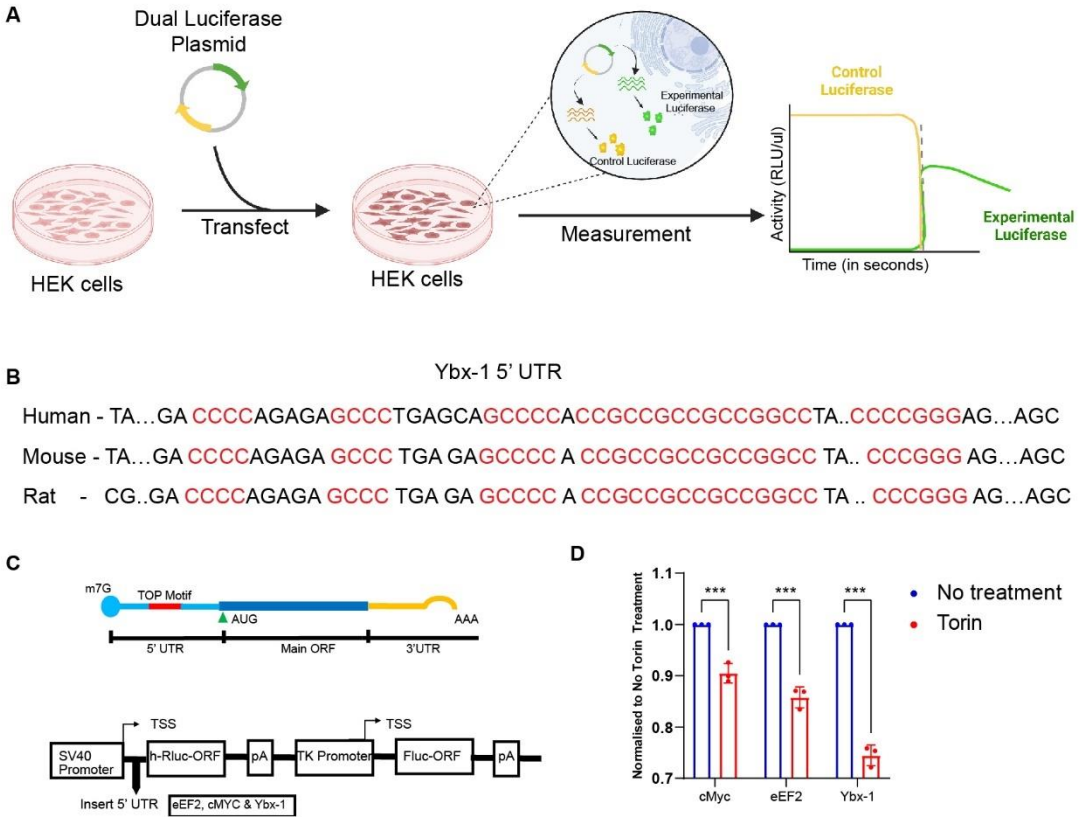

Figure 4.3: Ybx-1 has a 5' TOP motif. (A) Experimental design of Dual luciferase assay in HEK cells(B) 5' UTR region of Ybx-1 with TOP-like motifs that are conserved (highlighted in red) (C) Plasmid construct for Dual luciferase (D) luciferase results from lysates treated with Torin. 3 different plasmids were used i.e., eEF2 (positive control), cMyc (negative control) and Ybx-1. The experiment was performed in triplicates with n = 3. T-test, *** - P ≤ 0.001. Error bars indicate mean ± SEM.

4.4 Ybx-1 control cell size and protein translation in NRVM

4.4.1 Ybx-1 knockdown reduces cell size and protein translation

Previously published papers have shown that depletion of Ybx-1 reduces cell growth and proliferation [60,89]. But the precise role of Ybx-1 in cardiomyocytes is yet to be discovered. To study the effect of Ybx-1 on NRVM, Ybx-1 was knocked down using siRNA. To mimic pathological heart growth in NRVMs, cells were treated with the α-1 receptor agonist phenylephrine (PE), which induces pathological cell growth in cardiomyocytes *in vitro* [90]. The effect of Ybx-1 on the cell size of NRVMs was evaluated by immunostaining after the knockdown and after overexpressing Ybx-1. Approximately 80% reduction in Ybx-1 levels was observed after treatment with siRNA. As expected, PE treatment resulted in a larger cell surface area, almost a 50% increase, than vehicle-treated cells in NRVMs transfected with a control siRNA. However,

Ybx-1 knockdown resulted in a 30% reduction in cell size, and the reduction was 10% after stimulation with PE for 24 hrs (Figure 4.4, A and B).

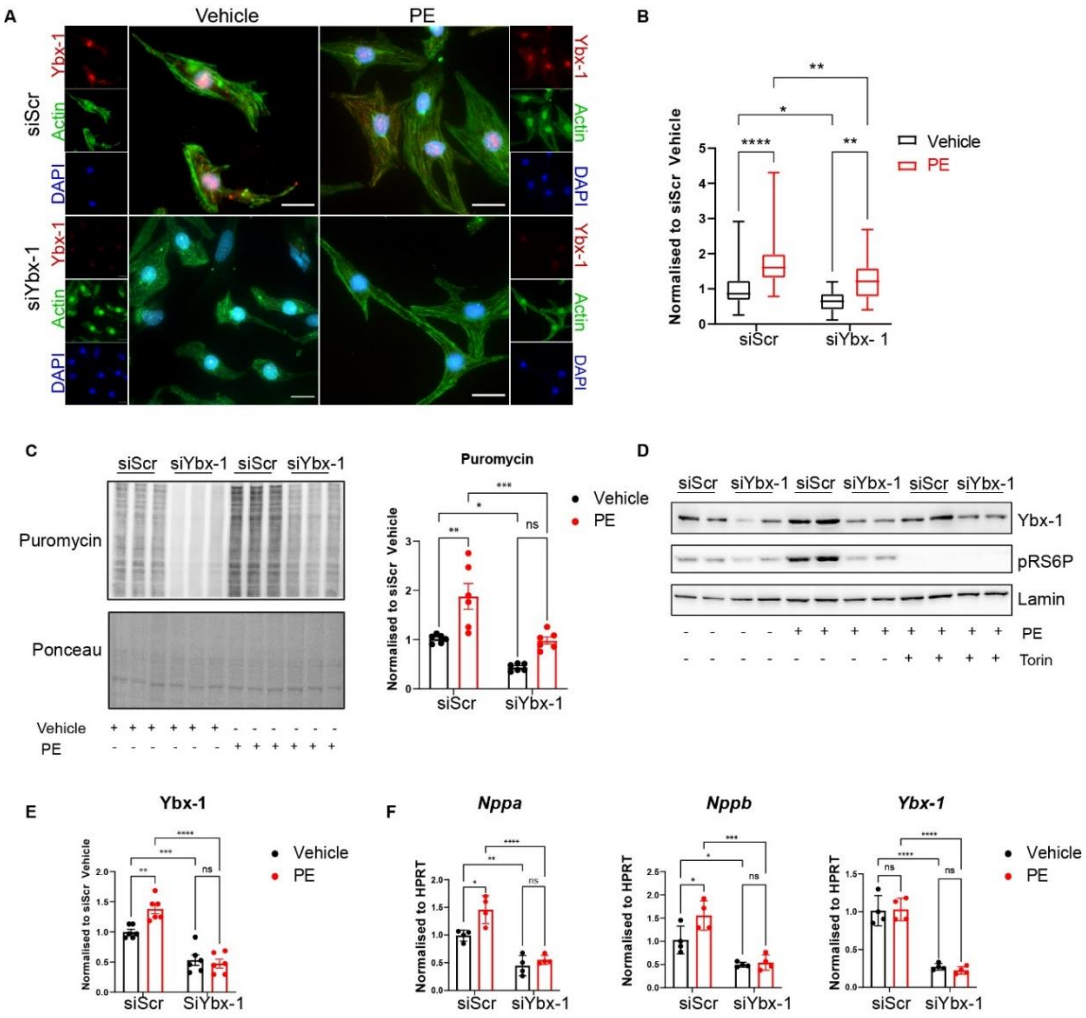

*Figure 4.4: Knockdown of Ybx-1 reduces cell size(*A)Immunofluorescence staining of neonatal rat cardiomyocytes for Ybx-1(red), sarcomeric actin(green) and nuclei(blue) after knockdown of Ybx-1(siYbx-1) or scramble(SiScr) with/without PE treatment. Scale bar 20μm. (B) Quantification of cell size measurements done using Fiji. Analyzed by One-way ANOVA. n>150 cells from n=3 independent experiments. (C) Representative immunoblot and quantification for puromycin on NRVM after knockdown with scrambled(SiScr) or Ybx-1(siYbx-1), followed by treatment with either vehicle(PBS) or PE(50uM) for 24 hrs. Ponceau staining was used as a control. N=6 per group (D)Representative immunoblot and quantification(E) for Ybx-1 protein levels in NRVM after knockdown of Ybx-1 and stimulation with PE. Phospho ribosomal S6 protein (pRS6) is used as a marker for the effect of PE treatment and mTOR pathway activation. Lamin is used as a control. N = 6 independent experiments (F) Quantitative PCR for expression levels of nppa, nppb and Ybx-1 in NRVM to confirm the knockdown and the PE treatment. T-test, * - P ≤ 0.05** - P ≤ 0.01, **** - P ≤ 0.0001. Error bars indicate mean ± SEM

Similarly, PE induced the expression of *Nppa* and *Nppb,* but the induction was blocked after the siRNA-mediated knockdown of Ybx-1. There is a 1.5-fold increase in Nppa and Nppb levels in the vehicle samples treated with PE compared to the vehicle-treated control. Interestingly, there is a 50%

reduction in the *Nppa* and *Nppb* levels in both vehicle and PE treated samples with Ybx-1 knocked down. To analyze the effect of Ybx-1 on the overall protein translation in NRVMs, a puromycin assay was performed after PE treatment and knockdown of Ybx-1. NRVM were treated with 0.5ug/ml puromycin for 30 mins before being harvested. A reduction in puromycin levels was observed for cardiomyocytes with Ybx-1 knocked down (Figure 4.4 C), suggesting that Ybx-1 knockdown reduces protein translation in NCRM at baseline.

Moreover, stimulation of cardiomyocytes with PE resulted in almost a 2-fold increase in overall protein synthesis, but this increase was completely blocked with the knock-down of Ybx-1. Immunoblotting confirmed upregulation of Ybx-1 after PE stimulation and successful knockdown of Ybx-1. Again, the increase of Ybx-1 was independent of changes in mRNA levels (Figure 4.4 D and E).

Ybx-1 was overexpressed in NRVM using adenovirus, followed by cell size measurements by immunostaining. Interestingly and surprisingly, there was a significant reduction in cell size after Ybx-1 overexpression (Figure 4.5 A and B). The effect of PE on cell size is also reduced in NRVM overexpressing Ybx-1 compared to control cells. Puromycin assay showed that the elevated levels of Ybx-1 resulted in reduced protein translation in NRVM, thereby highlighting that an optimal protein level of Ybx-1 is needed for cell growth (Figure 4.5 C). Immunoblots and qRT-PCR confirmed the Ybx-1 overexpression in NRVM (Figure 4.5 D and E).

4.4.2 Ybx-1 Overexpression reduces cell growth and protein translation

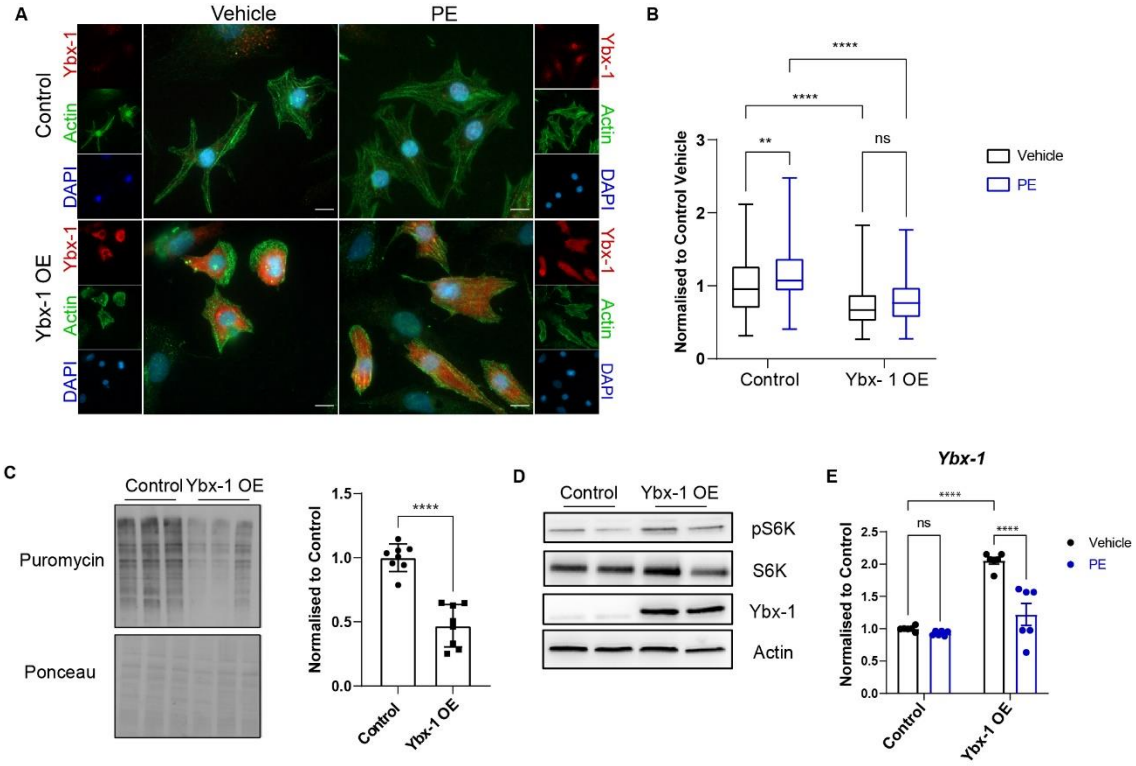

*Figure 4.5: Ybx-1 overexpression reduces cell size. (*A)Immunofluorescence staining of neonatal rat cardiomyocytes for Ybx-1(red), sarcomeric actin(green) and nuclei(blue) after overexpression of Ybx-1(Ybx-1 OE) or control virus(Control) with/without PE treatment. Scale bar 20μm. (B) Quantification of cell size measurements done using Fiji. Analysed by One-way ANOVA. n>150 cells from n=3 independent experiments. (C) Representative immunoblot and quantification for puromycin on NRVM after overexpression of Ybx-1, Ponceau staining was used as a control. N=6 per group (D)Representative immunoblot and quantification(E) for Ybx-1 protein levels in NRVM after Ybx-1 overexpression. Lamin is used as a control. N = 6 independent experiments (E) Quantitative PCR for expression levels of Ybx-1 in NRVM to confirm the overexpression and the PE treatment. T-test, * - P ≤ 0.05** - P ≤ 0.01, **** - P ≤ 0.0001. Error bars indicate mean ± SEM

4.5 Ybx-1 and Cap Dependent Translation

The previous research showed that Ybx-1 affects global translation, and studies have shown that Ybx-1 is involved with cap-dependent translation [75,77]. To study the effect of Ybx-1 on cap-dependent translation, cap immunoprecipitation was performed on NRVM. NRVM cells were lysed in a mild buffer and then coupled with m7GTP beads overnight. This process would help attach the cap structure to the beads and wash everything else that doesn't bind (Figure 4.6 A). Immunoblotting of the IP elutes showed that knocking down Ybx-1 reduced the binding of eIF4E and eIF4G to the cap

structure; surprisingly, there was no effect on the eIF4A protein levels (Figure 4.6 B). The unchanged levels of eIF4A were exciting as eIF4E, eIF4G, and eIF4A form a complex together at the cap structure. To confirm the results of the CAP IP, immunoprecipitation against eIF4G was performed. The IP elutes isolated from NRVM after the Ybx-1 knockdown showed results similar to the CAP IP (Figure 4.6 C). Ybx-1 knockdown resulted in reduced interaction between eIF4G and eIF4E. These results are fascinating as they could show the involvement of Ybx-1 in controlling global translation by stabilizing the CAP binding proteins.

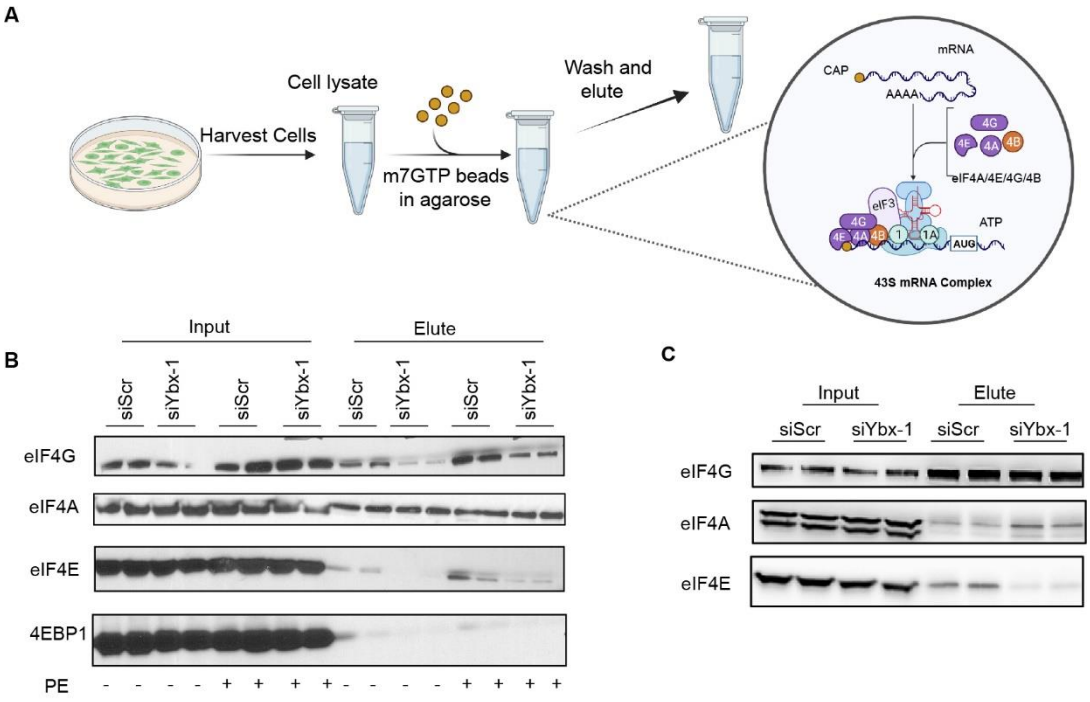

Figure 4.6: Ybx-1 is involved in cap-dependent translation. (A) Experimental setup for the cap immunoprecipitation. The proteins involved in the cap structure are magnified and zoomed in the figure. (B) Representative Immunoblot for the CAP IP using NRVM after knocking down Ybx-1 (SiYbx-1) or Scrambled (SiScr). (C) Immunoblot after immunoprecipitating against eIF4G in NRVM after Ybx-1 knockdown (siYbx-1) or scrambled (SiScr).

4.6 Identifying mRNAs bound to and regulated by Ybx-1

To identify the mRNAs bound to Ybx-1 during cardiac hypertrophy, immunoprecipitation against Ybx-1 was performed on NRVM treated with PE, followed by high throughput sequencing (RIP-Seq) (Fig 4.7 A). NRVM were cultured and stimulated with PE for 24 hours. Immunoprecipitation of Ybx-1 was confirmed with immunoblots (Fig 4.7 B). RNA was isolated from the cell

lysates, and after Ybx-1 IP was sequenced, RIP-Seq was performed in biological triplicates. The libraries were sequenced with the help of Prof. Matthias Hentze's group. The hits from the RIP-Seq data were plotted with p-values and fold change, and Ybx-1 was used as a positive control (Fig 4.7 C). There were 5154 transcripts found in the input samples, and of these, 15.36 % (792) transcripts were bound to Ybx-1. Ybx-1 mRNA was used as a positive control for the transcripts bound to Ybx-1 as it regulates itself [54] (Figure 4.7 D and E). RIP-PCR was used to validate the hits from the RIP-Seq data. *Ybx-1, Acta1, Foxp1, Aldoa, and Ide* were the positive controls, and Acat and Carns were the negative control (Fig 4.7 F). KEGG pathway enrichment was done with the significant hits from the sequencing data (Figure 4.7 G). Among Ybx-1-bound RNAs, transcripts encoding for mRNA involved in signaling pathways such as MAPK and PI3-Akt were significantly enriched.

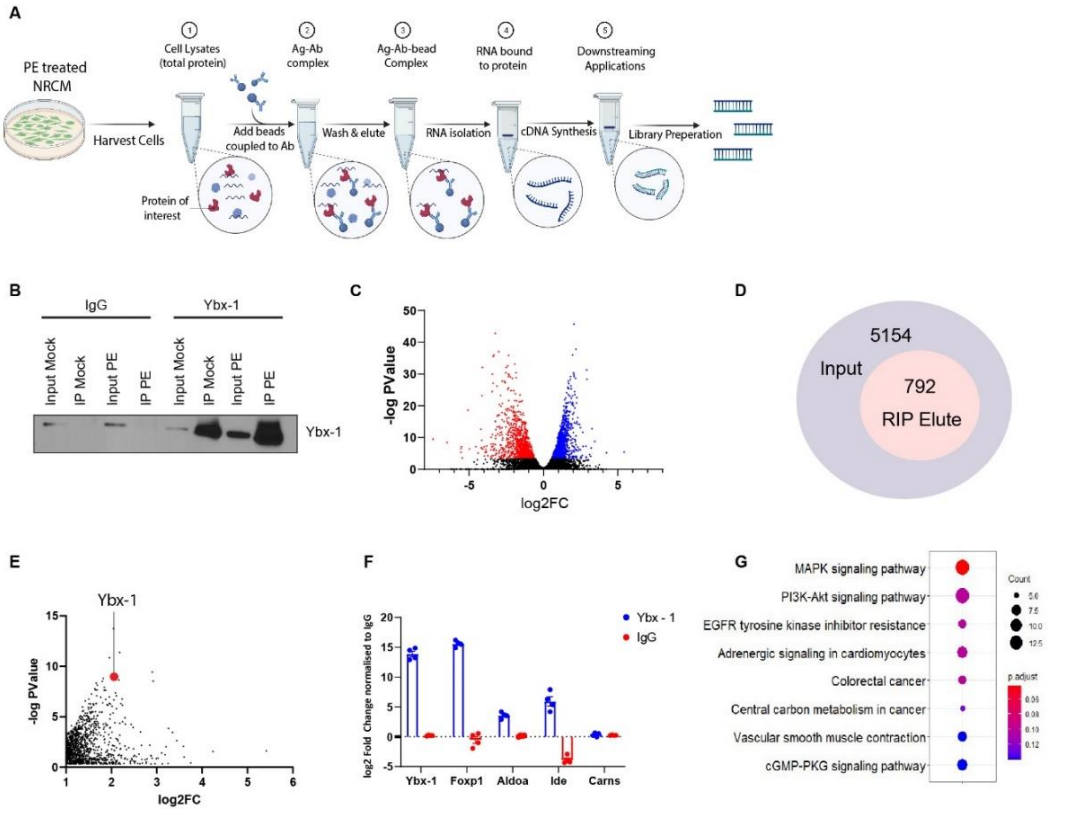

Figure 4.7: RIP Seq against Ybx-1. (A) Experimental set-up for RNA immunoprecipitation against Ybx-1 in NRVM treated with PE for 24 hours. (B) Immunoblot after immunoprecipitation against Ybx-1 in NRVM treated with/without PE (C) Volcano plot of mRNAs bound to Ybx-1 after IP. The red-coloured dots are depleted, and blue-coloured dots are enriched in NRVM elute after IP compared to the inputs. (D) The total amount of mRNAs identified in the input NRVM vs elutes after Ybx-1 after immunoprecipitation(E) The enriched mRNAs after Ybx-1 IP, with Ybx-1 highlighted in red (F) RIP qRTPCR of positive and negative controls after Ybx-1 IP (G)KEGG pathway analysis after immunoprecipitation against Ybx-1.

I further sequenced actively translating mRNAs by Ribosomal Sequencing [83] in NRVMs (Figure 4.8 A) after siRNA mediated KD of Ybx-1 compared to control NRVMs. Ribo-Seq analysis [83] identified in total 9638 translated transcripts. I used the downregulation of Ybx-1 as a positive control (Fig 4.8 B) and could identify 942 (9.7%) transcripts affected by the reduction in Ybx-1 levels in NRVM. In addition, 508 (5.2%) transcripts were identified to be significantly down-regulated when Ybx-1 is knocked down. GO term analysis of the Ribo-Seq list highlighted the mTOR pathway as one of the GO terms enriched in the KEGG pathway (Fig 4.8 C). To focus on mRNA targets affected by Ybx-1 knockdown and bound to Ybx-1, I overlapped the Ribo-Seq and RIP-Seq data. I also overlapped the TAC 2 Day Ribo Seq data to get 7 final common targets between the *in vitro* and *in vivo* data sets (Figure 4.8 D). The heat map of the 7 common targets shows that the 7 targets are downregulated in the Ybx-1 knocked down NRVMs (Fig 4.8 E). The transcript levels of the targets in the Ribo-Seq data with the Ybx-1 KD NRVM (Fig 4.8 F) showed that they were downregulated in the Ybx-1 KD samples compared to the control. eEF2 seemed like a promising target as previous papers have shown upregulated in TAC mice [91].

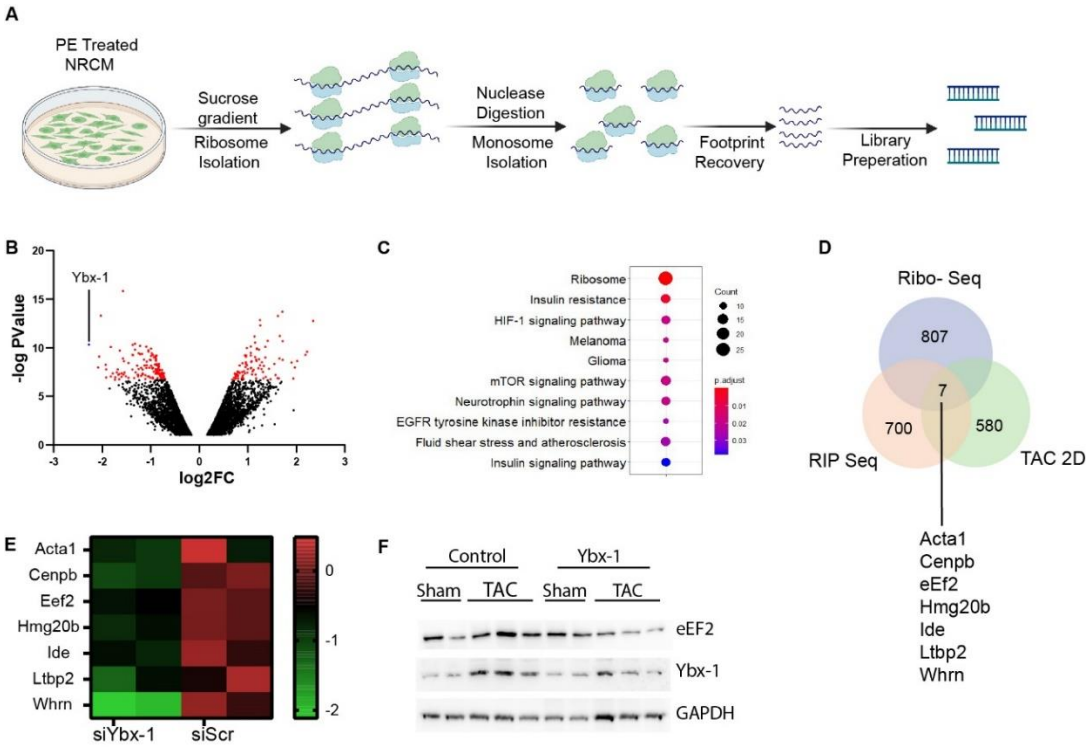

Figure 4.8: RiboSeq in hypertrophic NRVM after Ybx-1 knockdown. (A)Schematic representation of Ribosomal sequencing in NRVM treated with PE for 24 hrs. (B) Volcano plot for upregulated and downregulated mRNAs after Ybx-1 knockdown with significant hits highlighted in red. Ybx-1 is used as a positive control due to its downregulation in the knockdown. (C) KEGG pathway analysis of mRNAs regulated after Ybx-1 knockdown (D) Venn diagram showing the overlap of the mRNAs affected by Ybx-1 knockdown, upregulated during TAC 2D and are bound to Ybx-1. (E)Heatmap of 7 common targets and the difference in expression levels in scrambled and Ybx-1 knockdown (Ybx-1 KD) (F)Representative immunoblot for expression levels for Ybx-1, eEF2 and GAPDH in sham and TAC 2 weeks with and without Ybx-1 knockdown

4.7 Ybx-1 translationally upregulates eEF2 during Cardiac Hypertrophy

Activation of the mTOR pathway reduces EF2 phosphorylation by eEF2 Kinase (eEF2K), and previous papers have shown eEF2 to be upregulated during cardiac hypertrophy [91]. The RIP-Seq data revealed eEF2 mRNA bound to Ybx-1, and experiments showed down-regulation of eEF2 on a protein level in Ybx-1 knockdown samples. To validate the causal role of eEF2 in the phenotype after Ybx-1 knockdown, the eEF2 expression in NRVM needed to increase on a protein level or the activity of eEF2 needed to increase in Ybx-1 knockdown samples. Firstly, an eEF2K inhibitor was used to reduce phosphorylation of eEF2 [20,21]. Inhibition of phosphorylation activated eEF2 activity and resulted in increased protein synthesis as well as NRVMs size. NRVM were stimulated with 100 uM eEF2K inhibitor (A-484954) for 24 hours after Ybx-1 was knocked down. Cell size measurements were

done after immunostaining, and treatment of A-484954 restored the cellular size after Ybx-1 knockdown. eEF2K inhibitor-treated samples showed an increase in cell size, which was visible even after Ybx-1 knockdown (Figure 4.9 A and B). Puromycin assay after stimulating NRVM with eEF2K inhibitor for 24 h showed increased protein synthesis (Figure 4.9 C and D), and phosphorylation of eEF2 was significantly reduced in the samples treated with the eEF2K inhibitor (Figure 4. E). In contrast, no significant change in the mRNA levels of *eEF2* was observed in the NRVM (Figure 4.8 F). A-484954 rescued the defective overall protein synthesis back to levels observed in control cells.

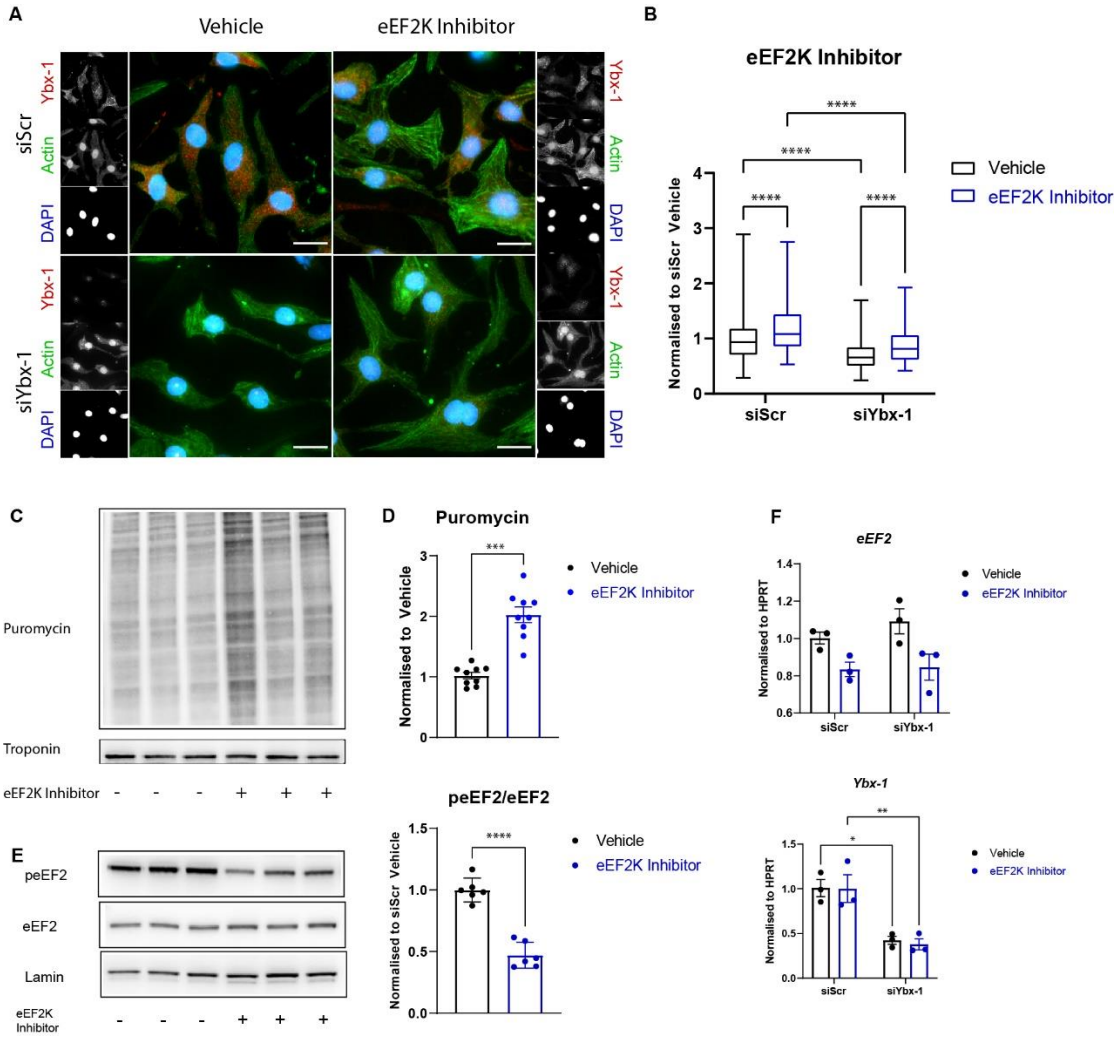

Figure 4.9: Effect of eEF2K Inhibitor on NRVM.(A)Immunofluorescence staining of neonatal rat cardiomyocytes for Ybx-1(red), sarcomeric actin(green) and nuclei(blue) after knockdown of Ybx-1(siYbx-1) or scramble(SiScr) with/without eEF2k inhibitor treatment for 24 hours. Scale bar 20μm. (B) Quantification of cell size measurements done using Fiji. Analysed by One-way ANOVA. n>150 cells from n=3 independent experiments. (C) Representative immunoblot and quantification(D) for puromycin on NRVM after treatment with eEF2K inhibitor. Troponin staining was used as a control. n=6 per group (E)Representative immunoblot and quantification(E) for peEF2 protein levels in NRVM after

eEF2k inhibition with A-484954 for 24 hours (F) qRTPCR levels of eEF2 and Ybx-1 after Ybx-1 knockdown and treatment with eEF2K inhibitor. t-test, * - P ≤ 0.05** - P ≤ 0.01, *** - P ≤ 0.001,**** - P ≤ 0.0001. Error bars indicate mean ± SEM

In addition to a pharmacological approach, I overexpressed eEF2 using an adenoviral vector. Similarly, to pharmacological eEF2 activation, increased eEF2 levels increased protein synthesis and NRVMs size (Figure 4.9 A-D). Again, decreased cell size after Ybx-1 knockdown depended on eEF2 levels as increased eEF2 expression restored NRVMs after Ybx-1 knockdown. Furthermore, immunoblots confirmed successful overexpression of eEF2 (Figure 4.9 E). In summary, those data suggest that reduced levels of eEF2 are causal for the decreased NRVMs size after Ybx-1 depletion. Moreover, the data also indicate that increased translational elongation contributes to cell growth in NRVMs.

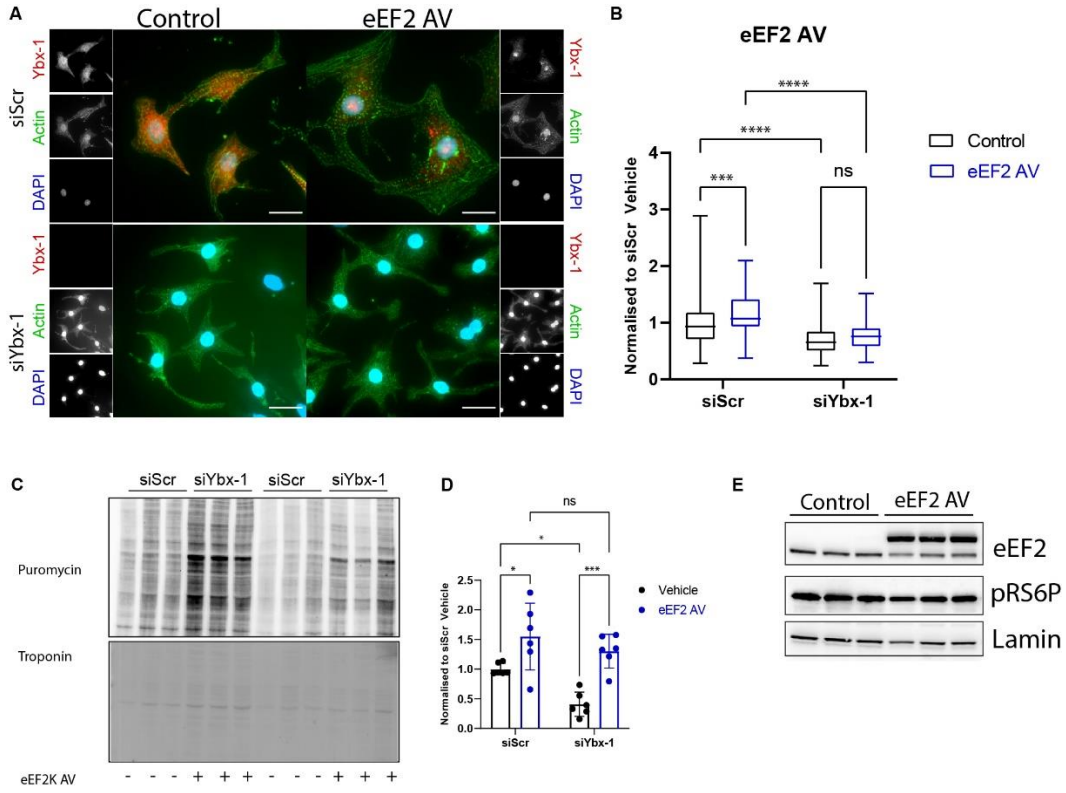

*Figure 4.10: Effect of eEF2 overexpression on NRVM (*A)Immunofluorescence staining of neonatal rat cardiomyocytes for Ybx-1(red), sarcomeric actin(green) and nuclei(blue) after knockdown of Ybx-1(siYbx-1) or scramble (SiScr) with/without eEF2 overexpression (eEF2 AV). Scale bar 20μm. (B) Quantification of cell size measurements done using Fiji. Analyzed by One-way ANOVA. n>150 cells from n=3 independent experiments. (C) Representative immunoblot and quantification(D) for puromycin on NRVM after Ybx-1 knockdown and eEF2 overexpression (eEF2 AV). Ponceau staining was used as a control. n=6 per group (E)Immunoblot of NRVM after treating them with eEF2 overexpression (eEF2 AV) eEF2 shows up higher than the endogenous expression levels due to a tag. t-test, * - P ≤ 0.05** - P ≤ 0.01, *** - P ≤ 0.001,**** - P ≤ 0.0001. Error bars indicate mean ± SEM

4.8 Ybx-1 affects pathological growth in cardiomyocytes *in vivo*

Finally, to analyze the effect of Ybx-1 *in vivo,* I used shRNA targeting Ybx-1 to knock down Ybx-1 in mice. Mice were injected with control AAV9 shRNA as well as against Ybx-1. Three weeks after the injection, TAC surgeries were performed by Dr Xue Li from AG Leuschner (Figure 4.10 A). Cardiac function in Ybx-1 knockdown mice was assessed by ejection fraction, fractional shortening, and heart weight to body ratio. Ybx-1 knockdown mice showed preserved fractional shortening and ejection fraction after TAC surgeries (Figure 4.11 B-D). Immunoblotting was done to confirm the reduction in Ybx-1 levels. Heart lysates from TAC mice showed increased Ybx-1 levels; however, Ybx-1 knockdown mice showed low levels of Ybx-1 that remained unchanged after TAC surgery even at an mRNA level (Figure 4.11 E-F). Furthermore, Ybx-1 knockdown did not change the levels of fetal gene markers generally upregulated in the adult heart during stress, such as *Nppa* and *Col1a1* (Figure 4.11 F). Immunoblotting of eEF2 in adult Ybx-1 KD mice hearts showed a reduction in eEF2 levels on a protein level in Ybx-1 knockdown samples (Fig 4.7 F).

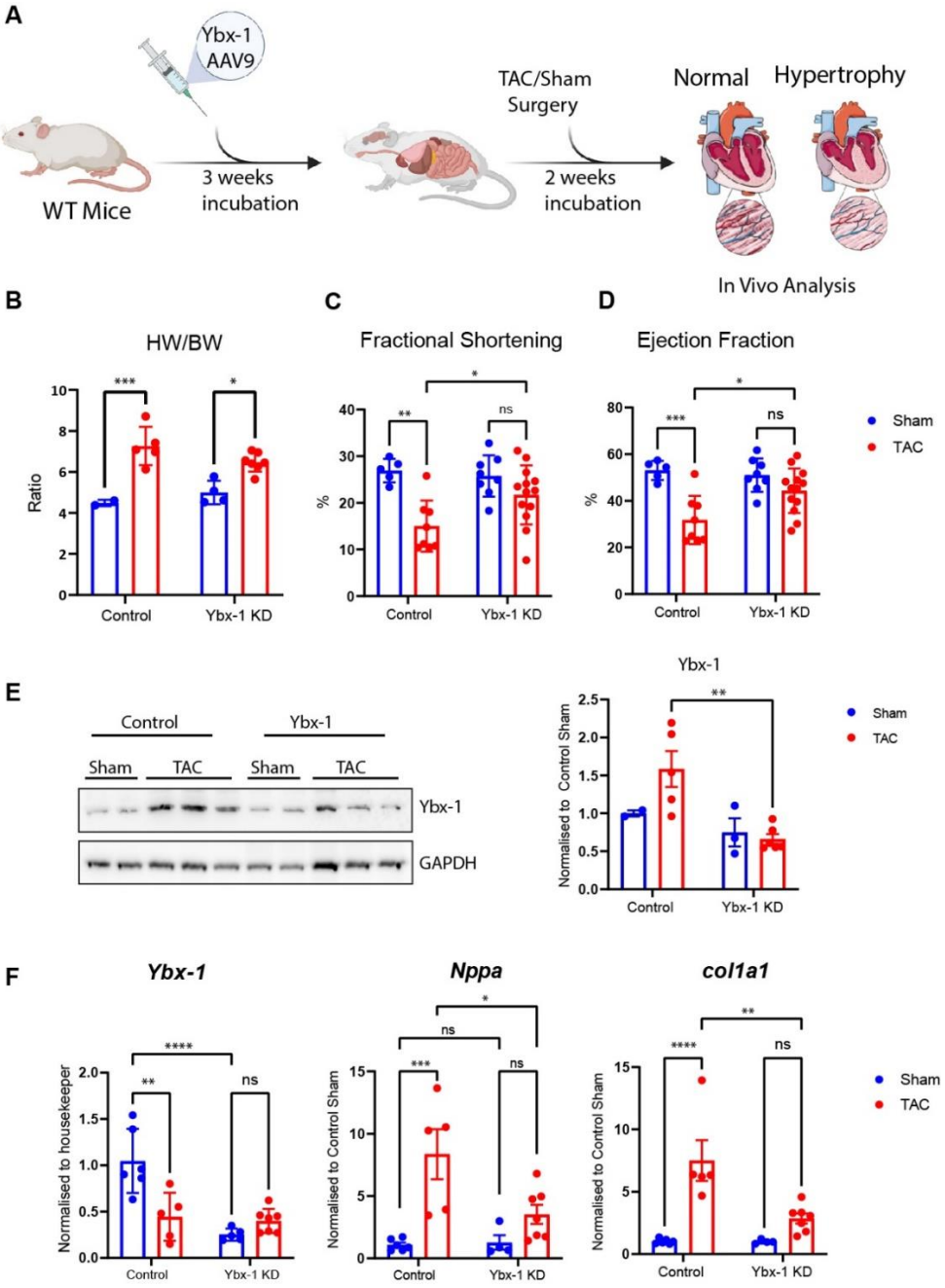

Figure 4.11: Ybx-1 knockdown preserves heart function *in vivo* during cardiac hypertrophy. *(A)Experimental design for injecting Ybx-1 knockdown in vivo and TAC 2-week surgeries in vivo. 2-month-old mice were injected with AAV9 shRNA against Ybx-1 or control, and then 3 weeks later, TAC surgeries were performed. 2 weeks after the TAC or sham, echoes were performed, and mice were sacrificed for further analysis. (B)Heart Weight to Body Weight (HW/BW) ratio, (C)Fractional Shortening and (D) Ejection fraction for sham and TAC mice in control or Ybx-1 knockdown (Ybx-1 KD) mice 2 weeks after TAC. n ≥ 2 (E)Representative immunoblot and quantification for Ybx-1 in adult mouse left ventricle samples 2 weeks after TAC for control and Ybx-1 KD mice. (F) Ybx-1, nppa, Col1a1 mRNA levels in vivo after TAC surgery in control and Ybx-1 KD mice. n ≥ 5 Analysed by one-way ANOVA * - P ≤ 0.05 ** - P ≤ 0.01, *** - P ≤ 0.001. Error bars indicate mean ± SEM*

5 Discussion

Cardiac hypertrophy is a disease that results in cardiac remodeling and dysfunction along with an increase in protein synthesis, especially in cardiomyocytes [14,15,94]. According to studies, a subset of mRNAs' translational activity is preferentially regulated during cardiac hypertrophy. There are also multiple complex pathways involved in this process in cardiomyocytes. Understanding post-transcriptional control of gene expression would be vital in unravelling the fate of mRNA or the regulation of a protein level, thereby developing new therapeutic interventions for this disease. Post-transcriptional gene regulation is controlled partly by RNA binding proteins in the cell. Understanding the role of some of the vital RBPs and their binding partners could provide a more comprehensive and precise picture of the translational landscape in the cardiomyocyte. This research, Ybx-1 was identified as a critical regulator of protein translation in cardiomyocytes during cardiac hypertrophy.

In this project, Ybx-1 is identified as an RNA binding protein translationally upregulated in cardiomyocytes during cardiac hypertrophy *in vitro* and *in vivo*. Ybx-1 is also shown to bind to different kinds of RNA. Secondly, knocking down or overexpressing Ybx-1 affected cardiac growth and protein translation. Thirdly, mRNAs bound to Ybx-1 and regulated during cardiac hypertrophy are identified. Interestingly, eEF2 is regulated by Ybx-1 and is shown to be involved in cardiac growth and hypertrophy. Finally, the knockdown of Ybx-1 is shown to preserve heart function *in vivo* during cardiac hypertrophy. Thus, Ybx-1 has been shown to translationally regulate cell growth and protein level in cardiomyocytes during cardiac hypertrophy by binding with eEF2.

5.1 RNA Binding Proteins Involved in Cardiac Hypertrophy

5.1.1 Ybx-1 is translationally regulated during cardiac hypertrophy

This study used data from previously published papers [82,90] to identify 86 mTOR responsive RNA binding proteins in NRVM. The 86 RBPs were crossed with 677 TAC upregulated transcripts to finally get a list of 9 RBPs regulated during cardiac hypertrophy. Ybx-1 was one of the 9 proteins and was interestingly only regulated on a translational level. The role of Ybx-1 in various cell types, such as cancer cells and neurocytes, has been studied; however, the role of Ybx-1 in cardiomyocytes is still to be discovered(ref). Ybx-1 levels remained unchanged in RNA seq data at different time points after TAC, whereas there was an upregulation of Ybx-1 two days after TAC. Previously published papers [61,85,95,96] have shown a correlation between Ybx-1 expression level and the mTOR pathway. However, the precise mechanism is still unknown. In this study, Ybx-1 levels increased or decreased in response to mTOR pathway activation or inactivation in cardiomyocytes. Ybx-1 protein levels were reduced in response to Torin 1, a known mTORC1 inhibitor. Ybx-1 mRNA levels remained unchanged after mTORC1 inhibition *in vitro* or TAC surgery *in vivo*. Thus, the study shed light on the translational control of Ybx-1 by the mTOR pathway in cardiac myocytes during cardiac hypertrophy.

5.1.2 Ybx-1 – RNA Binding Protein in Cardiomyocyte

Ybx-1 is a vital protein for a cell to function. It has multiple roles in a mammalian cell and is known to bind to RNA and DNA [55,96,97]. To analyze the function of Ybx-1, it is vital to first identify if Ybx-1 binds to RNA or DNA in the cardiomyocyte. UV rays were used to crosslink protein-RNA interaction *in vitro*, and then RNA isolation was used to isolate RBPs and RNA. The complex capture protocol was first optimized with NRVM, and silver staining was used to show that multiple proteins bound to RNA were eluted after the complex capture. Next, RNAse digestion is used to get rid of RNA in the RBP-RNA complex and then immunoblot was used to confirm that Ybx-1 binds to

RNA In NRVM. Ybx-1, as an RNA binding protein, is involved in splicing, mRNA stability, export, degradation, apoptosis and mRNA packaging [54,66,98].

Ybx-1 is a stress protein found both in the nucleus and cytoplasm. Studies have shown that Ybx-1 is involved in stress granule formation via tiRNA-derived stress-induced RNA in some cell types [85]. The cold shock domain of Ybx-1 is shown to interact with tRNA, resulting in inhibition of translation and induction of stress granules. To check if Ybx-1 still binds to tRNA, cardiac myocyte *in vitro* isolation of small RNAs was done after crosslinking. Immunoblotting confirmed the presence of Ybx-1 bound to small RNAs in NRVM. The function of Ybx-1 binding to tRNA in cardiomyocytes is still unexplored and unknown. The study showed that Ybx-1 binds to tRNA *in vitro*, but the exact function still has to be explored.

5.1.3 Translational Control of Ybx-1 by mTOR

Cardiomyocyte cellular function is crucially dependent on the expression of ribosomal proteins and other elements needed for protein synthesis. As mentioned before, cardiac hypertrophy involves increased protein synthesis. Protein synthesis requires much energy; thus, it's crucial to have a gatekeeper that checks that the energy levels are right before starting the program. An excellent candidate for such a gatekeeper is the 5' TOP-like motif, which is present in transcripts encoding all human ribosomal proteins and various proteins necessary for translation [87]. The 5’ TOP-like motif is highly conserved for Ybx-1 between different species. mTORC1 signaling inhibition has been shown to reduce translation of transcripts with 5’ TOP-like motif. Dual luciferase assay with plasmid inserted with 5’UTR region of Ybx-1 helped validate the presence of TOP-like motif as a reduction in luciferase activity was observed for cells treated with Torin1 as compared to the control. These experiments helped further corroborate the translational control of Ybx-1 by the mTOR pathway in cardiomyocytes.

5.2 Ybx-1 in translation and cell growth

5.2.1 Ybx-1 in cardiomyocyte cell growth and overall protein translation

Multiple studies have highlighted the function of Ybx-1 in multiple cellular functions such as mRNA localisation and stability and translational and transcriptional control [79,96,98–101]. The importance of Ybx-1 in a cell is highlighted by the fact that Ybx-1 deletion is embryonically lethal *in vivo* due to growth reduction and deficiencies in neural development [96]. Cardiac hypertrophy is a disease involving increased cardiac myocytes' cell size; therefore, cell size experiments were done with cardiomyocytes to study the effect of Ybx-1 knockdown *in vitro*. NRVMs were stressed with phenylephrine to mimic cardiac hypertrophy. Reducing Ybx-1 protein expression level resulted in 30% smaller NRVMs even during cardiac hypertrophy. This data correlates with previously published papers on Ybx-1 and its role in cell size growth [60,66]. Ybx-1 affects overall protein translation, and the study here highlighted that reducing Ybx-1 reduces overall protein translation in cardiac hypertrophic myocytes and blocks an increase in protein synthesis in NRVM *in vitro*. Blunted growth by Ybx-1 reduction also reduced the expression level of hypertrophy markers Nppa and Nppb on an mRNA level. Thus, it was hypothesised that Ybx-1 knockdown reduces cell growth in cardiomyocytes by affecting overall protein translation.

The role of Ybx-1 as a potential biomarker for cancer has been studied extensively [54,60,72,102]. Elevated Ybx-1 levels are a marker for cell proliferation and metastatic cancer. However, the effect of overexpressing Ybx-1 in cardiomyocytes has not been studied. Cardiomyocytes do not proliferate; therefore, the effect of Ybx-1 overexpression in cardiomyocytes is a big contradiction to previously published data. In this study, Ybx-1 overexpression in NRVMs reduces cell size *in vitro* and blunts cardiac hypertrophic growth *in vitro*. In addition, Ybx-1 overexpression reduced overall protein translation in NRVMs, as evident by the Puromycin assay. Multiple reasons could contribute to the reduction in protein translation due to increased Ybx-1 protein levels. One of the potential reasons could be that

interaction of Ybx-1 with mRNA happens through the cold shock domain, causing the development of substantial multimeric Ybx-1 complexes. Such huge complexes pack mRNA fragments and make them inaccessible for translation [63].

Studies have also shown that high levels of Ybx-1 as compared to mRNA in the cell cause the Ybx-1 displacement from eIF4F and PABP, resulting in inhibition of translation. The study here shows that the relationship between Ybx-1 and translation is dependent on the Ybx-1 concentration in the cell. Therefore, there needs to be an optimum level of Ybx-1 in the cell for standard protein translation, and any changes in the Ybx-1 protein levels result in decreased protein translation in cardiomyocytes.

5.2.2 Ybx-1 stabilizes initiation complex in cardiomyocytes

Protein translation in a eukaryotic cell happens in three stages, i.e., initiation, elongation and termination. As Ybx-1 controls overall protein translation in the cell, one of the first places to look for the effect of Ybx-1 is the initiation step of protein translation. The initiation step is often considered the rate liming step of protein translation [103] and the role of Ybx-1 in initiation was studied by analysing its effect on cap-dependent translation. Evdokimova V. et al. showed that Ybx-1 stabilises 5' cap-dependent mRNAs [77]. The cap-immunoprecipitation with NRVM showed that knockdown of Ybx-1 surprisingly reduces the binding of eIF4E and eIF4G to the cap structure *in vitro*. This finding is unexpected in two ways; firstly, no study has shown that Ybx-1 directly affects the cap structure. Secondly, the eIf4F complex sits on the cap structure with 3 vital initiation factors, i.e., eIF4G, eIF4A and eIF4E; here, eIF4E and eIF4G have reduced binding, whereas eIF4A have unchanged levels in the immunoprecipitation. These results were surprising; therefore, they were validated with an immunoprecipitation against eIF4G in NRVM, and identical results were observed with the IP. The reduction in eIF4G and eIF4E could be the potential contributor to the reduction in protein translation in cardiomyocytes, and Ybx-1 could be involved in stabilising the cap structure. This conclusion, however, still needs to be validated.

5.2.3 Ybx-1 knockdown protects heart function during cardiac hypertrophy

So far, this study has shown that Ybx-1 knockdown reduces cell growth by affecting overall protein translation *in vitro*. The next step was the analysis of Ybx-1 knockdown *in vivo*. Ybx-1 was knockdown in mice hearts *in vivo* by using an shRNA targeting Ybx-1 with an AAV9. TAC surgery was performed on mice 3 weeks after AAV9 injections, and Ybx-1 knockdown blunted cell growth 2 weeks after TAC. In addition, Ybx-1 knockdown resulted in a reduced heart weight/body weight ratio 2 weeks after TAC surgery. With blunted growth, cardiac function was also preserved in Ybx-1 knockdown mice two weeks after TAC. Preserved ejection fraction and fractional shortening were found for Ybx-1 knockdown mice. Interestingly, Ybx-1 knockdown also blunted the increase in hypertrophic markers Nppa and col1a1. The role of Ybx-1 in hypertrophy has not been studied to date, and this study sheds light on the protective nature of reducing Ybx-1 levels *in vivo* in cardiac hypertrophy.

5.3 Ybx-1 Binding Partners in Hypertrophic Cardiomyocyte

5.3.1 eEF2 mRNA binds to Ybx-1

Identifying the mRNA binding partners of Ybx-1 is essential to understanding the function of this RBP in cardiac hypertrophy. In this study, RIP-seq was used to identify 5154 transcripts in the input and out of those, 792 transcripts were bound to Ybx-1 during cardiac hypertrophy. Ybx-1 is a protein that regulates itself; therefore, it was used as a positive control for the RIP-PCR in NRVM. Positive (eEF2, Ide, Foxp1, Acta1) and negative controls (Acat, Carns) from the RIP-seq data were used for the RIP-PCR to validate the mRNA targets found. After RIP-seq, targets regulated by Ybx-1 knockdown were also identified using Ribosomal Profiling. A translatome in NRVMs after Ybx-1 knockdown in cardiac hypertrophy *in vitro* was generated, and 942 transcripts were found to be affected by Ybx-1 knockdown *in vitro*. Most

transcripts (508) were downregulated after Ybx-1 knockdown in hypertrophic cardiomyocytes, which shows that Ybx-1 knockdown reduces overall protein translation in cardiomyocytes.

Overlapping the RIP-Seq data, Ribo-Seq data from the Ybx-1 knockdown samples and Ribo-Seq data with TAC 2-day samples showed 7 targets of interest. Out of these seven targets, eEF2 seemed the most promising. RIP-PCR and immunoblotting NRVM validated eEF2. eEF2 is an elongation factor and could also affect the overall protein translation in cardiomyocytes. The previous experiments in this study were focused on translation initiation; however, this result seemed to divert the focus towards the elongation process of the protein translation. Previous work has also shown eEF2 to be elevated in mice hearts after TAC surgery and cardiac hypertrophy [91]. mTOR pathway has shown to be involved in elevating eEF2 protein levels, and the data from this study shows that there may also be an alternative regulation of eEF2 in cardiomyocytes by Ybx-1.

5.3.2 Translational Control of eEF2 by Ybx-1

To understand how Ybx-1 regulates eEF2, eEF2 levels on a protein level and mRNA level were checked. No changes were observed in the mRNA levels of eEF2 after Ybx-1 knockdown in NRVMs; therefore, this study showed that Ybx-1 controls eEF2 protein levels translationally. Knocking down Ybx-1 reduces eEF2 protein levels, and rescue experiments were performed in Ybx-1 knockdown NRVMs. Two methods were used to increase eEF2 protein levels in cardiomyocytes, i.e., the eEF2K inhibitor A-484954 and an eEF2 overexpression virus. The eEF2K inhibitor reduces the phosphorylation of eEF2 and thus makes more eEF2 free for protein translation.

Interestingly both the methods resulted in the rescue of cell growth after Ybx-1 knockdown in cardiomyocytes. This results in to conclude that eEF2 is responsible for reducing cell growth after Ybx-1 knockdown in hypertrophic cardiomyocytes. One of the potential reasons for Ybx-1 being involved with eEF2 could be the mRNA stabilization of eEF2 by Ybx-1. In the present study, the interplay between Ybx-1 and eEF2 is identified for the first time.

6 Conclusion

RNA binding proteins are emerging as critical players in post-transcriptional protein regulation, and Ybx-1 is one such RBP that has been studied in various cell types. Ybx-1 is identified to be an RBP that is involved in cardiac hypertrophy. Ybx-1 levels in hypertrophic cardiomyocytes are controlled translationally by the mTOR pathway. The function of Ybx-1 in hypertrophic cardiomyocytes is analysed for the first time. Ybx-1 is identified as an RNA binding protein that also interacts with tRNAs in cardiomyocytes. The binding of Ybx-1 with different RNAs sheds light on the potential of this RBP having many different roles in the cardiomyocyte. RBPs control protein translation by involving in different aspects of the process. This study highlighted the role of Ybx-1 in the initiation complex and its stability in cardiomyocytes. Knocking down Ybx-1 resulted in reduced binding of initiation factors eIF4E and eIF4G to the cap complex, thereby reducing protein translation in Ybx-1 knockdown cardiomyocytes.

Manipulation of Ybx-1 protein expression level by knocking down and overexpressing Ybx-1 revealed its regulatory role in cardiac growth and protein translation. Ybx-1 seemed to have a bell shape regulatory role in cardiomyocytes, i.e., a certain level of Ybx-1 is required by cardiomyocytes to function correctly, and any dysregulation (increase or decrease) of Ybx-1 protein level results in reduced cell growth and protein translation in cardiomyocytes. An increase or decrease of Ybx-1 levels also stunted cardiac growth and markers during hypertrophy *in vitro*.

For the first time in this study, the binding partners of Ybx-1 during cardiac hypertrophy were identified, and a translatome of targets affected due to Ybx-1 knockdown was created. Interestingly, eEF2 was identified as an mRNA translationally regulated by Ybx-1 during cardiac hypertrophy in cardiomyocytes. The interplay between eEF2 and Ybx-1 was identified using RIP-Seq and Ribosomal sequencing. Surprisingly, eEF2 was translationally controlled by Ybx-1 in hypertrophic cardiomyocytes. Overexpression of eEF2

rescued the phenotypic changes in cardiomyocytes *in vitro* caused due to Ybx-1 knockdown. This study shows that eEF2 is responsible for the reduction in cell growth after Ybx-1 knockdown. The role of Ybx-1 in elongation seems vital for cardiomyocytes during hypertrophy.

Interestingly Ybx-1 knockdown data *in vivo* showed that Ybx-1 preserved heart function *in vivo* two weeks after TAC surgery. Ybx-1 protected cardiomyocytes from hypertrophic cell growth *in vivo*, and samples with reduced Ybx-1 levels also showed a reduction in eEF2 protein levels. Ybx-1 knockdown also reduced cardiac hypertrophy markers Nppa and col1a1 *in vivo*.

In conclusion, the presented data shows the importance of Ybx-1 in regulating cell growth and protein translation in cardiac cells in response to pathological stress.

7 Limitations of the study

Ybx-1 is an RNA binding protein and identifying its binding partners has been the first step in analysing its function in cardiomyocytes. This study successfully identified transcripts that bind to Ybx-1 during cardiac hypertrophy. The next step would be to identify where those transcripts bind to Ybx-1, and this could be achieved by utilising techniques such as eCLIP (enhanced crosslinked immunoprecipitation) in cardiomyocytes. These techniques allow us to study the precise interaction of protein-mRNA and manipulate their interaction. Such methods help study what happens in the cell if the protein-mRNA interaction is inhibited and give a more specific function of the RBP in the system.

The *in vivo* data in this study has data after two weeks of TAC; however, there is a need to study shorter and longer TAC time points to study the response of Ybx-1. Data after 4 weeks of TAC were analysed; however, due to the self-regulation of Ybx-1, the knockdown effect of Ybx-1 is lost. 4 weeks after TAC surgery, upregulation of Ybx-1 is seen in the mice's hearts, and no difference was seen in the knockdown mice and the control mice. Therefore, there is a need to create a knockout inducible mouse model of Ybx-1 to study the effect of Ybx-1 on mice hearts. A paper published by Konermann et al. ([104]) highlighted the use of Crispr VI-D for *in vivo* applications, and work on Crispr has been started in the lab. However, the process is still ongoing and requires optimisation *in vitro* before it can be used *in vivo*.

8 Outlook

Cardiac diseases are driven by changes in the protein and RNA levels in the organ. Analysing the molecular mechanism for these changes will direct the invention of therapeutic mediations. The Post-transcriptional mechanisms behind these diseases are still unknown and must be explored. Studying the role of RNA binding proteins presents a vital way of understanding and controlling gene expression in the myocardium. RNA Binding proteins function in many different ways, and fully elucidating these mechanisms could present new and powerful approaches to treating or preventing heart failure or heart diseases.

This study's data and literature shed light on the post-transcriptional regulatory role of Ybx-1 on gene expression in cardiac cells in response to hypertrophic stimuli. Ybx-1 was identified to be a critical regulatory RNA Binding protein involved in cardiac hypertrophy in this study. Ybx-1 has been involved in cell growth and proliferation; however, its role in cardiac cells remains unexplored. The effect of Ybx-1 protein levels on cardiac growth and protein translation was identified in this study. Consistent with previously published data about Ybx-1, the knockdown of this protein showed a reduction in cell growth and protein translation in cardiomyocytes. Overexpression of Ybx-1 has been used as a biomarker for detecting cancer proliferation; however, surprisingly, in cardiomyocytes, Ybx-1 seemed to reduce cell growth and protein translation after overexpression. Optimum levels of Ybx-1 were found to be needed for normal cardiac cell function. *In vivo* data from this study is the first time we can see a cardioprotective effect of Ybx-1 knockdown during cardiac hypertrophy two weeks after TAC. However, knockout data is still missing from this research.

Data from the translatome of Ybx-1 knocked down cardiomyocytes, and mRNAs binding with Ybx-1 showed elongation factor eEF2 as an mRNA binding partner for Ybx-1. eEF2 offers an exciting new avenue to target for treatment and prevention of cardiac diseases. Studies into eEF2 and its role in hypertrophy have suggested that cardiac hypertrophy is partly regulated by increased protein synthesis via eEF2K/eEF2 signaling[105,106]. How Ybx-1

regulates eEF2 expression is still to be explored. A recent publication by Perner et al. in acute myeloid leukaemia identified eEF2 mRNA as a binding partner of Ybx-1 and the role of Ybx-1 in RNA stability in cancer cells [95].

Further RNA stability experiments need to be conducted with eEF2 mRNA and Ybx-1 in cardiomyocytes to specify the exact role that Ybx-1 has in the cardiac cells. Results from this study with pharmacological eEF2K inhibitor and eEF2 overexpression showed that Ybx-1 affects cell growth in cardiomyocytes by the eEF2/eEF2k pathway. Utilising pharmacological eEF2K activators such as nelfinavir in cardiac hypertrophic cells could be a potential therapeutic avenue. Research by De Gassart A et al. showed that activation of eEF2K by nelfinavir reduced cell proliferation and inhibited can progression in colorectal cancer [107]. eEF2K activation has not been studied in cardiac cells, and therefore, experiments first need to be conducted on the effect of eEF2K activation during cardiac hypertrophy.

Altogether the data here paints a clearer image of how Ybx-1 affects post-transcriptional changes in cardiomyocytes during hypertrophy and provides a resource to study the regulation of proteins in cardiomyocytes during cardiac hypertrophy by Ybx-1.

9 References

1. McMurray JJ, Pfeffer MA. Heart failure. *Lancet*. 2005;365(9474):1877-1889. doi:10.1016/S0140-6736(05)66621-4
2. Virani SS, Alonso A, Aparicio HJ, et al. Heart Disease and Stroke Statistics-2021 Update: A Report From the American Heart Association. *Circulation*. 2021;143(8):e254-e743. doi:10.1161/CIR.0000000000000950
3. Tsao CW, Aday AW, Almarzooq ZI, et al. Heart Disease and Stroke Statistics-2022 Update: A Report From the American Heart Association. *Circulation*. 2022;145(8):e153-e639. doi:10.1161/CIR.0000000000001052
4. Tanai E, Frantz S. Pathophysiology of Heart Failure. *Compr Physiol*. 2015;6(1):187-214. doi:10.1002/cphy.c140055
5. Linzbach AJ. Hypertrophy, hyperplasia and structural dilatation of the human heart. *Adv Cardiol*. 1976;18(0):1-14. doi:10.1159/000399507
6. Bernardo BC, Weeks KL, Pretorius L, McMullen JR. Molecular distinction between physiological and pathological cardiac hypertrophy: experimental findings and therapeutic strategies. *Pharmacol Ther*. 2010;128(1):191-227. doi:10.1016/j.pharmthera.2010.04.005
7. Modesti PA, Vanni S, Bertolozzi I, et al. Early sequence of cardiac adaptations and growth factor formation in pressure- and volume-overload hypertrophy. *Am J Physiol Heart Circ Physiol*. 2000;279(3):H976-85. doi:10.1152/ajpheart.2000.279.3.H976
8. Weeks KL, McMullen JR. The athlete's heart vs. the failing heart: can signaling explain the two distinct outcomes? *Physiology (Bethesda)*. 2011;26(2):97-105. doi:10.1152/physiol.00043.2010
9. Shimizu I, Minamino T. Physiological and pathological cardiac hypertrophy. *J Mol Cell Cardiol*. 2016;97:245-262. doi:10.1016/j.yjmcc.2016.06.001
10. Oldfield CJ, Duhamel TA, Dhalla NS. Mechanisms for the transition from physiological to pathological cardiac hypertrophy. *Canadian Journal of Physiology and Pharmacology*. 2020;98(2):74-84. doi:10.1139/cjpp-2019-0566
11. Grossman W, Jones D, McLaurin LP. Wall stress and patterns of hypertrophy in the human left ventricle. *J Clin Invest*. 1975;56(1):56-64. doi:10.1172/JCI108079
12. Tirziu D, Giordano FJ, Simons M. Cell Communications in the Heart. *Circulation*. 2010;122(9):928-937. doi:10.1161/CIRCULATIONAHA.108.847731

13. Tham YK, Bernardo BC, Ooi JY, Weeks KL, McMullen JR. Pathophysiology of cardiac hypertrophy and heart failure: signaling pathways and novel therapeutic targets. *Arch Toxicol*. 2015;89(9):1401-1438. doi:10.1007/s00204-015-1477-x

14. Samak M, Fatullayev J, Sabashnikov A, et al. Cardiac Hypertrophy: An Introduction to Molecular and Cellular Basis. *Med Sci Monit Basic Res*. 2016;22:75-79. doi:10.12659/MSMBR.900437

15. Heineke J, Molkentin JD. Regulation of cardiac hypertrophy by intracellular signalling pathways. *Nat Rev Mol Cell Biol*. 2006;7(8):589-600. doi:10.1038/nrm1983

16. Thoreen CC. The molecular basis of mTORC1-regulated translation. *Biochem Soc Trans*. 2017;45(1):213-221. doi:10.1042/BST20160072

17. Laplante M, Sabatini DM. mTOR signaling in growth control and disease. *Cell*. 2012;149(2):274-293. doi:10.1016/j.cell.2012.03.017

18. Balasubramanian S, Johnston RK, Moschella PC, Mani SK, Tuxworth Jr. WJ, Kuppuswamy D. mTOR in growth and protection of hypertrophying myocardium. *Cardiovasc Hematol Agents Med Chem*. 2009;7(1):52-63. doi:10.2174/187152509787047603

19. Morita M, Gravel SP, Hulea L, et al. mTOR coordinates protein synthesis, mitochondrial activity and proliferation. *Cell Cycle*. 2015;14(4):473-480. doi:10.4161/15384101.2014.991572

20. Nojima H, Tokunaga C, Eguchi S, et al. The mammalian target of rapamycin (mTOR) partner, raptor, binds the mTOR substrates p70 S6 kinase and 4E-BP1 through their TOR signaling (TOS) motif. *J Biol Chem*. 2003;278(18):15461-15464. doi:10.1074/jbc.C200665200

21. Loewith R, Jacinto E, Wullschleger S, et al. Two TOR complexes, only one of which is rapamycin sensitive, have distinct roles in cell growth control. *Mol Cell*. 2002;10(3):457-468. doi:10.1016/s1097-2765(02)00636-6

22. Xu L, Brink M. mTOR, cardiomyocytes and inflammation in cardiac hypertrophy. *Biochim Biophys Acta*. 2016;1863(7 Pt B):1894-1903. doi:10.1016/j.bbamcr.2016.01.003

23. Hua H, Kong Q, Zhang H, Wang J, Luo T, Jiang Y. Targeting mTOR for cancer therapy. *J Hematol Oncol*. 2019;12(1):71. doi:10.1186/s13045-019-0754-1

24. Wu CW, Storey KB. mTOR Signaling in Metabolic Stress Adaptation. *Biomolecules*. 2021;11(5). doi:10.3390/biom11050681

25. Holz MK, Ballif BA, Gygi SP, Blenis J. mTOR and S6K1 mediate assembly of the translation preinitiation complex through dynamic protein interchange and ordered phosphorylation events. *Cell*. 2005;123(4):569-580. doi:10.1016/j.cell.2005.10.024

26. Sonenberg N, Hinnebusch AG. Regulation of translation initiation in eukaryotes: mechanisms and biological targets. *Cell*. 2009;136(4):731-745. doi:10.1016/j.cell.2009.01.042

27. Ben-Sahra I, Manning BD. mTORC1 signaling and the metabolic control of cell growth. *Curr Opin Cell Biol*. 2017;45:72-82. doi:10.1016/j.ceb.2017.02.012

28. Tee AR, Blenis J. mTOR, translational control and human disease. *Semin Cell Dev Biol*. 2005;16(1):29-37. doi:10.1016/j.semcdb.2004.11.005

29. Petersen RO, Baserga R. Nucleic acid and protein synthesis in cardiac muscle of growing and adult mice. *Exp Cell Res*. 1965;40(2):340-352. doi:10.1016/0014-4827(65)90267-3

30. di Liegro CM, Schiera G, di Liegro I. Regulation of mRNA transport, localization and translation in the nervous system of mammals (Review). *Int J Mol Med*. 2014;33(4):747-762. doi:10.3892/ijmm.2014.1629

31. Zeitz MJ, Smyth JW. Translating Translation to Mechanisms of Cardiac Hypertrophy. *J Cardiovasc Dev Dis*. 2020;7(1). doi:10.3390/jcdd7010009

32. Calkhoven CF, Muller C, Leutz A. Translational control of gene expression and disease. *Trends Mol Med*. 2002;8(12):577-583. doi:10.1016/s1471-4914(02)02424-3

33. Nagai R, Low RB, Stirewalt WS, Alpert NR, Litten RZ. Efficiency and capacity of protein synthesis are increased in pressure overload cardiac hypertrophy. *Am J Physiol*. 1988;255(2 Pt 2):H325-8. doi:10.1152/ajpheart.1988.255.2.H325

34. Nagatomo Y, Carabello BA, Hamawaki M, Nemoto S, Matsuo T, McDermott PJ. Translational mechanisms accelerate the rate of protein synthesis during canine pressure-overload hypertrophy. *Am J Physiol*. 1999;277(6):H2176-84. doi:10.1152/ajpheart.1999.277.6.H2176

35. Spriggs KA, Bushell M, Willis AE. Translational regulation of gene expression during conditions of cell stress. *Mol Cell*. 2010;40(2):228-237. doi:10.1016/j.molcel.2010.09.028

36. Halbeisen RE, Galgano A, Scherrer T, Gerber AP. Post-transcriptional gene regulation: from genome-wide studies to principles. *Cell Mol Life Sci*. 2008;65(5):798-813. doi:10.1007/s00018-007-7447-6

37. Knight JRP, Garland G, Pöyry T, et al. Control of translation elongation in health and disease. *Disease Models & Mechanisms*. 2020;13(3). doi:10.1242/dmm.043208

38. Taha E, Gildish I, Gal-Ben-Ari S, Rosenblum K. The role of eEF2 pathway in learning and synaptic plasticity. *Neurobiology of Learning and Memory*. 2013;105:100-106. doi:10.1016/j.nlm.2013.04.015

39. Montanaro L, Sperti S, Testoni G, Mattioli A. Effect of elongation factor 2 and of adenosine diphosphate-ribosylated elongation factor 2 on translocation. *Biochemical Journal*. 1976;156(1):15-23. doi:10.1042/bj1560015

40. Nairn AC, Matsushita M, Nastiuk K, et al. Elongation Factor-2 Phosphorylation and the Regulation of Protein Synthesis by Calcium. In: ; 2001:91-129. doi:10.1007/978-3-662-09889-9_4

41. Delaidelli A, Jan A, Herms J, Sorensen PH. Translational control in brain pathologies: biological significance and therapeutic opportunities. *Acta Neuropathologica*. 2019;137(4):535-555. doi:10.1007/s00401-019-01971-8

42. Faller WJ, Jackson TJ, Knight JRP, et al. mTORC1-mediated translational elongation limits intestinal tumour initiation and growth. *Nature*. 2015;517(7535):497-500. doi:10.1038/nature13896

43. Corbett AH. Post-transcriptional regulation of gene expression and human disease. *Curr Opin Cell Biol*. 2018;52:96-104. doi:10.1016/j.ceb.2018.02.011

44. Gerstberger S, Hafner M, Tuschl T. A census of human RNA-binding proteins. *Nat Rev Genet*. 2014;15(12):829-845. doi:10.1038/nrg3813

45. Kelaini S, Chan C, Cornelius VA, Margariti A. RNA-Binding Proteins Hold Key Roles in Function, Dysfunction, and Disease. *Biology (Basel)*. 2021;10(5). doi:10.3390/biology10050366

46. Castello A, Fischer B, Eichelbaum K, et al. Insights into RNA biology from an atlas of mammalian mRNA-binding proteins. *Cell*. 2012;149(6):1393-1406. doi:10.1016/j.cell.2012.04.031

47. Quattrone A, Dassi E. The Architecture of the Human RNA-Binding Protein Regulatory Network. *iScience*. 2019;21:706-719. doi:10.1016/j.isci.2019.10.058

48. Liao Y, Castello A, Fischer B, et al. The Cardiomyocyte RNA-Binding Proteome: Links to Intermediary Metabolism and Heart Disease. *Cell Rep*. 2016;16(5):1456-1469. doi:10.1016/j.celrep.2016.06.084

49. Blech-Hermoni Y, Ladd AN. RNA binding proteins in the regulation of heart development. *Int J Biochem Cell Biol*. 2013;45(11):2467-2478. doi:10.1016/j.biocel.2013.08.008

50. Chothani S, Schafer S, Adami E, et al. Widespread Translational Control of Fibrosis in the Human Heart by RNA-Binding Proteins. *Circulation*. 2019;140(11):937-951. doi:10.1161/CIRCULATIONAHA.119.039596

51. Chothani S, Adami E, Ouyang JF, et al. deltaTE: Detection of Translationally Regulated Genes by Integrative Analysis of Ribo-seq and RNA-seq Data. *Curr Protoc Mol Biol*. 2019;129(1):e108. doi:10.1002/cpmb.108

52. Lennermann D, Backs J, van den Hoogenhof MMG. New Insights in RBM20 Cardiomyopathy. *Curr Heart Fail Rep*. 2020;17(5):234-246. doi:10.1007/s11897-020-00475-x

53. de Bruin RG, Rabelink TJ, van Zonneveld AJ, van der Veer EP. Emerging roles for RNA-binding proteins as effectors and regulators of cardiovascular disease. *Eur Heart J*. 2017;38(18):1380-1388. doi:10.1093/eurheartj/ehw567

54. Lyabin DN, Eliseeva IA, Ovchinnikov LP. YB-1 protein: functions and regulation. *Wiley Interdiscip Rev RNA*. 2014;5(1):95-110. doi:10.1002/wrna.1200

55. En-Nia A, Yilmaz E, Klinge U, Lovett DH, Stefanidis I, Mertens PR. Transcription Factor YB-1 Mediates DNA Polymerase α Gene Expression. *Journal of Biological Chemistry*. 2005;280(9):7702-7711. doi:10.1074/jbc.M413353200

56. Shah A, Lindquist JA, Rosendahl L, Schmitz I, Mertens PR. Novel Insights into YB-1 Signaling and Cell Death Decisions. *Cancers (Basel)*. 2021;13(13):3306. doi:10.3390/cancers13133306

57. Fan X, Xie X, Yang M, et al. YBX3 Mediates the Metastasis of Nasopharyngeal Carcinoma via PI3K/AKT Signaling. *Front Oncol*. 2021;11:617621. doi:10.3389/fonc.2021.617621

58. Matsumoto K, Bay BH. Significance of the Y-box proteins in human cancers. *J Mol Genet Med*. 2005;1(1):11-17. doi:10.4172/1747-0862.1000005

59. Lyabin DN, Ovchinnikov LP. Selective regulation of YB-1 mRNA translation by the mTOR signaling pathway is not mediated by 4E-binding protein. *Sci Rep*. 2016;6:22502. doi:10.1038/srep22502

60. Johnson TG, Schelch K, Lai K, et al. YB-1 Knockdown Inhibits the Proliferation of Mesothelioma Cells through Multiple Mechanisms. *Cancers (Basel)*. 2020;12(8). doi:10.3390/cancers12082285

61. Lyabin DN, Eliseeva IA, Ovchinnikov LP. YB-1 synthesis is regulated by mTOR signaling pathway. *PLoS One*. 2012;7(12):e52527. doi:10.1371/journal.pone.0052527

62. Evdokimova V, Ovchinnikov LP, Sorensen PH. Y-box binding protein 1: providing a new angle on translational regulation. *Cell Cycle*. 2006;5(11):1143-1147. doi:10.4161/cc.5.11.2784

63. Eliseeva IA, Kim ER, Guryanov SG, Ovchinnikov LP, Lyabin DN. Y-box-binding protein 1 (YB-1) and its functions. *Biochemistry (Mosc)*. 2011;76(13):1402-1433. doi:10.1134/S0006297911130049

64. Yang XJ, Zhu H, Mu SR, et al. Crystal structure of a Y-box binding protein 1 (YB-1)–RNA complex reveals key features and residues interacting with RNA. *Journal of Biological Chemistry*. 2019;294(28):10998-11010. doi:10.1074/jbc.RA119.007545

65. Zhang J, Fan JS, Li S, et al. Structural basis of DNA binding to human YB-1 cold shock domain regulated by phosphorylation. *Nucleic Acids Res*. 2020;48(16):9361-9371. doi:10.1093/nar/gkaa619

66. Kohno K, Izumi H, Uchiumi T, Ashizuka M, Kuwano M. The pleiotropic functions of the Y-box-binding protein, YB-1. *Bioessays*. 2003;25(7):691-698. doi:10.1002/bies.10300

67. Heinemann U, Roske Y. Cold-Shock Domains—Abundance, Structure, Properties, and Nucleic-Acid Binding. *Cancers (Basel)*. 2021;13(2):190. doi:10.3390/cancers13020190

68. Skabkin MA, Evdokimova V, Thomas AAM, Ovchinnikov LP. The Major Messenger Ribonucleoprotein Particle Protein p50 (YB-1) Promotes Nucleic Acid Strand Annealing. *Journal of Biological Chemistry*. 2001;276(48):44841-44847. doi:10.1074/jbc.M107581200

69. Zasedateleva OA, Krylov AS, Prokopenko DV, et al. Specificity of Mammalian Y-box Binding Protein p50 in Interaction with ss and ds DNA Analyzed with Generic Oligonucleotide Microchip. *Journal of Molecular Biology*. 2002;324(1):73-87. doi:10.1016/S0022-2836(02)00937-3

70. Smith MR, Costa G. RNA-binding proteins and translation control in angiogenesis. *The FEBS Journal*. Published online November 28, 2021. doi:10.1111/febs.16286

71. Lasham A, Moloney S, Hale T, et al. The Y-box-binding Protein, YB1, Is a Potential Negative Regulator of the p53 Tumor Suppressor. *Journal of Biological Chemistry*. 2003;278(37):35516-35523. doi:10.1074/jbc.M303920200

72. Lyabin DN, Doronin AN, Eliseeva IA, Guens GP, Kulakovskiy I v, Ovchinnikov LP. Alternative forms of Y-box binding protein 1 and YB-1 mRNA. *PLoS One*. 2014;9(8):e104513. doi:10.1371/journal.pone.0104513

73. Evdokimova VM, Wei CL, Sitikov AS, et al. The Major Protein of Messenger Ribonucleoprotein Particles in Somatic Cells Is a Member of the Y-box Binding Transcription Factor Family. *Journal of Biological Chemistry*. 1995;270(7):3186-3192. doi:10.1074/jbc.270.7.3186

74. Evdokimova VM, Kovrigina EA, Nashchekin D v., Davydova EK, Hershey JWB, Ovchinnikov LP. The Major Core Protein of Messenger Ribonucleoprotein Particles (p50) Promotes Initiation of Protein Biosynthesis in Vitro. *Journal of Biological Chemistry*. 1998;273(6):3574-3581. doi:10.1074/jbc.273.6.3574

75. Svitkin Y v, Ovchinnikov LP, Dreyfuss G, Sonenberg N. General RNA binding proteins render translation cap dependent. *EMBO J*. 1996;15(24):7147-7155.

76. Minich WB, Ovchinnikov LP. Role of cytoplasmic mRNP proteins in translation. *Biochimie*. 1992;74(5):477-483. doi:10.1016/0300-9084(92)90088-V

77. Evdokimova V, Ruzanov P, Imataka H, et al. The major mRNA-associated protein YB-1 is a potent 5' cap-dependent mRNA stabilizer. *EMBO J*. 2001;20(19):5491-5502. doi:10.1093/emboj/20.19.5491

78. Nekrasov MP, Ivshina MP, Chernov KG, et al. The mRNA-binding Protein YB-1 (p50) Prevents Association of the Eukaryotic Initiation Factor eIF4G with mRNA and Inhibits Protein Synthesis at the Initiation Stage. *Journal of Biological Chemistry*. 2003;278(16):13936-13943. doi:10.1074/jbc.M209145200

79. Evdokimova V, Ovchinnikov LP, Sorensen PH. Y-box binding protein 1: providing a new angle on translational regulation. *Cell Cycle*. 2006;5(11):1143-1147. doi:10.4161/cc.5.11.2784

80. Sangermano F, Delicato A, Calabrò V. Y box binding protein 1 (YB-1) oncoprotein at the hub of DNA proliferation, damage and cancer progression. *Biochimie*. 2020;179:205-216. doi:10.1016/j.biochi.2020.10.004

81. Shurtleff MJ, Yao J, Qin Y, et al. Broad role for YBX1 in defining the small noncoding RNA composition of exosomes. *Proceedings of the National Academy of Sciences*. 2017;114(43). doi:10.1073/pnas.1712108114

82. Doroudgar S, Hofmann C, Boileau E, et al. Monitoring Cell-Type-Specific Gene Expression Using Ribosome Profiling In Vivo During Cardiac Hemodynamic Stress. *Circ Res*. 2019;125(4):431-448. doi:10.1161/CIRCRESAHA.119.314817

83. Riechert E, Kmietczyk V, Stein F, et al. Identification of dynamic RNA-binding proteins uncovers a Cpeb4-controlled regulatory cascade during pathological cell growth of cardiomyocytes. *Cell Rep*. 2021;35(6):109100. doi:10.1016/j.celrep.2021.109100

84. Asencio C, Chatterjee A, Hentze MW. Silica-based solid-phase extraction of cross-linked nucleic acid-bound proteins. *Life Sci Alliance*. 2018;1(3):e201800088. doi:10.26508/lsa.201800088

85. Goodarzi H, Liu X, Nguyen HCB, Zhang S, Fish L, Tavazoie SF. Endogenous tRNA-Derived Fragments Suppress Breast Cancer Progression via YBX1 Displacement. *Cell*. 2015;161(4):790-802. doi:10.1016/j.cell.2015.02.053

86. Meyuhas O, Kahan T. The race to decipher the top secrets of TOP mRNAs. *Biochimica et Biophysica Acta (BBA) - Gene Regulatory Mechanisms*. 2015;1849(7):801-811. doi:10.1016/j.bbagrm.2014.08.015

87. Cockman E, Anderson P, Ivanov P. TOP mRNPs: Molecular Mechanisms and Principles of Regulation. *Biomolecules*. 2020;10(7):969. doi:10.3390/biom10070969

88. Philippe L, Vasseur JJ, Debart F, Thoreen CC. La-related protein 1 (LARP1) repression of TOP mRNA translation is mediated through its cap-binding domain and controlled by an adjacent regulatory region. *Nucleic Acids Research*. 2018;46(3):1457-1469. doi:10.1093/nar/gkx1237

89. Miao X, Wu Y, Wang Y, et al. Y-box-binding protein-1 (YB-1) promotes cell proliferation, adhesion and drug resistance in diffuse large B-cell lymphoma. *Exp Cell Res*. 2016;346(2):157-166. doi:10.1016/j.yexcr.2016.07.003

90. Simpson P. Stimulation of hypertrophy of cultured neonatal rat heart cells through an alpha 1-adrenergic receptor and induction of beating through an alpha 1- and beta 1-adrenergic receptor interaction. Evidence for independent regulation of growth and beating. *Circ Res*. 1985;56(6):884-894. doi:10.1161/01.res.56.6.884

91. Kameshima S, Okada M, Ikeda S, Watanabe Y, Yamawaki H. Coordination of changes in expression and phosphorylation of eukaryotic elongation factor 2 (eEF2) and eEF2 kinase in hypertrophied cardiomyocytes. *Biochem Biophys Rep*. 2016;7:218-224. doi:10.1016/j.bbrep.2016.06.018

92. Kodama T, Okada M, Yamawaki H. Eukaryotic elongation factor 2 kinase inhibitor, A484954 inhibits noradrenaline-induced acute increase of blood pressure in rats. *J Vet Med Sci*. 2019;81(1):35-41. doi:10.1292/jvms.18-0606

93. Kodama T, Okada M, Yamawaki H. Mechanisms underlying the relaxation by A484954, a eukaryotic elongation factor 2 kinase inhibitor, in rat isolated mesenteric artery. *J Pharmacol Sci*. 2018;137(1):86-92. doi:10.1016/j.jphs.2018.04.006

94. Zeitz MJ, Smyth JW. Translating Translation to Mechanisms of Cardiac Hypertrophy. *J Cardiovasc Dev Dis*. 2020;7(1). doi:10.3390/jcdd7010009

95. Perner F, Schnoeder TM, Xiong Y, et al. YBX1 mediates translation of oncogenic transcripts to control cell competition in AML. *Leukemia*. 2022;36(2):426-437. doi:10.1038/s41375-021-01393-0

96. Kwon E, Todorova K, Wang J, et al. The RNA-binding protein YBX1 regulates epidermal progenitors at a posttranscriptional level. *Nature Communications*. 2018;9(1):1734. doi:10.1038/s41467-018-04092-0

97. Perner F, Schnoeder TM, Xiong Y, et al. YBX1 mediates translation of oncogenic transcripts to control cell competition in AML. *Leukemia*. 2022;36(2):426-437. doi:10.1038/s41375-021-01393-0

98. Skabkina O v., Skabkin MA, Popova N v., Lyabin DN, Penalva LO, Ovchinnikov LP. Poly(A)-binding Protein Positively Affects YB-1 mRNA Translation through Specific Interaction with YB-1 mRNA. *Journal of Biological Chemistry*. 2003;278(20):18191-18198. doi:10.1074/jbc.M209073200

99. Evdokimova V, Tognon C, Ng T, et al. Translational Activation of Snail1 and Other Developmentally Regulated Transcription Factors by YB-1 Promotes an Epithelial-Mesenchymal Transition. *Cancer Cell*. 2009;15(5):402-415. doi:10.1016/j.ccr.2009.03.017

100. Jürchott K, Bergmann S, Stein U, et al. YB-1 as a Cell Cycle-regulated Transcription Factor Facilitating Cyclin A and Cyclin B1 Gene Expression. *Journal of Biological Chemistry*. 2003;278(30):27988-27996. doi:10.1074/jbc.M212966200

101. Stickeler E. The RNA binding protein YB-1 binds A/C-rich exon enhancers and stimulates splicing of the CD44 alternative exon v4. *The EMBO Journal*. 2001;20(14):3821-3830. doi:10.1093/emboj/20.14.3821

102. Gong H, Gao S, Yu C, et al. Effect and mechanism of YB-1 knockdown on glioma cell growth, migration, and apoptosis. *Acta Biochim Biophys Sin (Shanghai)*. 2020;52(2):168-179. doi:10.1093/abbs/gmz161

103. Londei P. Translation Initiation Models in Prokaryotes and Eukaryotes. In: *ELS*. Wiley; 2009. doi:10.1002/9780470015902.a0000541.pub2

104. Konermann S, Lotfy P, Brideau NJ, Oki J, Shokhirev MN, Hsu PD. Transcriptome Engineering with RNA-Targeting Type VI-D CRISPR Effectors. *Cell*. 2018;173(3):665-676.e14. doi:10.1016/j.cell.2018.02.033

105. Wang L, Proud CG. Regulation of the phosphorylation of elongation factor 2 by MEK-dependent signalling in adult rat cardiomyocytes. *FEBS Letters*. 2002;531(2):285-289. doi:10.1016/S0014-5793(02)03536-6

106. Everett AD, Stoops TD, Nairn AC, Brautigan D. Angiotensin II regulates phosphorylation of translation elongation factor-2 in cardiac myocytes. *American Journal of Physiology-Heart and Circulatory Physiology*. 2001;281(1):H161-H167. doi:10.1152/ajpheart.2001.281.1.H161

107. de Gassart A, Demaria O, Panes R, et al. Pharmacological <scp>eEF</scp> 2K activation promotes cell death and inhibits cancer progression. *EMBO Rep*. 2016;17(10):1471-1484. doi:10.15252/embr.201642194

V. Acknowledgements

First and foremost, I would like to express my thanks to my supervisor, Dr Mirko Volkers, for allowing me the chance to work on this intriguing research and for his constant scientific and motivational support and direction, particularly over the last year.

I want to thank Prof. Dr. Marc Freichel for assuming the position as chair of the examination committee, helping with my roadblocks in the in vivo research, and for evaluating my thesis. I would also like to thank Prof. Heineke for providing me with his supervision as a TAC team supervisor during my PhD. I am also grateful to Prof. Dr Thomas Weiland and Dr Daniela Duarte Campos for being members of my examination committee.

I want to thank Prof. Dr Matthais Hentze for providing guidance and help with my project. Without his team's help, especially Thileepan Sekaran, I wouldn't be able to sequence my data. I would also like to acknowledge the help of Dr Xue Li in testing and completing TAC surgeries.

Also, I would like to acknowledge everyone from the Völkers' lab for their stimulating work environment and participation and engagement in this project. Furthermore, I want to thank Verena, Claudi and Lonny for all their technical and experimental assistance. Finally, I would like to highlight the help I have received from Verena Kamuf-Schenk with experiments, optimizations and guidance in the last few years.

More than ever, I would like to thank Dr Aga Gorska, Dr Vivien Kmietczyk and Ellen Malovrh for all the coffee and lunch breaks, for keeping me motivated and for always being helpful colleagues and good friends.

I am very thankful to all of the people in the AZIII I have had the pleasure to work with during the last four years.

I want to thank my friends, Angela, Aditya and Sweta, for their incredible friendship, support, and active participation in each other's lives, even from a distance.

I am deeply grateful to my parents and sister, who have always supported my career and life choices. My father has been a calming, supportive pillar in my life, and without him, I wouldn't have managed to finish my PhD.

In the end, nobody has been more important to me in pursuing my PhD than Vineet Dalal, my best friend, who has always been kind, supportive and helpful to me during all these years, even when times were rough and stressful.

VI. Papers Published

1. Kmietczyk V. et al (2019) m6A-mRNA methylation regulates cardiac gene expression and cellular growth. PMID: 30967445
2. Sanlialp A, et al. (2020) Saraf-dependent activation of mTORC1 regulates cardiac growth. PMID:32173353
3. Gorska AA, et al. (2021) Muscle Specific Cand2 is translationally upregulated by mTORC1 and promotes cardiac remodeling. PMID: 34605609
4. Riechert E, et al. (2021) Identification of dynamic RNA-binding proteins uncovers a CPEB4-controlled regulatory cascade during pathological cell growth of cardiomyocytes. PMID: 33979607